" A DESIGN THEORY FOR HARMONIC TRANSISTOR OSCILLATORS"

by

CHOW HON YEAN, B.Sc., A.R.C.S.

A Thesis submitted for the Degree of

DOCTOR OF PHILOSOPHY

of the

UNIVERSITY OF LONDON

Department of Electrical Engineering,

Imperial College of Science and Technology,

January, 1968.

ABSTRACT

In this thesis, the oscillation mechanism behind the transistor oscillator is examined. The controlling variable of the nonlinear action is identified to be the voltage across the emitter base junction. Since the oscillator is deliberately designed to produce sinusoidal voltages, the system can be linearized. Such a linearized system is characterized by the large signal "Y" parameters.

In order to achieve oscillation the transistor has to be embedded with lossless elements (energy storage elements). A geometrical model has been constructed to relate the embedding network to the active device. The condition for steady state oscillation is represented by a locus in three dimensional space. Each point on the locus correspond to an oscillator configuration. Each configuration correspond to a nonlinear dynamical system, whose solution is the observed oscillation generated by the circuit. In order for the configuration to be a useful oscillator circuit, it must satisfy the condition for soft excitation and have a stable limit cycle. Methods for testing these conditions are suggested. The effect of dissipative loads on the geometrical model is studied. Amplitude and frequency sensitivity expressions with respect to small parameter variations are derived. The mechanism of frequency stability is examined.

ACKNOWLEDGEMENTS

The author wishes to express his deep gratitude to his supervisor Dr. R. Spence of the Electrical Engineering Department, Imperial College, London for his encouragement and guidance during the course of this work. Thanks are also due to his many colleagues in the Circuit Theory Laboratory, in particular E. J. Purslow, B. Y. Ozal, V. Arandjelovic, M. Vehovec, J. M. Garduno, Drs. P. D. van der Puije and J. W. Bandler for their interest, encouragement and discussions.

Financial support provided by the Ministry of Technology (S.R.D.E.) in the form of a research contract is gratefully acknowledged.

TABLE OF CONTENTS

List of Principal Symbols

a	amplitude of oscillation
a_o	amplitude of steady oscillation
b	base terminal of transistor
B	susceptance
B_B	total susceptance of "arm" opposite base terminal of embedded transistor in gyrator representation
B_b	susceptance of "arm" opposite base terminal of transistor in gyrator representation
B_b^+	susceptance of external embedding "arm" opposite base terminal of transistor in gyrator representation
B_E, B_C	defined similarly as B_B, but for the emitter and collector terminals respectively
B_e, B_c	defined similarly as B_b, but for the emitter and collector terminals respectively
B_e^+, B_c^+	defined similarly as B_b^+, but for the emitter and collector terminals respectively
c	collector terminal of transistor
C	capacitance
C^+	capacitance used in embedding network
C_c	collector-base junction capacitance
e	emitter terminal of transistor
E	voltage source
E_{ee}	voltage of d.c. source for emitter-base bias

E_{cc}	voltage of d.c. source for collector-base junction bias
G	conductance
G_B	total conductance of "arm" opposite base terminal of embedded transistor in gyrator representation
G_b	conductance of "arm" opposite base terminal of transistor in gyrator representation without embedding
G_b^+	conductance of external embedding "arm" opposite base terminal of transistor in gyrator representation
G_E, G_C	defined similarly as G_B, but for the emitter and collector terminals respectively
G_e, G_c	defined similarly as G_b, but for the emitter and collector terminals respectively
G_e^+, G_c^+	defined similarly as G_b^+, but for the emitter and collector terminals respectively
j	$\sqrt{-1}$
L	inductance
L	load e.g. y_L = load admittance
M	real part of circuit determinant involving large signal transistor parameters
m	real part of circuit determinant involving small signal transistor parameters
N	imaginary part of circuit determinant involving large signal parameters
n	imaginary part of circuit determinant involving small signal transistor parameters

P	$G_B G_E + G_E G_C + G_C G_B + G_O^2 - B_O^2$
p	$-2G_O B_O$
P(X)	power dissipation in circuit element X
Q	quality factor of tuned circuit $Q = \omega L/r$
q	$2Q/\omega_o$
R	resistance
r	small resistance e.g. in $\omega L/r$
S	source e.g. y_S = source admittance
s	complex frequency $s = \sigma + j\omega$
U	unilateral gain factor
v_{eb}	emitter-base a.c. voltage
v_c	voltage opposite collector terminal in the three terminal representation of the transistor $v_{eb} \equiv v_c$
Y,y	admittance
Y_{11} etc.	large signal transistor "y" parameters
y_{11} etc.	small signal transistor "y" parameters
Z,z	impedance
ω	angular frequency also called frequency for short in the thesis
ω_o	angular frequency of steady state oscillation
	real part of complex frequency
δ, Δ	increment e.g. δa or Δa
τ	period of oscillation

Σ summation e.g. $\Sigma G_B G_E = G_B G_E + G_E G_C + G_C G_B$;

$B_B B_E + B_E B_C + B_C B_B = \Sigma B_B B_E$

$\triangle$ circuit determinant

$\triangle^+$ determinant of embedding network

INDEX OF FIGURES.

INDEX OF FIGURES.(Ctd.)

INDEX OF TABLES.

Chapter 1

Introduction

1.1 Historical Background.

The theory of oscillation has a long history, going back to the days when classical mechanics was formulated. Even the phenomenon of synchronization goes back to Huygens (1629-1695). He observed that two clocks were slightly unsynchronized when suspended on a thin wood board. The lack of accuracy and controllability made experimental investigation and exploitation of the phenomena very difficult. However the theoretical study of oscillatory phenomena went on and became absorbed into the realm of nonlinear differential equations. Early contributions include Lindstedt[1], Poincare[2], Helmholtz[3] and Lyapunov[4]. These pioneers laid down the foundation, on which later workers built up the general theories of nonlinear oscillations.

Just prior to the 1920's the new field of electronics made its appearance. The design of electronic amplifiers and electronic oscillators posed new problems. Experiments on them have provided a wealth of results demanding theoretical interpretations. The advent of electronics brought renewed interests in nonlinear theory. Van der Pol[5] proposed his elegant theory, which treats the type of second order equation bearing his name. By varying only one parameter, the transition of a system from the linear to the nonlinear domain is explained. The magnitude of this parameter will decide whether oscillation is to

be almost sinusoidal or of a relaxation nature. Noted contributors in this post-electronic period include Lienard[6], Krylov-Bogolinbov[7], Andronov-Witt[8] etc.

In this thesis work is directed to the study of nearly sinusoidal oscillators i.e. a transistor oscillator whose output voltage waveform is nearly sinusoidal. From this point onwards any mention of oscillator is taken to mean the above type unless stated otherwise.

Some of the problems facing the designer of transistor oscillators were also known to earlier workers concerned with vacuum tube oscillators. Vacuum tube oscillators were used very early on in radio communication. The requirements on these circuits were dependent on their particular applications. For example, in a power oscillator the magnitude of the oscillatory current is of prime importance, whereas oscillators used in beat-tone audio-frequency generators and superheterodyne receivers are required to possess a high degree of frequency stability. In a book by Thomas[9], he listed some properties of which knowledge is desirable in general. These are:-

(1) The magnitude and constancy of amplitude of the oscillation.

(2) The harmonic content of the oscillation.

(3) The efficiency of the d.c. to a.c. conversion.

(4) The value and stability of the oscillation frequency.

(5) The rate of "build-up" of the oscillation.

The problem of designing the most suitable circuit for any particular

purpose involves adjustment of these factors to coincide as nearly as possible with the requirements under consideration. He also enumerated the factors governing the performance of vacuum tube oscillators. These are:-

(1) The conditions required to start and maintain oscillation.

(2) The mechanism by which the oscillation amplitude is limited.

(3) The frequency of oscillation and its dependence on the maintaining conditions.

These properties were studied by many authors. Corbeiller[10] was interested in the maintenance of oscillation in electrical circuits. Groszkowski[11] showed that in any self-maintained oscillation system there is a balance of both "real" and "imaginary" power. Pierce[12] and Vigoureux[13] worked on crystal oscillators.

Most of the phenomena of vacuum tube oscillators were understood by the time the transistor appeared. However the ideas of feedback amplifiers carried over into the analysis of oscillator circuits cause some confusion over the classification of oscillator circuit configurations. Since there was no unified treatment many authors invented their own circuits, which were later named after them. Such authors include Hartley[14], Colpitts[15], Pierce[12], Miller[16], Lampkin[17] etc. These circuit configurations are shown in Fig. 1.1.

The internal feedback in transistor can give rise to potential instability over a range of frequencies. Terminations for the

potentially unstable network to oscillate can always be found. Sometimes the internal feedback of the transistor might not be sufficient to lead to oscillation at the desired frequency with terminations alone. In order to realize an oscillator at this frequency, lossless embedding elements (external feedback) are normally employed. The effect of lossless embedding is to change the state of potential stability of the network. The effect of terminating the network with dissipative loads is to change its state of activity. Consideration of these properties had led to the formulation of active two-port theory. The basis was laid by Llewellyn[18] and Mason[19,20] and has since been extended by many authors connected with the design of stable amplifier gain; notably by Cheng[21] and Stern[22]. Page and Boothroyd[23] applied this theory to the deliberate design for potential instability in networks containing a transistor. More recently Spence[24] has carried this one step further by his derivation of design expressions for the maximally loaded oscillator.

In the works mentioned above, the transistor is treated as a two-port. It is characterized by the relationships between port currents and port voltages. Such a characterization is normally restricted to linear operation of the device. Mason[19,20] has derived an expression, called the unilateral gain expression U, based on the transistor small signal parameters. When U is greater than unity, the device is active and would be able to give power gain. U normally falls with frequency. The frequency for which U is unity, is called the maximum frequency of oscillation, f_m. For an active device to be

useful as an amplifier, its power gain must be stable over the designed range of frequencies. The boundary between inherent stability and potential instability at any frequency is marked by stability factors. The commonly used stability factors are Stern's[22] and Venkateswaran's[25] stability factor. They are represented by k_i and η_i respectively. At the boundary of stability both these factors are equal to unity. When either of them is less than unity, the two-port is said to be potentially unstable and a pair of passive terminations can be found which will induce oscillation.

Activity and potential instability are two valuable concepts for transistor oscillator design. By optimising k_i with respect to the lossless embedding, Page and Boothroyd were able to design for maximal potential instability of the network. If the dissipative load conductance of the optimised network were less than a maximum value, then the network can be made to oscillate. The condition for oscillation is unfortunately more involved than that presented by the authors mentioned above. To proceed any further, a more general approach is required. Spence considered the case of the maximally loaded oscillator. By setting U of the network equal to unity it is possible to obtain expressions for maximum loads across any port of the three terminal active device (transistor). Spence derived expressions for the embedding network required to induce oscillation under this condition of maximum loading. These expressions have the property that only invariants of the device and device self-immittances are involved, no feedback path needs be identified and no reference to a "common"

device terminal is required. The later property is appropriate to a discussion of oscillators, since in an oscillator there is no identifiable common terminal.

1.2 The Condition for Oscillation

The oscillator circuits when designed, have to be self-excited and self-sustaining, i.e. when the switch of the circuit is closed, some arbitrary small noise impulse will start the system oscillating and this oscillation will ultimately reach exactly the same stationary state regardless of the initial conditions. The limit cycle in nonlinear theory has precisely such properties. Poincare[2] showed that the differential equation of the form $\dot{x} = X(x,y)$; $\dot{y} = Y(x,y)$ admits occasionally special solutions represented by closed curves in the phase plane - limit cycles. Every trajectory beginning sufficiently near a limit cycle approaches it either as time tends to infinity or time tends to minus infinity; i.e. the trajectory either winds itself upon the limit cycle or unwinds from it. Three types of limit cycles are shown in Fig. 1.2.

Any system in which the oscillatory phenomenon starts spontaneously from rest and reaches its stationary state on the limit cycle is said to exhibit soft-excitation. The stationary state of such systems does not depend on the initial conditions but depends uniquely on the parameters of the system, i.e. the final stationary solution is uniquely

determined by the differential equation. Graphically the soft excited oscillation is represented by a trajectory unwinding from an unstable focus point F into the limit cycle C. This case is shown in Fig. 1.3a. There is also the dual case of the trajectory unwinding from a semi-stable limit cycle into a stable focus point as shown in Fig. 1.3b. In this case soft excitation will not be possible. Any sustained oscillation in a physical system has the same nature as a limit cycle.

The concept of the limit cycle is a powerful one in explaining oscillatory phenomena qualitatively. Many attempts had been made to establish a criterion for the existence of limit cycles in non-linear systems. However these criteria e.g. Poincare's index test and Bendixson's[26] negative criterion cannot be applied to transistor oscillator design. Although classical methods connected with the study of limit cycles are not directly applicable here, the line of thought and the qualitative model of the oscillation mechanism which they have created are useful as a mental framework to refer to while searching for a new approach.

The oscillation mechanism involves a stationary state and an unstable initial state (unstable focus point). Growing oscillation in the vicinity of the focus point has a small amplitude which increases exponentially. This initial state can be described by a linear equation. In linear network theory, Laplace transformation can be applied and the superposition of signals holds. Within the linear framework, concepts of immittances and complex frequencies can be used to fascilitate

analysis. One of the most powerful tool available for investigating the stability of linear systems is the Nyquist[27] frequency plot. It is instructive to review Nyquist's method briefly. In order to do this, we refer to Fig. 1.4. Nyquist had shown that the stability of any linear system can be investigated graphically by plotting some characteristic quantity of the system in the complex frequency plane. Nyquist's criterion for the system shown in Fig. 1.4 will be stated as follows:-

> If the function $G(j\omega) = 1 - H(j\omega)K(j\omega)$ is plotted on the complex plane for all real frequencies ω running from $-\infty$ to $+\infty$, the number of times this locus encircles the origin is equal to $N(z) - N(p)$, where $N(z)$ is the number of zeros of $G(s)$ with positive real parts, $N(p)$ is the number of poles of $G(s)$ with positive real parts.

If the above system is to possess any self induced oscillation, then the equation below must be satisfied.

$$\left[1 - H(s)\, K(s) \right] x(t) = 0 \qquad (1.1)$$

The only possible values of the complex frequency variable "s", which can lead to non-zero solutions for $x(t)$ are those which satisfy the equation,

$$G(s) = 1 - H(s)\, K(s) = 0 \qquad (1.2)$$

If all roots of equation (1.2) have negative real parts, the system will be asymptotically stable; if at least one of the roots has a positive

real part, the system will be unstable.

Bode[28] developed the idea of the return difference and expressed it in terms of the network matrix:

$$G(s) = \Delta / \Delta^{\circ} \tag{1.3}$$

where Δ and Δ° represent respectively the determinant of the total network matrix and the same determinant with the feedback element set to zero. This is illustrated in Fig. 1.5. In this example the feedback element y_{21} will be set to zero i.e. $\Delta^{\circ} = \Delta|_{y_{21}=0}$

For all non zero values of $\Delta^{\circ} = 0$, the condition for $G(s) = 0$ will be equivalent to having a singular matrix for the network.

$$\Delta(s) = 0 \tag{1.4}$$

The quasi stationary state can be obtained by setting $s = j\omega$,

$$\Delta(j\omega) = 0 \tag{1.5}$$

Equation (1.5) forms the basis of the linear design theory. It will be shown in this thesis that a linear theory of transistor oscillator is not adequate.

1.3 Aim of the Thesis

At the present time transistor oscillators cannot be designed satisfactorily without resort to empirical methods, and the intuition of the experienced designer. Hafner[29] has called oscillator design an art. Although experienced circuit designers can obtain good results using empirical methods, it is however desirable to have a design theory which can give a step by step procedure towards the final product. The advent of such a procedure would be especially welcome to manufacturers of integrated oscillator circuits. In order to arrive at a new approach it is necessary to have a better understanding of the oscillation mechanism in transistor circuits.

It has been stated in Section 1.1 that for self-sustained oscillation to exist, the system must possess some arbitrary stable limit cycle. The linear theory of transistor oscillator design, uses small signal parameters of the transistor. Therefore it cannot predict the properties of the final stationary state. A method which can be applied to the nonlinear (large signal level) region of operation, has to be found. An unwelcome feature of the earlier linear theory is the requirement of selecting a feedback path. In fact the theory was carried over from the linear feedback amplifier. The transistor is a three terminal device. To describe it by two-port parameters, leads to some confusion in "classifying" the numerous oscillator circuit configurations. Cote[30,31], Brodie[32] and Pritchard[33] had discussed this problem. An approach which does not require the identification of any feedback path will be desirable. Finally there

are the properties and factors governing the performance of the oscillator. Thomas[9] discussed these for the vacuum tube. However these factors have to be re-examined for transistor circuits.

The difficulties met with in transistor oscillator design, are due to the nonrational frequency and amplitude dependence of the transistor parameters. This makes it impossible to write down the differential equation which describes the dynamic behaviour of the circuit. Therefore the classical methods of nonlinear theory are not applicable here. But nevertheless self-sustained oscillations in electrical circuits are manifestations of nonlinear actions. The existence of nonlinear action is easily demonstrated by altering any one of the oscillator circuit parameters. Both the amplitude and frequency of oscillation change in order to maintain oscillation.

Two things are evident from the above discussions. These are:- (1) It will be very unlikely that a general design theory can stem from the analytical methods of classical nonlinear theory.(2) The old design theory based on transistor small signal parameters is found to be inadequate. A new approach has to be found. There is the need to overcome the noncompatibility of the design theory which is linearized and the physical theory which is nonlinear. Until this is done there can be little hope to find quantitative answers to questions like the ones listed below:-

(1) Which is the circuit parameter responsible for amplitude limiting?

(2) Can the transistor oscillator be loaded between any two terminals,

and how will loading affect its performance?

(3) What is the effect of small variations of circuit parameters on the frequency and amplitude of oscillation?

(4) How can the frequency of oscillation be stabilized most efficiently?

These questions form the guide line of the research carried out for this thesis.

1.4 Layout of the Thesis

The main aim of this thesis is to find a reliable procedure for the design of transistor oscillators. The proposed theory is a union of linear network theory and nonlinear system theory.

It is felt that the best introduction to the physics behind the transistor oscillator is in fact to examine an idealised model. In Chapter 2 the Ebers Moll model of the transistor is used to build up a physical model of the system. This reveals certain features which are important for later mathematical formulations. Chapter 3 is concerned with a discussion of the mathematical techniques useful to the proposed theory. Chapter 2 and Chapter 3 form the basis of a quantitative design theory proposed in Chapter 4. This theory relies heavily on harmonic linearization and the exploitation of symmetrical circuit representation. Chapter 5 is connected with the experimental

verification of the proposed theory by means of design examples. The final conclusion and suggestions for further research are given in Chapter 6.

1.5 Statement of Originality

An initial survey of design methods for transistor harmonic oscillators has revealed short comings of the linear theory based on small signal transistor parameters. Classical nonlinear theory cannot be applied because of the complicated nonlinear action in the transistor oscillator. An additional complication is the nonrational dependence of the transistor parameters on frequency. To overcome these difficulties, two well tried techniques are used. These are: (1) Symmetrical Representation; (2) Linearization. On applying these techniques, the behaviour of the oscillatory solutions of the transistor oscillator can be studied in terms of circuit elements directly. The following results are found:

(1) The controlling variable for the nonlinear action in the transistor oscillator is the port voltage v_{eb}.

(2) The transistor can be characterized for nonlinear operation by the large signal "Y" parameters.

(3) The use of large signal "Y" parameters is in fact the Describing Function Method. The justification for using this method is that Aizerman's Filter Hypothesis can always be made to hold.

(4) The large signal "Y" parameters can be measured on a transformer ratio-arm bridge for the specified signal level v_{eb} and frequency f_o.

(5) A geometrical model for the condition of steady state oscillation has been constructed.

(6) Points on the locus of steady state oscillation correspond to oscillator configurations.

(7) Depending on its position in the "geometry", the oscillator configuration can either belong to the basic Colpitts or Hartley configuration.

(8) Only those configurations, which satisfy the criterion for steady state stability and the criterion for soft excitation, correspond to useful circuit configurations.

(9) Methods of testing for these criteria are suggested.

(10) The effect of loading the oscillator with dissipative elements is to alter the "geometry". For any given state $S(a_o, \omega_o)$ there exist a maximum load and an unique embedding network associated with it.

(11) If the locus of steady state oscillation is a closed one, then there exist bounds on the lossless embedding elements.

(12) Expressions for amplitude and frequency sensitivity have been derived.

(13) The mechanism of achieving high frequency stability is found to be connected with the high frequency gradient of the maximum load of the given device. (Note: The maximum load is related to the unilateral gain factor U of the device;
e.g. $G_c^+ = [(U-1)/U][(G_o^2 + B_o^2)/(G_b + G_e)]$).

(14) Expressions for efficiency of operation have been derived. For a heavily loaded transistor, the efficiency of converting d.c. to a.c. power is found to be very small. To obtain

reasonable output power and preserve stability it is the author's opinion that the best way is to use a buffer stage and an amplifier in conjunction with the oscillator.

To the best knowledge of the author, the results presented in this thesis are original.

1.6 References

1. A. Lindstedt, Mem. de l'Ac. Impen de St. Petersburg, 31, 1883.
2. H. Poincare, J. des Math., (3), 7, 1881.
3. H. Helmholtz, "Sensation of tone", Longmans, Green, (London), 1895.
4. M. A. Liapunov, Ann. de Toulouse, Paris, Vol. 9, 1907.
5. van d. Pol, "The triode as a generator of oscillations", Radio Rev., Vol. 1, pp.701-754, 1920. "On relaxation oscillations", Phil. Mag., Vol. 2, pp.978-992, 1926.
6. A. Lienard, Rev. Gen. de l'Electricite 23, 1928.
7. N. Krylov and N. Bogolinbov, "Introduction to nonlinear mechanics", Ann. of Math. Studies, No. 11, Princeton, 1947.
8. A. Andronov and A. Witt, Arch. für Elektrotech., 24, 1930.
9. H. A. Thomas, "Theory and design of valve oscillators", Chapman and Hall Book Co., 1951.
10. Le Corbeiller P., "The nonlinear theory of maintenance of oscillation", J. Inst., Electr. Engrs., Vol. 79, pp.361-378, 1936.
11. J. Groszkowski, "Frequency of self oscillations", Pergamon Press, 1964.
12. G. W. Pierce, "Piezo-electric crystal resonator and crystal oscillations applied to the precision calibration of wave-meters", Proc. Amer. Acad. Arts. Sci., 59, p.81, 1923.
13. P. Vigoureux, "Quartz Vibrators and their Applications", His Majesty's Stationery Office, 1950.

14. Hartley, see ref. 9.

15. Colpitts, see ref. 9.

16. Miller, see ref. 9.

17. Lampkin, see ref. 9.

18. F. B. Llewellyn, "Some fundamental properties of transmission systems", Proc. IRE, Vol. 40, No. 3, pp.271-283, March, 1952.

19. S. J. Mason, "Power gain in feedback amplifiers", IRE Trans. on Ct. Th., Vol. CT-1, No.2, pp.20-25, June, 1954.

20. S. J. Mason, "Some properties of three-terminal devices', IRE Trans. on Ct. Th., Vol. CT-4, No.4, pp.330-332, Dec. 1957.

21. C. C. Cheng, "Neutralization and unileterization", IRE Trans. on Ct. Th., Vol. Ct. Th., Vol. CT-2, No. 2, pp.138-145, June 1955.

22. A. P. Stern, "Stability and power gain of tuned transistor amplifiers", Proc. IRE, Vol. 45, No. 3, pp.335-343, March 1957.

23. D. F. Page and A. R. Boothroyd, "Instability in two port active networks", IRE Trans. on Ct. Th., Vol. CT-5, No. 2, pp.133-139, June 1958.

24. R. Spence, "A theory of maximally loaded oscillators", Trans. IEEE on Ct. Th., Vol. CT-13, p.58, March 1966.

25. S. Venkateswaran and Boothroyd, "Power gain of bandwidth of tuned transistor amplifier stages", Proc. IEE, Vol. 106 B, Suppl. 15, pp. 518-529, May 1959.

26. I. Bendixson, Acta Math. 24, 1901.

27. H. Nyquist, "Regeneration theory", Bell System Technical Journal, Vol. 11, 1932, pp.126-147.

28. H. W. Bode, "Network analysis and feedback amplifier design", D. van Nostrand Book Co., 1959.

29. E. Hafner, "Analysis and design of crystal oscillators", Technical Report, U.S. Army Electronics Laboratories, Fort Monmouth, New Jersey, May 1964.

30. A. J. Cote, "Matrix analysis of oscillator and transistor applications", IRE Trans. on Ct. Th., CT-5, September 1958.

31. A. J. Cote, "Matrix analysis of RL and RC oscillators", IRE Trans. on Ct. Th., CT-6, pp. 232-233, June 1959.

32. J. H. Brodie, "Matrix analysis of oscillators", IRE Trans. on Ct. Th., CT-7, 1, March 1960.

33. R. L. Pritchard, "Discussion of Matrix Analysis of Transistor Oscillators", IRE Trans. on Ct. Th., CT-8, 2, June 1961.

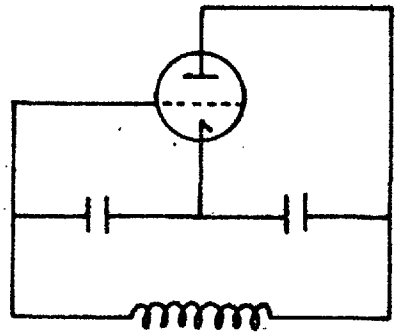

(a) Colpitts oscillator

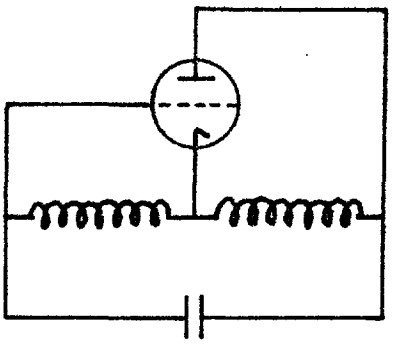

(b) Hartley oscillator

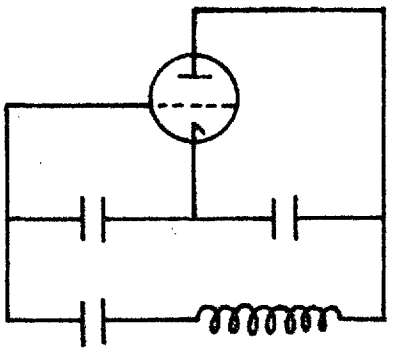

(c) Clapp oscillator

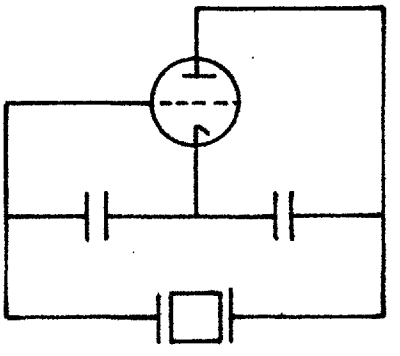

(d) Pierce oscillator

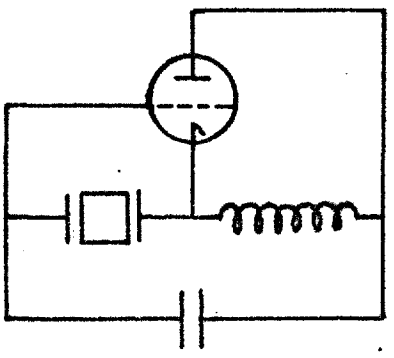

(e) Miller oscillator

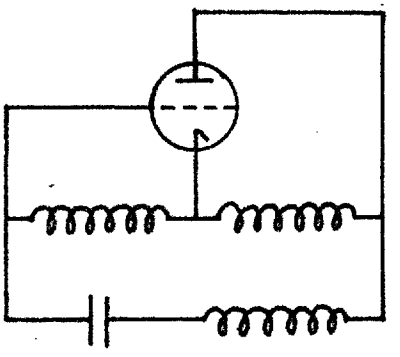

(f) Lampkin oscillator

Fig. 1.1 The diversity of oscillator configurations

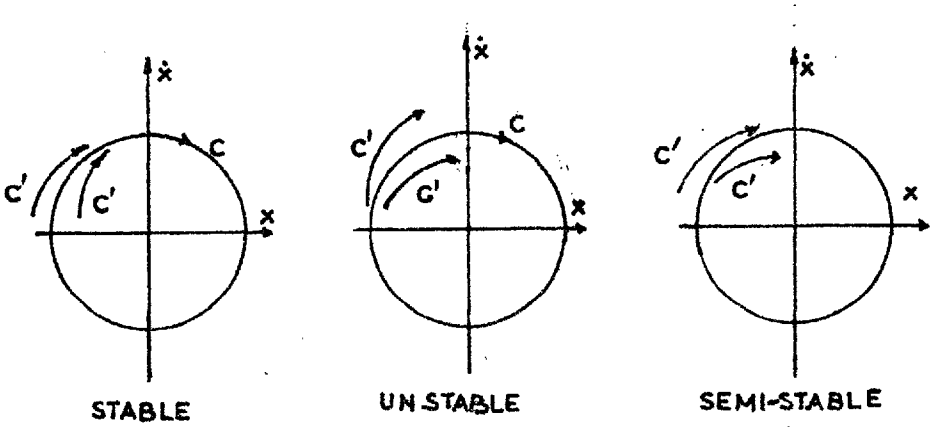

Fig. 1.2 Types of limit cycles

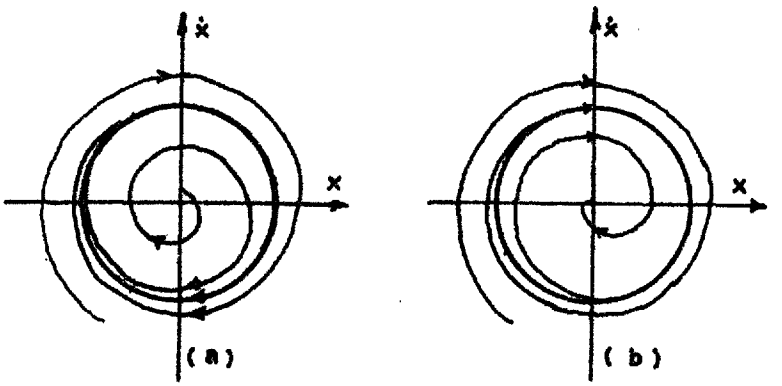

Fig. 1.3 (a) Stable limit cycle with unstable focus point (b) semi-stable limit cycle with stable focus point

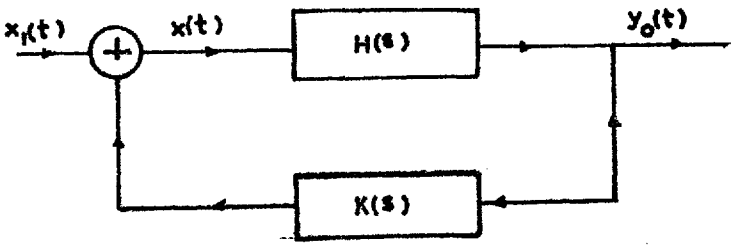

Fig. 1.4 Return difference

notations:

s complex frequency

H(s) transfer function of amplifier

K(s) transfer function of feedback network

$x_i(t)$ input signal , $y_o(t)$ output signal

definition:

$G(s) = 1 - H(s)K(s)$, return difference of system.

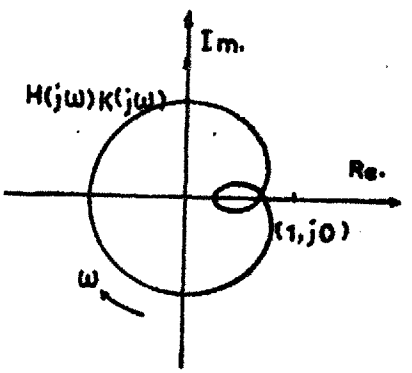

The critical point for the system is (1, j0).

Fig. 1.5 Example of a Nyquist plot

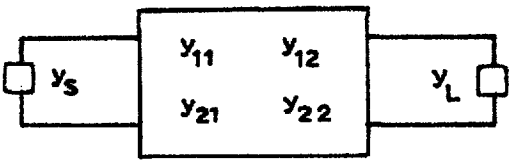

$$G(s) = \frac{\Delta}{\Delta|_{y_{21}}} = \frac{y_1 y_2 - y_{12} y_{21}}{y_1 y_2}$$

$$y_1 = y_s + y_{11}$$

$$y_2 = y_L + y_{22}$$

Fig. 1.6 Return difference of a terminated two-port

Chapter 2

An Idealized Model of the Transistor Oscillator

2.1 Introduction

A well designed oscillator would be one which produces stable oscillation within limits of the specified performances. The complexity of the equations encountered with oscillator circuits and the difficulty of characterizing the transistor (at high frequencies and large signal operation) prevent analysis for the general case. Hafner[1] has pointed out that the success of any analysis of the transistor oscillator depends on the judicious selection of the approximation that have to be made to keep the problem tractable and upon the proper formulation of the analytical expressions in such a manner that they are most susceptible to interpretation. On one hand the designer is faced with the difficulties due to the nonlinear action and on the other hand it is well recognized that only nonlinear theory can provide a conceptual basis for solution of the problem. It is therefore of prime importance to overcome the above mentioned difficulties set by the presence of complicated nonlinearities.

2.2 Ebers Moll Model of the Transistor is a Useful Aid for the Present Investigation

The use of equivalent circuits is only justified if they simplify the analysis and produce acceptable agreement in the subsequent calculations. An equivalent circuit which can reproduce the great number of transistor properties will be extremely complicated and would not help in simplifying the already elusive problem of transistor oscillator design. In view of the complexity, it would be instructive to study a low frequency model of the transistor oscillator. Any salient features revealed in such a study will help to form a strategy to solving the general problem. For this purpose, the set of d.c. characteristics provided by the Ebers Moll[2] equations are employed. These are:-

(For pnp transistors in common-base configuration)

$$I_E = I_{EBS}\left[\exp(qV_{EB}/kT)-1\right] - \alpha_r I_{CBS}\left[\exp(qV_{CB}/kT)-1\right] \qquad (2.1a)$$

$$I_C = I_{CBS}\left[\exp(qV_{CB}/kT)-1\right] - \alpha_f I_{EBS}\left[\exp(qV_{EB}/kT)-1\right] \qquad (2.1b)$$

where,

α_f, α_r = common base forward or reverse current gain respectively

I_{CBS}, I_{EBS} = saturation currents with open collector or open emitter respectively

V_{EB} = emitter-base voltage

V_{CB} = collector-base voltage.

The general shape of Ebers Moll curves and the model on which they are based are shown in Fig. 2.1 and Fig. 2.2.

The first step towards utilizing the transistor in any operational circuit is to fix its quiscent point. In doing this the maximum ratings and the state of operation must be taken into consideration. Fig. 2.3 shows the different regions of operation for the common-emitter configuration. Nonlinear effects will only set in appreciably if the a.c. operation reaches out into either the saturation or the cut off region. The effect of saturation is a severe distortion of collector voltage waveform, while that of cut-off is a severe distortion of the collector current.

2.3 Self Adjustment of the D.C. Conditions when Operating at Large Signal Level.

The transistor nonlinearity which contributes towards amplitude limiting and stability of oscillation is asymmetric. This means that the d.c. bias of the transistor readjust itself to large signal levels. Consider now the biasing network, shown in Fig. 2.4. Ebers Moll equations can be rewritten in the form below

$$\begin{bmatrix} I_E \\ I_C \end{bmatrix} = \frac{1}{1-\alpha_f\alpha_r} \begin{bmatrix} I_{EBO} & -\alpha_r I_{CBO} \\ -\alpha_f I_{EBO} & I_{CBO} \end{bmatrix} \begin{bmatrix} \exp\left[q(E_{ee}-I_eR_e+v_{eb})/kT\right]-1 \\ \exp\left[q(E_{cc}-I_cR_c+v_{cb})/kT\right]-1 \end{bmatrix} \quad (2.2)$$

where,

I_{EBO}, I_{CBO} = leakage currents with open collector or open emitter respectively.

I_e , I_c = d.c. components of I_E and I_C respectively.

v_{eb}, v_{cb} = excitation voltages shown in Fig. 2.4.

The d.c. component of the distorted current is equal to the first term of the Fourier series expansion for the exponential terms. The new d.c. currents at large signal operation are:-

$$I_e = + \frac{I_{EBO}}{1-\alpha_f\alpha_r} \frac{1}{\tau} \int_\tau \exp(q(E_{ee}-I_eR_e+v_{eb})/kT)dt - \frac{I_{EBO}}{1-\alpha_f\alpha_r}$$
$$- \frac{\alpha_r I_{CBO}}{1-\alpha_f\alpha_r} \frac{1}{\tau} \int_\tau \exp(q(E_{cc}-I_cR_c+v_{cb})/kT)dt + \frac{\alpha_r I_{CBO}}{1-\alpha_f\alpha_r} \qquad (2.3)$$

$$I_c = \frac{-\alpha_f I_{EBO}}{1-\alpha_f\alpha_r} \frac{1}{\tau} \int_\tau \exp(q(E_{ee}-I_eR_e+v_{eb})/kT)dt + \frac{\alpha_f I_{EBO}}{1-\alpha_f\alpha_r}$$
$$+ \frac{I_{CBO}}{1-\alpha_f\alpha_r} \frac{1}{\tau} \int_\tau \exp(q(E_{cc}-I_cR_c+v_{cb})/kT)dt - \frac{I_{CBO}}{1-\alpha_f\alpha_r} \qquad (2.4)$$

where τ is the period of oscillation.

Assume that the transistor has been designed to produce sinusoidal voltages; $v_{eb} = |v_{eb}| \cos \omega t$ and $v_{cb} = |v_{cb}| \cos \omega t$. Since the collector is normally well biased into the reverse region, $(E_{cc}-I_cR_c)$ is negative and $\exp(q(E_{cc}-I_cR_c)/kT)$ is very small. The second and fourth terms contribute negligibly to the d.c. currents. Therefore

expressions (2.3) and (2.4) can be rewritten as

$$I_e = \frac{I_{EBO}}{1-\alpha_f\alpha_f} I_o(x) \exp(q(E_{ee}-I_eR_e)/kT) \qquad (2.5)$$

where,

$$x = q\,|v_{eb}|\,/kT$$

$$I_o(x) = \frac{1}{\tau}\int_{\tau} \exp(q\,v_{eb}/kT)dt$$

$$I_c = -\alpha_f I_e \qquad (2.6)$$

The d.c. bias condition of the transistor can be obtained by constructing the load line for the family of curves represented by equation (2.5) and (2.6). These have the form shown in Fig. 2.5.

2.4 The Current Waveforms at Steady State Oscillation

The bias points of the transistor oscillator will readjust themselves to different amplitudes of the steady state oscillation. The new quiscent voltages will be given by $V_{EBQ} = (E_{ee} - I_eR_e)$ and $V_{CBQ} = (E_{cc} - I_c R_c)$. The a.c. component of I_E and I_C are obtained from relationship (2.2),

$$i_e = \frac{I_{EBO}}{1-\alpha_f\alpha_r} \exp\left[q(V_{EBQ}+v_{eb})/kT\right] - \frac{\alpha_r I_{CBO}}{1-\alpha_f\alpha_r} \exp\left[q(V_{CBQ}+v_{cb})/kT\right] \qquad (2.7)$$

$$i_c = \frac{-\alpha_f I_{EBO}}{1-\alpha_f\alpha_r} \exp\left[q(V_{EBQ}+v_{eb})/kT\right] + \frac{I_{CBO}}{1-\alpha_f\alpha_r} \exp\left[q(V_{CBQ}+v_{cb})/kT\right] \tag{2.8}$$

The components of i_e and i_c can be examined separately as functions of v_{eb} and v_{cb}. The components of i_e are shown in Fig. 2.6. It is noticed that the component of i_e due to the excitation voltage v_{cb} can be very small if V_{CBQ} is well in the negative region.

At steady state oscillation v_{cb} and v_{eb} are related by the circuit matrix. Therefore the waveform of i_e will be determined on fixing V_{CBQ}, V_{EBQ} and v_{eb}. It will similarly be the case for the waveform of i_c. There are four possible combinations of the components of i_e or i_c; each giving a distinctly different waveform. These are shown in Fig. 2.7. Case (a) in Fig. 2.7 is the linear operation mode of the transistor. If instability does occur in case (a), the oscillation will grow until it either reaches a steady state or a self modulation state known as squegging.

Kontorovich[3], Bazhan[4] and Kaptsov[5] have analyzed the current waveform of transistor oscillators. The general procedure is to separate the distorted current into a part which can be expressed by a sinusoid through part of its period and the other part by a "discontinuity". By writing down the differential equations for the two separate parts of one total period and then fitting them at their common boundary, the above mentioned authors were able to obtain satisfactory agreement with observed waveforms. Since these investigations are rather restricted in their applications, their methods are not adopted here.

2.5 Classical Methods Used in the Analysis of Vacuum Tube Oscillators are not Suitable for the Transistor Oscillator

In classical nonlinear theory it has been pointed out that self excited oscillations can only occur in nonlinear systems. With vacuum tube oscillators the nonlinearity is easily traced to the plate current being a nonlinear function of the grid voltage. The nonlinear theory of vacuum tube oscillators has been worked out very thoroughly. A number of analytical and graphical methods for the analysis of such circuit exist. The methods of slowly changing amplitudes proposed by van der Pol[6] and the method of small parameters proposed by Andronov[7] are two examples of available methods.

Although transistor oscillator circuit configurations resemble those employing vacuum tubes, nevertheless the above methods for the analysis cannot be applied easily. This is because the specific properties of the transistor as determined by the physical process in the device are quite different from those found in the vacuum tube. A number of important differences exist between the vacuum tube and the transistor. The chief of these are:-

(a) Transistors show considerably greater high frequency effects.

(b) They have smaller input and sometimes output resistance which are further more dependent on the operating conditions.

(c) They possess internal feedback.

(d) The emitter and collector junction capacitances have appreciable value and have to be taken into consideration in the design procedure.

The complete description of all the properties of the transistor can be obtained only by the solution of the diffusion equations for the charge carriers, taking into account the geometry of the device and the boundary conditions. It is not possible to obtain a simple solution to their equations. Therefore the substitute of some equivalent model can only be an approximation. At high frequencies and large signal levels, there are no equivalent circuits of the transistor, which correspond well to the actual physical processes governing transistor action. If consideration is limited to small signal operation, then a suitable equivalent circuit may be substituted for analysis. The designer has to be aware of these complications. Any approach to transistor oscillator design would have to take these properties of the transistor into consideration.

2.6 The Describing Function

2.6.1 Filtered nonlinear systems and the describing function

It should be pointed out that the linear theory of transistor harmonic oscillator design manages to survive in spite of its shortcomings. One reason for this is because there is no way of writing down the system of nonlinear differential equations describing the oscillator system. The second reason is due to the frequency domain

analysis which the linear theory employs. This is very close to the line of thought of the practical designer. He can think in terms of immittance functions and relate the external circuit elements to the parameters of the transistor directly. A similar situation arose when the theoretical basis for nonlinear control system design was formulated. While second order systems lend themselves to a simple analysis in the phase plane, the majority of nonlinear systems are of a higher order and are not amenable to phase plane analysis. Workers in this field of study turned to the concept of a filtered nonlinear system, in which the harmonics (except the first) generated by the nonlinearities may be neglected. It is then possible to define a complex transmission ratio between an input and an output signal. However, in contrast to linear systems, this transmission ratio is a function, not only of the frequency of the input signal but also of its amplitude. Contributors to the development of these ideas include Nichols[8], Goldfarb[9], Lechtman[10], Oppelt[11], Dutilh[12], Loeb[13] and Kochenburger[14]. In this section the basis for the describing function method as treated in Naslin's[15] book is reviewed briefly and then adapted to the problem of transistor oscillator design.

2.6.2 The describing function as used in nonlinear control systems

Consider an element, the input and output variables of which are related by a time invariant nonlinear relationship, $y = f(x)$. This relationship may be one-valued or two-valued. In the latter case, y assumes different values for increasing and decreasing values of x. Also y may exhibit an odd or even symmetry, or may be asymmetric. Fig. 2.8 shows a number of nonlinear characteristics which are frequently met with in practice.

If x is a sinusoidal function of time, $x = X \sin(\omega_o t) = X \sin\Omega$ where $\Omega = \omega_o t$. Then y will be a periodic function with the same angular frequency ω as x. The period of $y(\Omega)$ will be 2π. For a given value of X, $y(\Omega)$ is readily obtained by means of a graphical construction. Fig. 2.9 shows such a construction for the system which exhibits a hysteresis effect. The phase shift due to the hysteresis effect is clearly visible.

In general, a function $y(\Omega)$ of period 2π can always be represented by a Fourier series expansion of the form

$$y(\Omega) = Y_o + \sum_{n=o}^{\infty} (A_n \sin(n\Omega) + B_n \cos(n\Omega)) \qquad (2.9)$$

The mean value Y_o and the coefficients A_n and B_n are:-

$$Y_o = \frac{1}{2\pi} \int_{-\pi}^{+\pi} y(\Omega)\, d\Omega \qquad (2.10a)$$

$$A_n = \frac{1}{\pi} \int_{-\pi}^{\pi} y(\Omega) \sin(n\Omega) d\Omega \qquad (2.10b)$$

$$B_n = \frac{1}{\pi}\int_{-\pi}^{\pi} y(\Omega)\cos(n\Omega)d\Omega \qquad (2.10c)$$

Consider now the system shown in Fig. 2.10. This comprises a non-linear element described by the relationship $y = f(\Omega)$ and a linear element of transmittance $L(j\omega) = G\exp(j\phi)$. The amplitudes and phases of the various harmonic components, as well as the mean value Y_o, are functions of the amplitude X of the input signal but are independent of the excitation frequency ω. After passing through the linear transmittance $L(j\omega)$, each harmonic component of $y(f)$ undergoes a change of amplitude and phase. Therefore the expression for the signal $z(t)$ is:-

$$z(t) = G(o)\,Y_o + \sum_{n=o}^{\infty} G(n\omega_o)Y_n \sin\left[n\omega_o t + \Phi(n\omega_o)\right] \qquad (2.11)$$

If a filter action is present in the system to suppress all harmonics with frequency above the fundamental frequency, then equation (2.11) can be simplified to

$$z(t) = G(o)Y_o + G(\omega_o)Y_1 \sin\left[\omega_o t + \Phi(\omega_o)\right] \qquad (2.12)$$

The output-input amplitude ratio and the phase shift $\Phi_1(\omega_o)$ may be combined to give a complex equivalent gain function N(X)

$$N(X) = \frac{Y_1(X)}{X}\exp\left[j\Phi_1(x)\right] \qquad (2.13)$$

This function is generally known as the describing function. The

amplitude and phase relationships between x and z are given by the generalized transmittance $N(X)\ L(j\omega_o)$, which is a function of both the amplitude X and the angular frequency ω_o of the input. For a one valued characteristic, exhibiting no hysteresis effect, N(X) is always a real function.

2.6.3 Characterizing the transistor at large signal operation with a describing function

The above ideas can be applied to the transistor when sinusoidal driving voltages appear at the input and output port. Consider the system in Fig. 2.11. To characterize the transistor for a.c. operation, we need four parameters i_e, v_{eb}, i_c and v_{eb}. These are two more than those required for the system shown in Fig. 2.10. It has been pointed out in Section 2.3 that for a normally biased common base transistor, the emitter and collector currents are given by the expressions

$$I_E = \frac{I_{EBO}}{1-\alpha_f\alpha_r} \exp\left[q(V_{EBQ}+ v_{eb})/kT\right] \qquad (2.14a)$$

$$I_C = -\alpha_f I_E \qquad (2.14b)$$

Expanding the expression (2.14a) in Fourier series and keeping the d.c.

and the first harmonic terms we get,

$$I_E = \frac{I_{EBO}}{1-a_f a_r} \frac{1}{T}\int_{\tau} \exp\left[q(V_{EBQ}+ v_{eb})/kT\right] dt$$

$$+ \frac{I_{EBO}}{1-a_f a_r} \cos(\omega_o t) \left\{ \frac{2}{\tau}\int_{\tau} \exp\left[q(V_{EBQ}+ v_{eb})/kT\right] \cos(\omega_o t)dt \right\} \quad (2.15)$$

It is noticed that because of the exponential function, the first harmonic comprises only the term involving the cosine function. Expression (2.15) consists of two component terms:

d.c. component term

$$I_e = \frac{I_{EBO}}{1-a_f a_r} \exp(q\, V_{EBQ}/kT) I_o(q\,|\,v_{eb}\,|\,/kT) \quad (2.16)$$

1st harmonic component term

$$I_e = \frac{I_{EBO}}{1-a_f a_r} \cos(\omega_o t) \exp(q\, V_{EBQ}/kT) I_1(q\,|\,v_{eb}\,|\,/kT) \quad (2.17)$$

where I_o and I_1 are the modified Bessel functions of zero and first order respectively. These are given by the respective integrals in expression (2.15).

For reasons which will be clear later, it is desirable to separate the nonlinear active part from the linear part of the system.

The nonlinear active part can now be characterized by the following quantities.

$$V_{EBQ}\ ,\ V_{CBQ}\ ,\ |v_{eb}|\ ,\ I_e,\ i_e,\ I_o \text{ and } i_c$$

It is noticed that y_{11_B} and y_{21_B} of the transistor admittance matrix are in fact given by,

$$y_{11} = \frac{1}{|v_{eb}|} \frac{I_{EBO}}{1-\alpha_f\alpha_r} \exp(q\, V_{EBQ}/kT) I_1(q\,|v_{eb}|/kT) \tag{2.18}$$

$$y_{21} = -\alpha_f\, y_{11} \tag{2.19}$$

Expression (2.18) is the describing function of the transistor for operation at large signal level and it is a real function. The quantities I_e, $I_c = -\alpha_f I_e$, y_{11} and $y_{21} = -\alpha_f y_{11}$ can now be used as design parameters for the transistor oscillator.

2.6.4 <u>The describing function applied to transistor oscillator design and the effects of higher harmonics</u>

Having characterized the transistor for operation at large signal levels, the task of oscillator design can now be considered. The mechanism behind the steady state oscillation in the transistor oscillator is explained in steps below:

STEP 1

Fig. 2.12 shows the ideal case when the biased transistor is subjected to purely sinusoidal excitation. The currents I_E and I_C which result from the quiscent bias voltages V_{EBQ}, V_{CBQ} and the sinusoidal voltages v_{eb} and v_{cb}, are composed of d.c. and harmonic components.

$$I_E = I_e + i_e(\omega_o) + i_e(2\omega_o) + i_e(3\omega_o) + \qquad (2.20)$$

$$I_e = \frac{I_{EBO}}{1-a_f a_r} \exp(X_{EQ}) \frac{1}{\tau} \int_\tau \exp(x_e)dt \qquad (2.21a)$$

$$i_e = \frac{I_{EBO}}{1-a_f a_r} \cos(n\omega_o t)\exp(X_{EQ}) \frac{2}{\tau} \int_\tau \exp(x_e)\cos(n\omega_o t)dt \qquad (2.21b)$$

where $X_{EQ} = q\, V_{EBQ}/kT$ and $x_e = q\,|v_{eb}|/kT$.

$n = 1, 2, 3.$

ω_o = angular frequency of the 1st harmonic.

It should be pointed out that the integrals are in fact the modified Bessel functions $I_o(x_e)$ and $I_n(x_e)$.

$$\frac{1}{\tau} \int_\tau \exp(x_e)dt = I_o(x_e) \qquad (2.22)$$

$$\frac{1}{\tau} \int_\tau \exp(x_e)\cos(n\omega_o t)dt = I_n(x_e) \qquad (2.23)$$

The relative content of the harmonic components for any given value of $|v_{eb}|$ will be decided by the relative values of $I_1(x_e)$, $I_2(x_e)$, $I_3(x_e)$ ... etc. These values vary in a manner shown in Fig. 2.13.

STEP 2

In order to maintain the currents I_E and I_C in Fig. 2.12, the network has to be completed by the use of external embedding. This is shown in Fig2.14. It should be pointed out that once the embedding is used, the a.c. exciting voltages cannot be sinusoidal any longer. The existence of higher harmonic components in I_E and I_C, would necessarily mean that the a.c. port voltages contain harmonics too. However, the content of higher harmonics in the port voltages can be made small by using an embedding with a good filtering characteristic. Fig. 2.15 shows the transistor oscillator represented in the form of a close-loop system. At the steady state, the harmonic voltages developed across the ports of the embedding network will be fixed. Since the embedding network is linear and passive, we can investigate its port current-voltage relationships for individual harmonic components. In order to do this we need to obtain the equivalent two-port impedance matrix for the embedding network.

$$\begin{bmatrix} z_{11}^{+} & z_{12}^{+} \\ z_{21}^{+} & z_{22}^{+} \end{bmatrix} = \begin{bmatrix} y_{22}^{+}/\Delta^{+} & -y_{12}^{+}/\Delta^{+} \\ -y_{21}^{+}/\Delta^{+} & y_{11}^{+}/\Delta^{+} \end{bmatrix} \qquad (2.24)$$

where, $\Delta^{+} = y_{11}^{+}y_{22}^{+} - y_{12}^{+}y_{21}^{+}$

The harmonic components of the port voltages can be written in terms of the "z^{+}" parameters.

The n^{th}. harmonic components are:-

$$v_{eb}(n\omega_o) = -\left[z_{11}^{+} - \alpha_f z_{12}^{+} \right] i_e(n\omega_o) \qquad (2.25)$$

$$v_{cb}(n\omega_o) = \left[z_{21}^{+} - \alpha_f z_{22}^{+} \right] i_e(n\omega_o) \qquad (2.26)$$

From expression (2.25) we can obtain the ratio $|v_{eb}(n\omega_o)|/|v_{eb}(\omega_o)| = k\,|i_e(n\omega_o)/i_e(\omega_o)|$, where k is a property of the embedding network. Therefore the excitation voltage v_{eb} can be very close to a sinusoid if a proper embedding network is chosen.

STEP 3

In the design of transistor harmonic oscillators, one of the demands is to have almost sinusoidal port voltages. This requires the choice of an embedding network which possesses good filtering characteristic. Higher harmonic voltages will then be attenuated rapidly by the embedding network, whatever the harmonic content of the port currents might be. We require $|\Delta^{+}|$ to be a minimum at the frequency of the first harmonic and to have large values for frequencies over the rest of the frequency spectrum. The desired frequency characteristics of the quantities $\left[z_{11}^{+} - \alpha_f z_{12}^{+} \right]$ and $\left[z_{21}^{+} - \alpha_f z_{22} \right]$ are of the form shown in Fig. 2.16.

STEP 4

The physical mechanism behind the transistor oscillator (when based on Ebers Moll equations) has been discussed. For the case of the harmonic oscillator, v_{eb} and v_{cb} are nearly sinusoidal in waveforms. It is then valid to use the method of describing functions. In

Section 2.6.3 it is shown that the parameter y_{11} of the transistor is in fact a describing function. The rest of the two-port parameters are: $y_{21} = -\alpha_f y_{11}$; $y_{12} \simeq 0$; $y_{22} \simeq 0$. The addition of an embedding network to the transistor is to modify the circuit matrix. For steady state oscillation to occur, the modified circuit matrix is required to be singular. However to ensure subsequent oscillation, the conditions for instability of the initial state and stability of the steady state must also be satisfied.

2.7 Stability of Steady State Oscillation

The d.c. component of the emitter current, I_e is dependent on the amplitude of the a.c. excitation voltage v_{eb}. In the transient state, when the oscillatory current varies in amplitude, the d.c. component I_e must also vary accordingly. Thus in principle, the stability of oscillation in the transistor can be predicted by examining the set of dynamic equations governing the variation of the d.c. bias points. Consider the circuit shown in Fig. 2.17. The d.c. currents are:-

$$I_{eo} = \frac{E_{ee} - V_{ebo}}{R_1} \qquad (2.27a)$$

$$I_{co} = \frac{E_{cc} - V_{cbo}}{R_2} \qquad (2.28a)$$

The relationships for any incremental changes in I_{eo} and I_{co} are

$$\frac{dI_e}{dt} = -\frac{1}{R_1}\frac{dV_{eb}}{dt} - C_1\frac{d^2V_{eb}}{dt^2} - C_3\frac{d^2}{dt^2}(V_{eb} - V_{cb}) \qquad (2.29a)$$

$$\frac{dI_c}{dt} = -\frac{1}{R_2}\frac{dV_{cb}}{dt} - C_2\frac{d^2V_{cb}}{dt^2} + C_3\frac{d^2}{dt^2}(V_{eb} - V_{cb}) \qquad (2.29b)^{*}$$

One of the voltages can be eliminated from the set of equations givesn by (2.29a) and (2.29b). On doing so we obtain a fourth order differential equation in one of the voltage variables. This new equation involves the time differential of I_e. In Section 2.6.3. it has been shown that I_e can be expressed in terms of the modified Bessel function $I_o(x)$. However at large signal operation any change in amplitude of oscillation will also involve a change in frequency. This means that dI_e/dt has to be evaluated taking into consideration frequency variation as well:

$$\frac{dI_e}{dt} = \frac{\partial I_e}{\partial |v_{eb}|}\frac{d|v_{eb}|}{dt} + \frac{\partial I_e}{\partial \omega}\frac{d\omega}{dt} \qquad (2.30)$$

An accurate treatment of the problem is beyond reach for the present moment. Clarke[16] gave an approximate treatment of the problem. Sato[17] presented a brief correspondence along the same line. It is felt here that, this line of study will not lead to a useful design criterion. A different approach is taken in this thesis.

---

* The voltage drop across L_2 is assumed to be negligibly small.

Consider the condition of oscillation for the transistor oscillator. We obtain this by setting the circuit determinant to zero.

$$\Delta = \begin{vmatrix} y_{11} + y_{11}^{+} & y_{12}^{+} \\ -\alpha_f y_{11} + y_{21}^{+} & y_{22}^{+} \end{vmatrix} = 0 \qquad (2.31)$$

where, $-\alpha_f y_{11} = y_{21}$ and y_{12}, $-y_{22}$ are both negligible.
Let us represent the real and imaginary part of Δ by M and N respectively. Then condition (2.31) becomes

$$M + jN = 0 \qquad (2.32)$$

Just as we have borrowed the concept of immittance to give a physical meaning to the describing function of the transistor, we are now to borrow the idea of a limit cycle from phase plane analysis. Condition (2.32) can be interpreted as the algebraic form of a limit cycle, associated with the steady state oscillation $v_{eb} = |v_{eb}| \cos \omega_o t$. This oscillation can be written simply as $v_{eb} = |v_{eb}| \exp(j \omega_o t)$. To investigate its stability, it is necessary to consider the effect of small perturbations on the limit cycle. We do this by replacing $v_{eb} = a_o \exp(j \omega_o t)$ with a function of time differing slightly from it by Δ a in amplitude, $j \Delta \omega$ in frequency and which is slightly perturbed by the increment σ. Thus we find

$$v_{eb}(\text{disturbed}) = (a_o + \Delta a) \exp\, j(\omega_o + \Delta\omega + j\sigma)t$$

The incremental quantities "a", ω and σ must satisfy the condition,

$$M(\omega_o + \Delta\omega + j\sigma, a_o + \Delta a) + jN(\omega_o + \Delta\omega + j\sigma, a_o + \Delta a) = 0 \qquad (2.33)$$

If equation (2.33) is limited to the first term of its Taylor expansion and if the real and imaginary parts are separately equated to zero, we obtain

$$\frac{\partial M}{\partial a}\Delta a + \frac{\partial M}{\partial \omega}\Delta\omega - \frac{\partial N}{\partial \omega}\sigma = 0 \qquad (2.34)$$

$$\frac{\partial N}{\partial a}\Delta a + \frac{\partial N}{\partial \omega}\Delta\omega + \frac{\partial M}{\partial \omega}\sigma = 0 \qquad (2.35)$$

Whence by eliminating $\Delta\omega$, we obtain

$$\left[\left(\frac{\partial M}{\partial \omega}\right)^2 + \left(\frac{\partial N}{\partial \omega}\right)^2\right]\sigma = \left[\frac{\partial M}{\partial a}\frac{\partial N}{\partial \omega} - \frac{\partial M}{\partial \omega}\frac{\partial N}{\partial a}\right]\Delta a \qquad (2.36)$$

The condition for the limit cycle to be stable is that the disturbed function should *increase with time* ($\sigma > 0$) if its amplitude is smaller than a_o and *decrease with time* ($\sigma < 0$) if its amplitude is larger than a_o, i.e.

$$\frac{\partial M}{\partial a}\frac{\partial N}{\partial \omega} - \frac{\partial M}{\partial \omega}\frac{\partial N}{\partial a} > 0 \qquad (2.37)$$

The above condition for the stability of the steady state oscillation was obtained by Loeb in France and Popov in the Soviet Union. This condition can also be derived geometrically by extending the graphical methods of Nyquist and Mikhailov.

2.8 Soft Excitation - Unstable Focus Point

The oscillator designer is not only interested in synthesizing a stable limit cycle, he must ensure that soft excitation takes place in the circuit. It is known experimentally that the oscillograph of the "build-up" of oscillation is of the general form shown in Fig. 2.18. On examining this picture, we noticed that there are three stages through which the oscillation passes. Initially the transistor is operated essentially in a linear domain. In this first stage, oscillation grows exponentially. Once the critical amplitude a_c is reached (see Fig. 2.19), nonlinear action sets in and there will be a damping down of the amplitude growth. In this second stage, both the growth decrement and frequency change continuously until the final steady state is reached. A more detail discussion of the stability of the initial state is given in Section 4.14.

2.9 Conclusion for Chapter 2

The Ebers Moll equations were used to investigate the physical mechanism of self oscillation in low frequency transistor oscillators. This study has revealed some salient features of such oscillator systems. These are:-

(1) At normal biasing conditions, only y_{11_B} and y_{21_B} of the common-

base transistor parameters, have appreciable values. y_{12_B} and y_{22_B} are very small quantities.

(2) The controlling voltage of the nonlinear system is found to be v_{eb}.

(3) y_{11_B} and y_{21_B} are in fact the describing functions of the transistor.

(4) Provided a strong filter action exists in the system, we can use the large signal "y" parameters as design parameters.

The oscillator dealt with in Chapter 2 is an idealized model, and yet its analysis present many difficulties. It is a general feature of nonlinear system that there is no sure way of establishing a soft excited stable limit cycle. Andronov and Chaikin[18] compared it to a game of chess:-

> "The present status of the theory for establishing the existence of limit cycles can best be compared to the game of chess. There exists no theory by means of which a game can be won. There do exist, however alternatives which enable a skilled partner to win a game starting from a given configuration on the chess board".

In face of these difficulties, the circuit designer must take a new approach. The method of frequency analysis developed for nonlinear control systems, is found to be a suitable basis for a new design strategy. In this new approach, the transistor is characterized by its large signal "y" parameters.

2.10 References

1. E. Hafner, "Analysis and design of crystal oscillators", Technical Report, U.S. Army Electronics Laboratories, Fort Monmouth, New Jersey, May, 1964.
2. J. J. Ebers and J. L. Moll, "Large signal behaviour of junction transistors", Proc. IRE 42, pp.1761-1772, December, 1954.
3. M. I. Kontorovich et al., "Investigation of a transistor LC-oscillator", Radiotekhnika i Elektronika, 5, No. 3, pp.439-449, 1960.
4. A. N. Bazhan and L. N. Kaptsov, "A transistor oscillator with limiting in the saturation region", Radiotekhnika i Elektronika, 4, No. 9, pp.1549-1556, 1959.
5. L. N. Kaptsov, "Some special features of transistor oscillators", Radiotekhnika i Elektronika, 2, No. 9, pp.1127-1137, 1957.
6. van d. Pol, "The triode as a generator of oscillations", Radio Rev., Vol. 1, pp.701-754, 1920.
7. A. Andronov and A. Witt, Arch. für Elektrotech., 24, 1930.
8. N. B. Nichols et. al., "Theory of servomechanisms", MIT Radiation Laboratory Series, Vol. 21, pp. 117-124, McGraw-Hill Book Co., 1947.
9. L. Goldfarb, "A few nonlinear phenomena in regulating systems", Automatika i Telemekhanika, 8, No. 5, Sept.-Oct., 1947.
10. Lechtman, "Calculation of Relay Servomechanisms", Avtomatika i Telemekhanika, 12, No. 1, Jan.-Feb., 1951.
11. W. Oppelt, "Locus curves method for regulators with friction", J.IEE (London), Vol. 94, Pt.IIA, Nos. 1 and 2, May 1947.

12. J. R. Dutilh, "Theorie des servomecanismes non-lineaires", La Radio Francaise, May 1950.

13. J. Loeb, "Les servomechismes non-lineaires", L'Onde Electrique, Nov. 1952.

14. R. J. Kochenburger, "A frequency response method for analysing and synthesizing contactor servo-mechanisms", Trans. American IEE, 69, I, p.270, 1950.

15. P. Naslin, "The dynamics of linear and nonlinear systems", Blackie, 1965.

16. K. K. Clarke, "Transistor sine wave oscillators - squegging and collector saturation", IEEE Trans. on Ct. Th., CT-3, No. 4, December 1966.

17. T. Saito et. al., "Normalized equations for two-mode feedback oscillators", Proc. IEEE, pp. 730-732, May, 1967.

18. A. A. Andronov and S. E. Chaikin, "Theory of Oscillations", United Scientific and Technical Press, 1937.

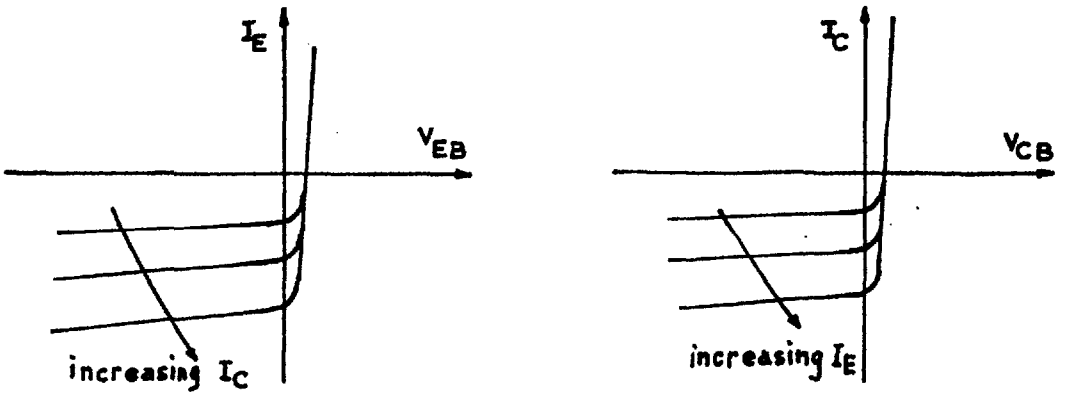

Fig. 2.1 General shape of Ebers Moll curves for the common-base configuration

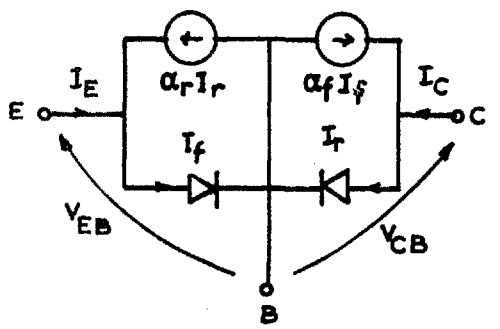

Fig. 2.2 Ebers Moll model of the transistor for the common-base configuration

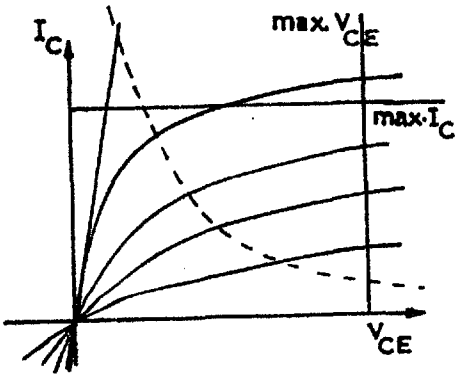

Fig. 2.3 Common-emitter characteristics showing regions of operation and maximum ratings

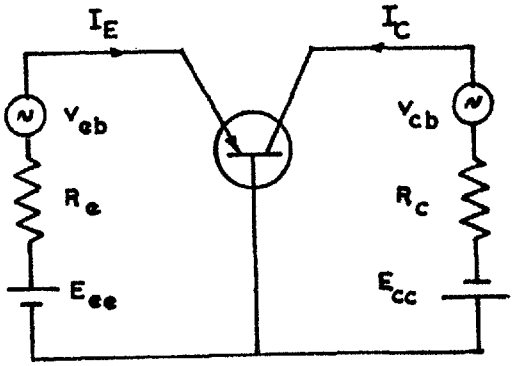

Fig. 2.4 D.C. bias of the transistor and large signal excitation by voltage v_{eb}

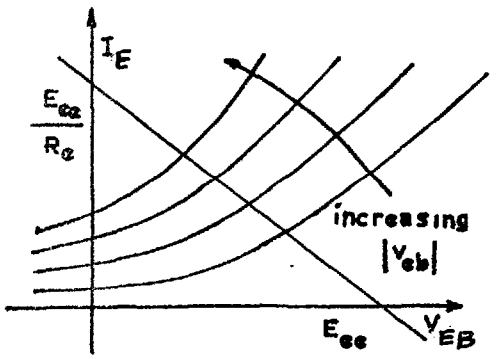

Fig. 2.5 Load line construction for determining I_e

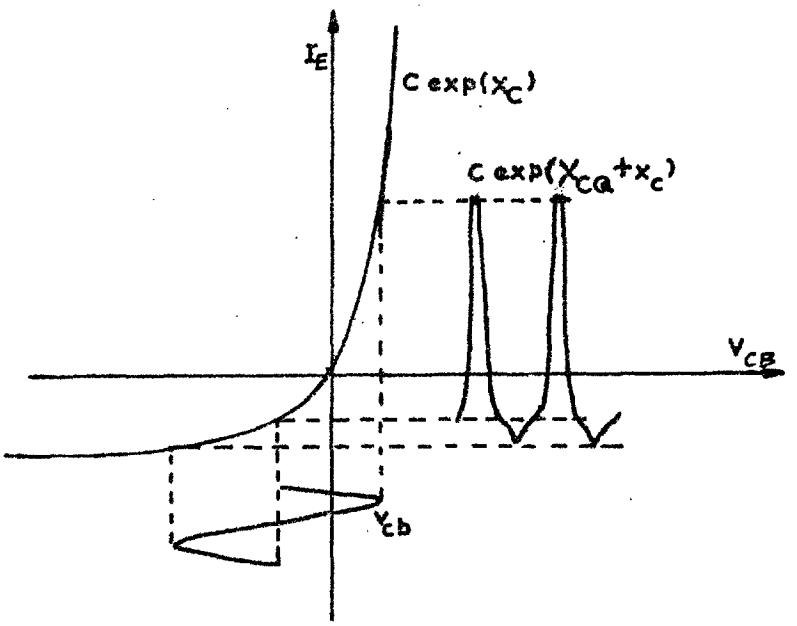

Fig. 2.6.a. The component of i_e due to v_{cb}

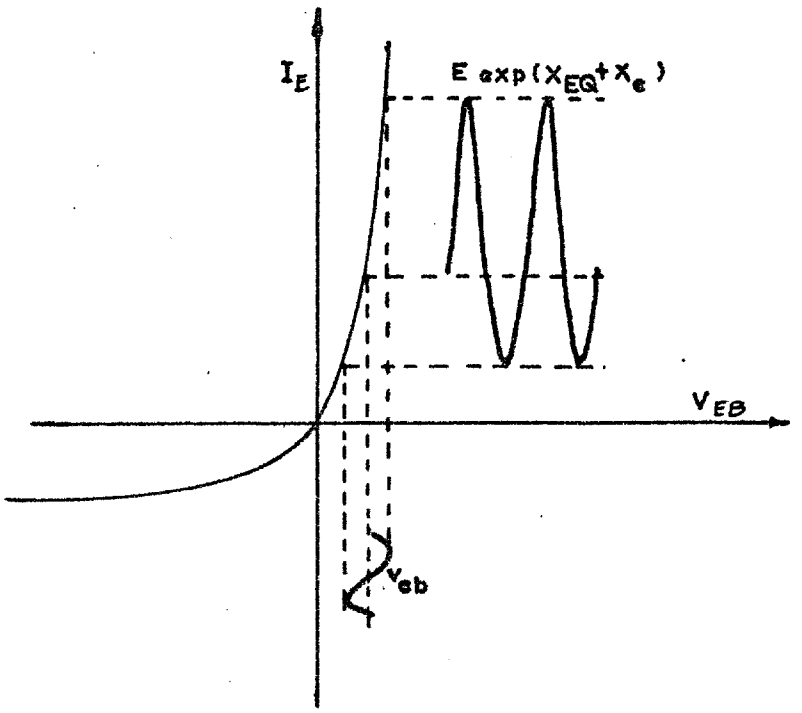

Fig. 2.6.b. The component of i_e due to v_{eb}

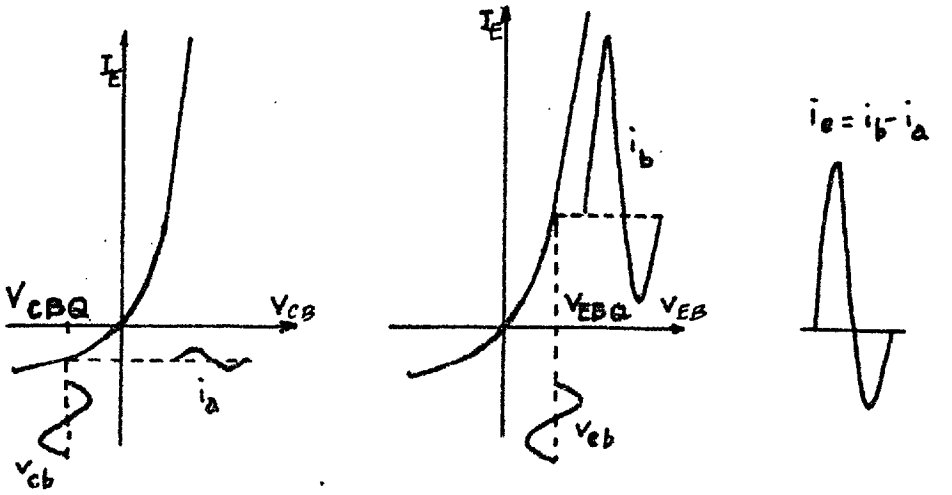

Fig. 2.7.a.

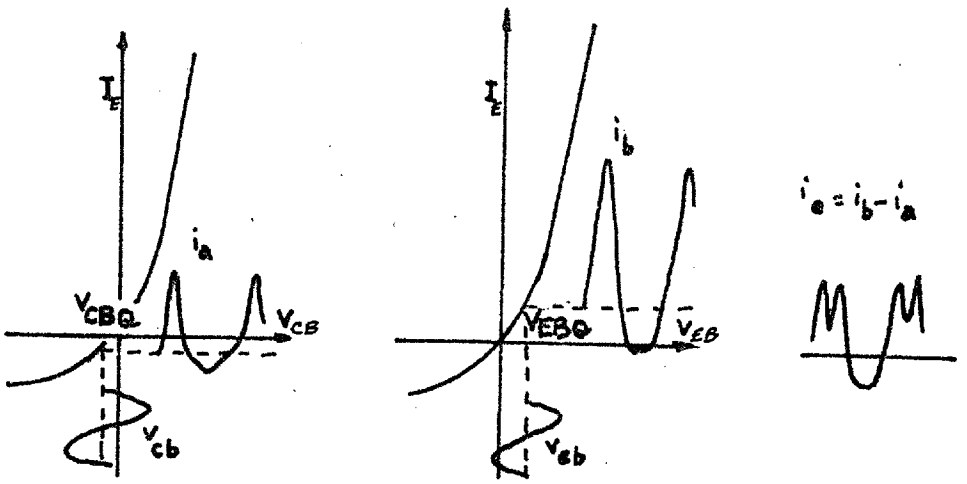

Fig. 2.7.b.

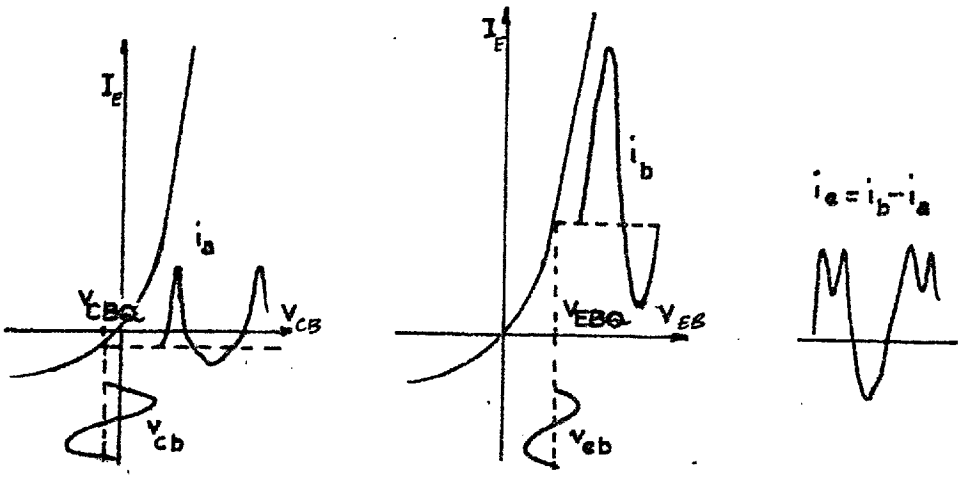

Fig. 2.7.c.

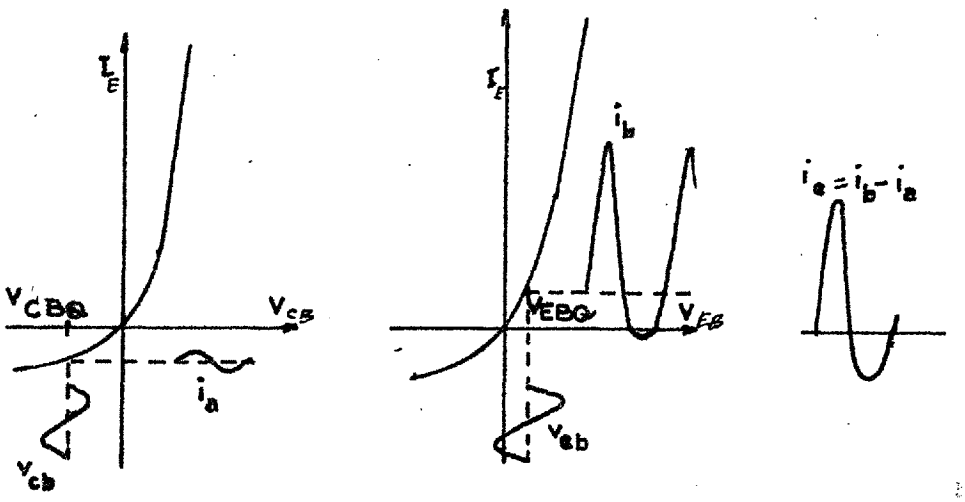

Fig. 2.7.d.

Fig. 2.7 The four distinctive types of current waveform for i_e

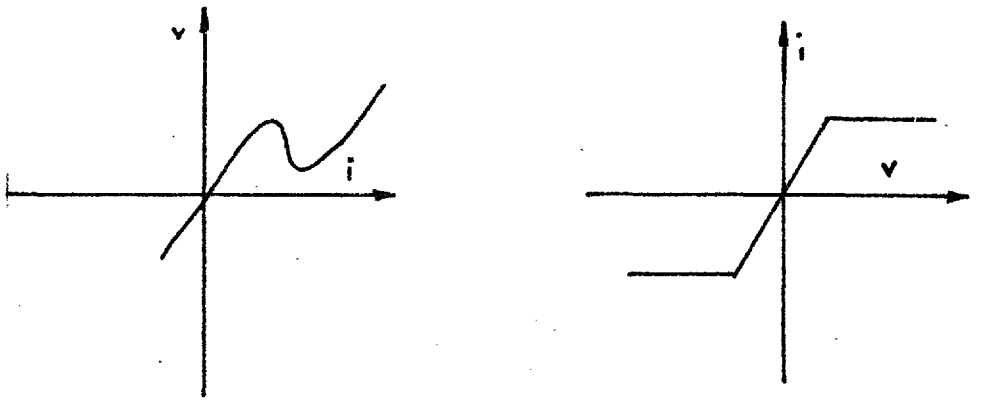

Fig. 2.8 (a) and (b)

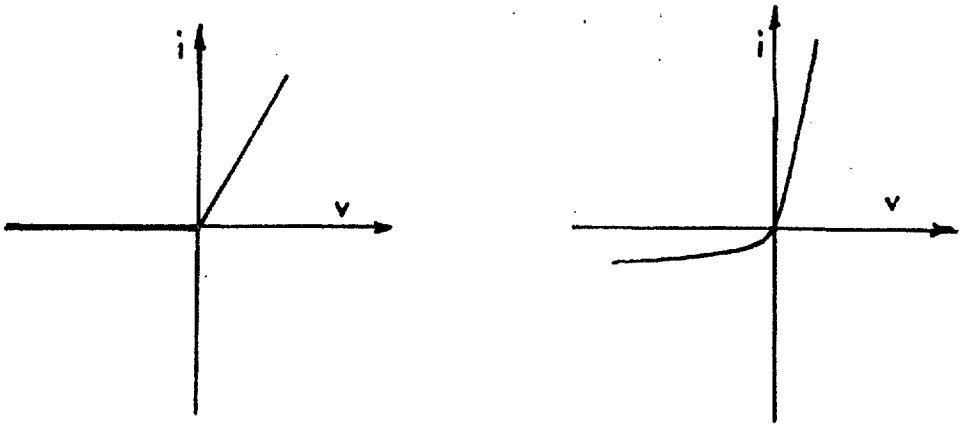

Fig. 2.8 (c) and (d)

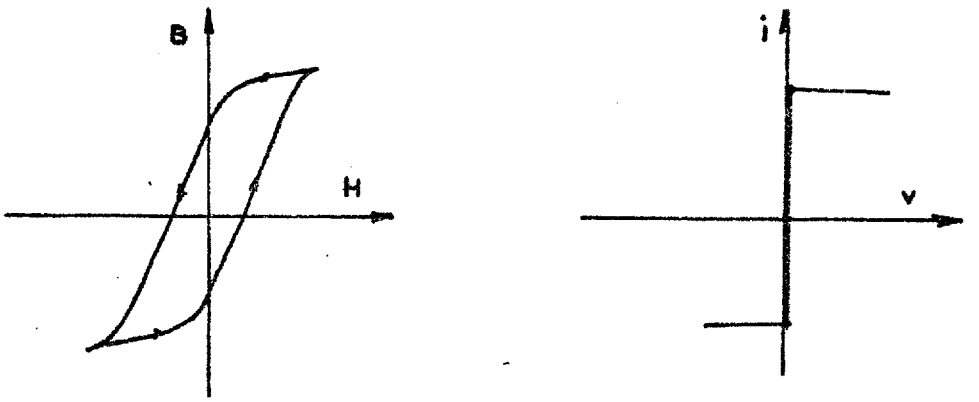

Fig. (e) and (f)

Fig. 2.8 Common types of nonlinearity

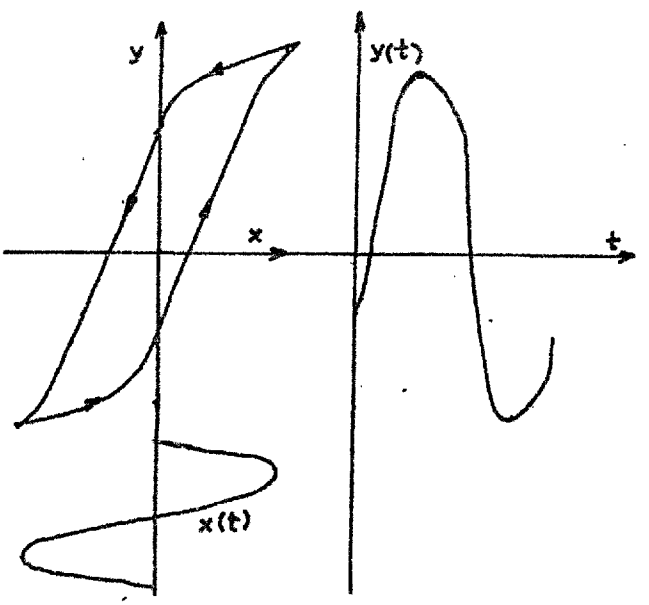

Fig. 2.9 Sinusoidal excitation of a nonlinearity

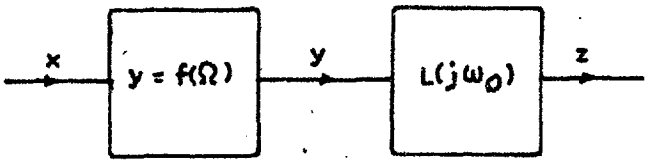

Fig. 2.10 A separable filtered nonlinear system

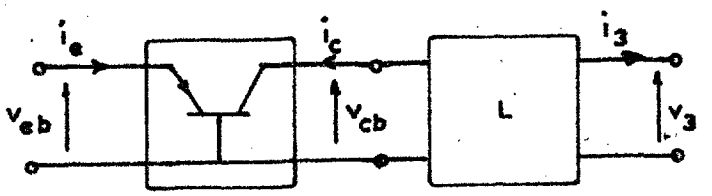

Fig. 2.11 Transistor cascaded with linear passive feedback network

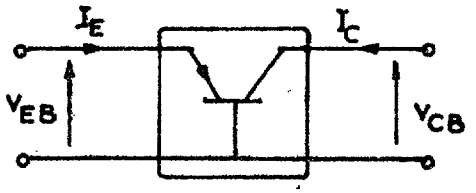

$$V_{EB} = V_{EBQ} + |v_{eb}| \cos(\omega_o t)$$
$$V_{CB} = V_{CBQ} + |v_{cb}| \cos(\omega_o t)$$

Fig. 2.12 The transistor driven by voltages V_{EB} and V_{CB} at the input and output ports

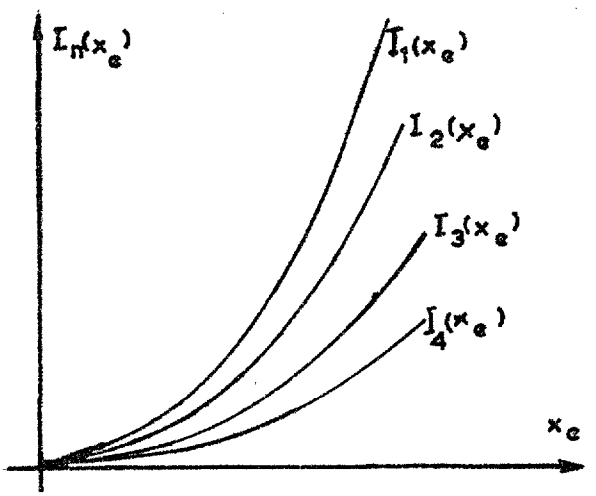

Fig. 2.13 The relative values of $I_n(x)$ for given values of x

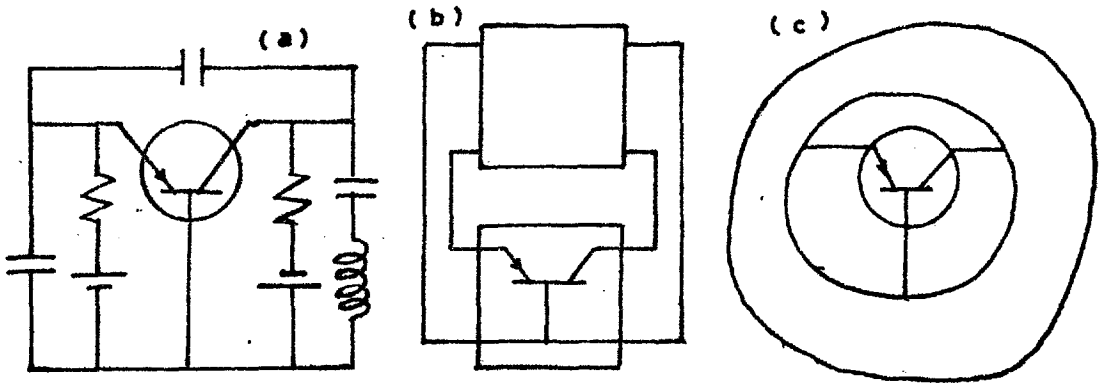

Fig. 2.14 A transistor embedded with external circuit elements to oscillate at a steady state. (a) a particular embedding (b) and (c) unspecified embeddings

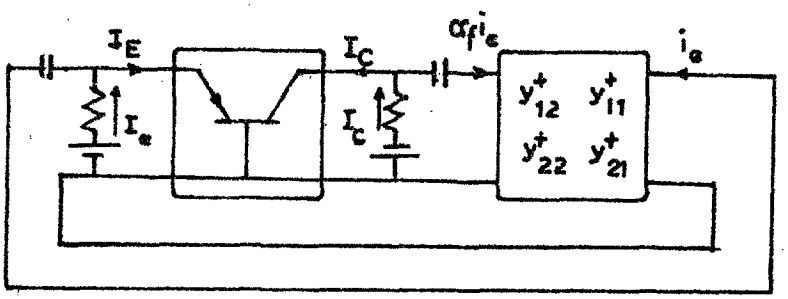

Fig. 2.15 The close-loop system representation of the transistor oscillator

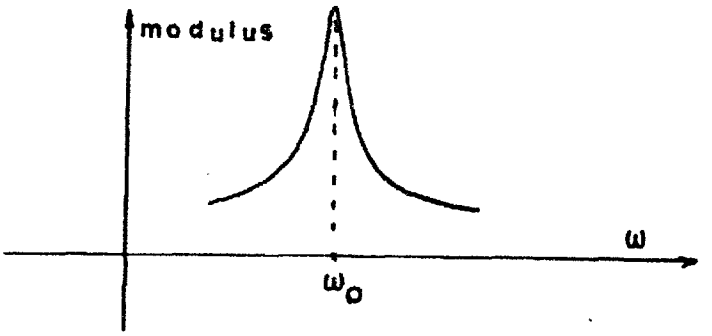

Fig. 2.16 Desired frequency characteristic of $z_{11}^{+} - \alpha_f z_{12}^{+}$ and $z_{21}^{+} - \alpha_f z_{22}^{+}$

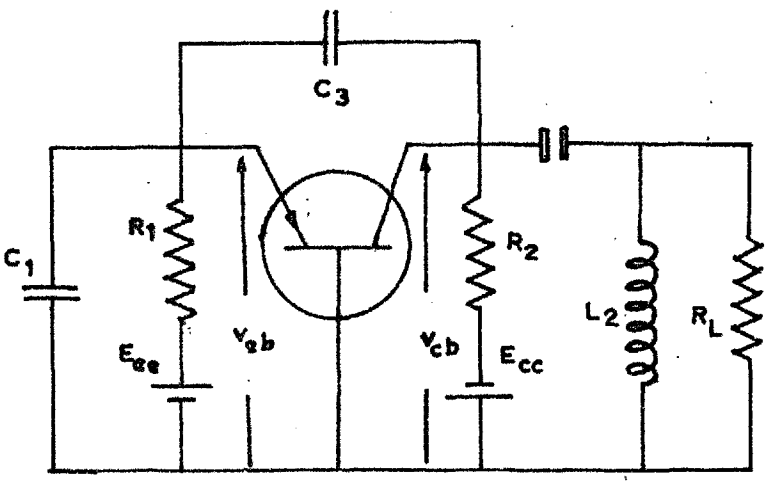

Fig. 2.17 A simple transistor oscillator circuit

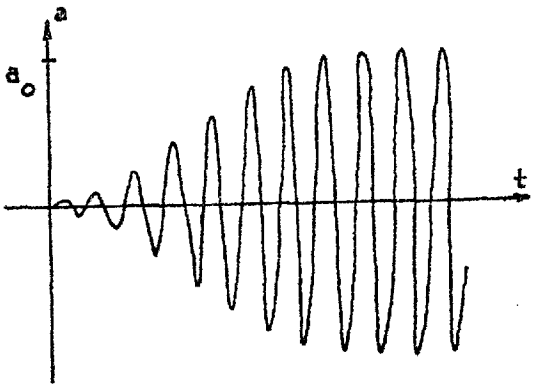

Fig. 2.18 The "build-up" of oscillation

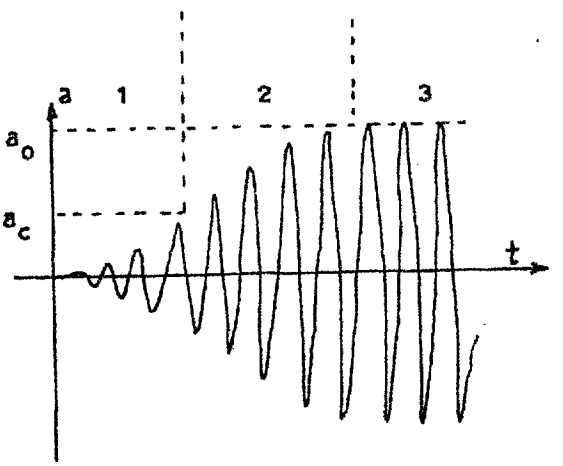

Fig. 2.19 The three stages of oscillation "build-up"

Chapter 3

Approximation Methods

3.1 Progress in the Study of Self Oscillation

In this section a survey of the available methods, which have been developed for the study of nonlinear systems and of self oscillation is presented. The object of such an exercise will be to relate the studies made in this thesis to the general development of the methods used for analysing and synthesizing nonlinear systems. By having an overall picture of the subject, the investigator can become more aware of both the limitations and the merits of his proposed approach, and thereby be more likely to steer his research in the correct direction.

The relationships between the different methods are given in Table 3.1. Poincare[1] is looked upon as a forerunner of modern nonlinear mechanics. He opened two major avenues of approach to the solution of problems of nonlinear mechanics.

(1) The topological methods of qualitative integration.

(2) The quantitative methods of approximations by expansion in terms of suitable parameters.

These methods were developed originally for the solution of problems in celestial mechanics. Barkhausen[2,3] was among the first scientists engaged in the study of oscillation in vacuum tube circuits. His doctorate thesis written on the above subject was published in 1907.

These problems drew the attention of van der Pol,[4,5,6] whose work has brought together the phenomena of harmonic oscillation, relaxation oscillation and the synchronization of oscillation under one common treatment. He invented the van der Pol equation, which has wide applications in the investigation of nonlinear systems. In their search for analytical methods to deal with nonlinear phenomena, Andronov and Witt[7,8] made use of the general theories worked out by Poincare and van der Pol. In their method, the oscillatory solution of van der Pol's equation is transformed into corresponding singular points and the criteria of Poincare are applied to study the stability of these points. The question of stability is an important aspect in nonlinear mechanics. The fundamental theorems connected with stability are due to Liapunov[9]. In nonlinear mechanics these theorems play a role similar to the Ruth-Hurwitz[10] theorem for linear systems. This direct nonlinear approach is limited to the study of certain systems. Its inability to cope with self oscillation is due to the absence of any developments leading to the establishment of topological concepts in the phase space. The phenomenon of self oscillation inevitably implies the existence of some stable limit cycles in phase space. Poincare was the originator of the concept of the limit cycle and he also invented the method called "Indices of Poincare" to infer indirectly the existence of limit cycles. A very useful graphical construction was invented by Lienard[11] for the study of phase trajectories associated with a nonlinear system. This is usually known as the method of isoclines. The trajectory representing

the solution to the nonlinear differential equation is constructed directly on the phase plane. If the trajectory eventually describes a closed path, then a limit cycle exists. If the limit cycle is stable, oscillatory solution will be realizable. The importance of the topological methods is that they provide a picture of the overall behaviour of the nonlinear system. However if one is only interested in nearly sinusoidal solutions, then the approximate methods of van der Pol and Krylov-Bogoluibov[12] will be more convenient. The method of equivalent linearization of Krylov-Bogoluibov led to the development of operational methods. These operational methods are commonly used in the study of self oscillations in nonlinear control systems. Popov[13] and Aizerman[14] are two important contributors to the study of self oscillation. Using the work of Krylov-Bogoluibov as a basis, they were able to build up a general theory of self oscillation. The works of the last four mentioned contributors are directly relevant to the study made in this thesis.

3.2 Popov's Classification of Nonlinear Systems

In the last Chapter, a simple resistive nonlinear system has been examined. This system is characterized by the set of equations

$$\begin{bmatrix} y_1 \\ y_2 \end{bmatrix} = \begin{bmatrix} f(x_1) & k_1 \\ k_3 f(x_1) & k_2 \end{bmatrix} \begin{bmatrix} x_1 \\ x_2 \end{bmatrix} \qquad (3.1)$$

where y_1 and y_2 are the current variables, x_1 and x_2 are the voltage variables and the "k"s are constants. The above system is the two-port equivalent of the relationship,

$$y_1 = f(x_1) \tag{3.2}$$

Unlike the electronic circuit designer, who is basically interested in the interrelation between the current and the voltage variables in a circuit, the control system engineer is interested in the relationships between output and input variables of a system. Frequently in the study of nonlinear control systems, it is possible to separate the nonlinear element such that the output variable x_2 is related to the input variable x_1 simply by

$$x_2 = F(x_1) \tag{3.3}$$

Expressions (3.2) and (3.3) are similar in form. There is a strong parallel between the problems found in transistor oscillator design and those arising from harmonic oscillations in nonlinear control systems. A close examination of the problems faced by the designer along the lines taken by control system engineers will be instructive. This may produce a correct approach to transistor oscillator design.

Many authors have suggested schemes for classifying nonlinear systems. Among these is Popov[13], who divided all nonlinear control systems and servomechanisms into three large classes:

(1) Nonlinear systems of the first class

The equation of the nonlinear element in these systems reduces to

any of the forms below,

$$x_2 = F(x_1) \tag{3.3}$$

$$F(\dot{x}_2, x_2) = c_1 x_1 \;, \quad F_1(\ddot{x}_2, x_2) + F_2(x_2) = c_1 x_1$$
$$x_2 = F(x_1, \dot{x}_1) \;, \quad x_2 = F_1(x_1) + F_2(\dot{x}_1) \tag{3.4}$$

In this class only the output variable (and its derivatives) or only the input variable (and its derivatives) enters into the nonlinear function. The block diagrams of such a class of system are shown in Fig. 3.1.

(2) Nonlinear systems of the second class

The second class of nonlinear systems includes such elements in which both the input and output variables enter into the nonlinear functional relationship. Examples of these relationships are:-

$$F_2(\dot{x}_2, x_2) = F_1(x) \;; \quad F_3(\dot{x}_2) + F_2(x_2) = F_1(x_1) \tag{3.5}$$

$$F(\dot{x}_2, x_2, x_1) = 0 \;; \quad F_2(x_2) + F_1(x_2, x_1) = 0 \tag{3.6}$$

The block diagrams of such systems will be of the forms shown in Fig. 3.1.

(3) Nonlinear systems of the third class

The third class systems are composed of two or more nonlinear elements separated from each other by linear parts. The block diagrams for these systems are shown in Fig.3.2.

We have seen in Chapter 2, that under normal biasing conditions, the common-base transistor parameters have the following features:

y_{12}; y_{22}

Complex quantities; very low value for both the real and imaginary parts; varies negligibly with changes in signal amplitudes and signal frequency.

y_{11}; y_{21}

Complex quantities; the values of the real and imaginary parts are much larger than those of y_{12} and y_{22}; values vary with the signal amplitude $|v_{eb}|$ and signal frequency.

These features are found to be preserved even at high frequency operation. Since y_{11} and y_{21} are functions of both signal amplitude and frequency, the simpler relationship (3.1) is no longer valid. The relationships of the system variables are:-

$$\begin{bmatrix} y_1 \\ y_2 \end{bmatrix} = \begin{bmatrix} f_1(x_1, \dot{x}_1) & k_1 \\ f_2(x_1, \dot{x}_1) & k_2 \end{bmatrix} \begin{bmatrix} x_1 \\ x_2 \end{bmatrix} \qquad (3.7)$$

A system of the form given by relationships (3.7) is classified as a first class second order nonlinear system under the Popov scheme. It is second order because there are two nonlinear elements and it is of the first class because they are controlled by the same variable. Equation (3.7) is the two-port equivalent of the two terminal case expressed by

$$x_2 = \left[f(x_1, \dot{x}_1) + k \right] x_1 \qquad (3.8)$$

The simplest system containing the element $f(x_1, \dot{x})$ and capable of producing harmonic oscillation will be a second order differential

equation of the form

$$\ddot{x} + F(x, \dot{x}) = 0 \tag{3.9}$$

Krylov and Bogoluibov established the method of "Equivalent Linearization", for solving second order nonlinear equations approximately. Most of the subsequent approximation methods developed for the study of nonlinear systems, including the design theory for harmonic oscillators proposed in this thesis derive their basis from the work of Krylov and Bogoluibov. Because of its wide application and because it is fundamental to other approximate methods in nonlinear theory. The method of "Equivalent Linearization" is reviewed below.

3.3 The Method of Equivalent Linearization

Krylov and Bogoluibov were interested in seeking a solution to equation (3.9) in the form of

$$x = a \sin (\omega_o t + \phi) \tag{3.10a}$$

$$\dot{x} = a\omega_o \cos (\omega_o t + \phi) \tag{3.10b}$$

where a and ϕ are slowly varying functions of time,

$$a = a(t) \; ; \quad \phi = \phi(t) \tag{3.11}$$

In order to solve equation (3.9), the nonlinear function $F(x,\dot{x})$ is written in the form

$$F(x, \dot{x}) = \omega_o^2 x + \mu f(x, \dot{x}) \tag{3.12}$$

Equation (3.9) becomes

$$\ddot{x} + \omega_o^2 x + \mu f(x, \dot{x}) = 0 \qquad (3.13)$$

For $\mu = 0$, equation (3.9) reduces to a simple equation whose solution is

$$x = a \sin(\omega_o t + \phi); \; \dot{x} = a\,\omega_o \cos(\omega_o t + \phi) \qquad (3.14)$$

For a quasi-linear equation when $\mu \neq 0$ but is small $\mu \ll 1$, it appears logical to retain the form of solutions (3.12), provided "a" and ϕ are considered to be slowly functions of time. Krylov and Bogoluibov have been able to find these functions. They take the form

$$\frac{da}{dt} = -\frac{1}{2\pi\omega_o} \int_0^{2\pi} F(a \sin u, a\,\omega_o \cos u)\cos u \, du \qquad (3.15)$$

$$\frac{d\phi}{dt} = -\omega_o + \frac{1}{2\pi\omega_o a} \int_0^{2\pi} F(a \sin u, a\,\omega_o \cos u)\sin u \, du \qquad (3.16)$$

where $u = \omega t + \phi$

Krylov and Bogoluibov then went on to introduce the method of equivalent linearization, whereby they showed that equation (3.13) can be linearized to the form

$$\ddot{x} + \omega_o^2 x = -\left[\frac{\mu}{\pi a} \int_0^{2\pi} f(x,\dot{x})\sin u \, du\right] x -$$

$$-\frac{1}{\omega_o}\left[\frac{\mu}{\pi a} \int_0^{2\pi} f(x,\dot{x})\cos u \, du\right] \dot{x} + O(\mu^2) \qquad (3.17)$$

Comparing equation (3.17) to equation (3.13) one sees that the nonlinear function $\mu f(x,\dot{x})$ has been linearized to the form

$$\mu f(x,\dot{x}) = q\,x + (q_1/\omega_o)\dot{x} \tag{3.18}$$

where,

$$q = \frac{\mu}{\pi a}\int_0^{2\pi} f(x,\dot{x})\sin u\,du \tag{3.19}$$

$$q_1 = \frac{\mu}{\pi a}\int_0^{2\pi} f(x,\dot{x})\cos u\,du \tag{3.20}$$

Owing to the presence of the residue $O(\mu^2)$, relationship (3.18) is satisfied up to an order of accuracy μ^2. The interested reader should refer to references 12 and 13.

3.4 Popov's Generalization of the Method of Equivalent Linearization to the Frequency Analysis of Nonlinear Systems

Krylov and Bogoluibov have established relationship (3.18) by analytical methods and have pointed out that even for more complicated higher order systems, the method of equivalent linearization can be effective. Popov has followed this recommendation and went on to formulate the very powerful method of harmonic linearization. Popov was more interested in substituting the nonlinearity in a system with a linearized expression. He pointed out that the nonlinear function $\mu(x, \dot{x})$ can be linearized directly without referring to the method of

averaging used by Krylov and Bogoluibov.

Let there be given some nonlinear function

$$x_2 = F(x, \dot{x}) \tag{3.21}$$

where, $x = a \sin(\omega_o t + \phi)$

then expression (3.21) becomes

$$x_2 = F(a \sin u, a\,\omega_o \cos u) \tag{3.22}$$

where, $u = \omega_o t + \phi$

Expanding the right hand side of the relationship (3.22), we obtain

$$x_2 = \frac{1}{2\pi}\int_0^{2\pi} F(x, \dot{x})\, du + \left[\frac{1}{\pi}\int_0^{2\pi} F(x, \dot{x}) \sin u\, du\right] \sin \omega t + \left[\frac{1}{\pi}\int_0^{2\pi} F(x, \dot{x}) \cos u\, du\right] \cos \omega t + \text{higher harmonics} \tag{3.23}$$

The first integral in this expansion is a constant (d.c.) quantity. If the higher harmonics and the d.c. term are neglected and if the relationships

$$\sin(\omega_o t + \phi) = x/a\ ; \quad \cos(\omega_o t + \phi) = \dot{x}/a\,\omega_o$$

are used, then expression (3.23) may be rewritten as

$$x_2 = q(a, \omega_o) + \left[q_1(a, \omega_o)/\omega_o\right] \dot{x}$$

where q and q_1 are quantities identical to those derived by Krylov and Bogoluibov.

Consider the simple system shown in Fig. 3.3. The transfer junction of the linear part is $W(p) = R(p)/S(p)$. We have the relationship

$$x = y - WF \tag{3.24}$$

At the onset of self oscillation, $y = 0$ and consequently $x = -z$. Equation (3.24) becomes

$$S(p)x + R(p)\,F(x, \dot{x}) = 0 \tag{3.25}$$

If the linear part filters out the higher harmonics present in the function F, then the solution to a first approximation is

$$x = a \sin u \quad ; \quad u = \omega_o t \tag{3.26}$$

If in addition no constant component is present,

$$\int_0^{2\pi} F(a \sin u,\ a\,\omega_o \cos u)\,du = 0 \tag{3.27}$$

then the condition for self-oscillation by the method of harmonic linearization is

$$\Delta = S(p) + R(p)\left[q + \frac{q_1}{\omega_o}\,p\right] = 0 \tag{3.28}$$

where, q and q_1 are given by expressions (3.19) and (3.20) respectively. For steady state operation $p = j\omega_o$. On separating the real and

imaginary parts of Δ, we obtain

$$\begin{aligned} \text{Re}\ \Delta\,(q, q_1, \omega_o) &= 0 \\ \text{Im}\ \Delta\,(q, q_1, \omega_o) &= 0 \end{aligned} \qquad (3.29)$$

The relationships (3.29) determine the amplitude "a" and the frequency ω of the periodic solution in terms of the coefficients of the characteristic equation, and therefore in terms of the parameters of the system considered. Thus it is possible to construct graphs of relationships a(k) and ω(k), where k is any one of the parameters of the system. From these graphs one may select the parameters of the system (or the range of possible parameters) which will give the required values of amplitude "a" and frequency ω of the self oscillation.

Any self oscillation observed in a system is in fact the stable periodic solution of the mathematical equations describing the system. If two or more periodic solutions are obtained (or one, without there being any assurance that the system will sustain stable oscillation), then it will be necessary to determine the stability of the periodic solution, using some stability criterion, e.g.

$$(\partial M/\partial a)\,(\partial N/\partial \omega) - (\partial M/\partial \omega)\,(\partial N/\partial a) > 0$$

This criterion was discussed in Section 2.7.

For systems with asymmetrical nonlinearity, there exists a slowly changing mean signal besides the self-oscillation. Consider the system shown in Fig. 3.3. The condition for self-oscillation

becomes

$$\left.\begin{aligned} S(p)x &= -R(p)\, F(x, \dot{x}) \\ x &= y - z \end{aligned}\right\} \qquad (3.30)$$

The variables x and z now have d.c. components x_c and z_c, upon which there will be superimposed the oscillations,

$$x = x_c + a \sin \omega_o t \quad ; \quad z = z_c + a_z \sin (\omega_o t + \phi) \qquad (3.31)$$

The harmonic linearization for asymmetric nonlinearity is

$$q = \frac{1}{\pi a} \int_0^{2\pi} F(x_c + a \sin \Omega,\ a\, \omega_o \cos \Omega) \sin \Omega \, d\Omega \qquad (3.32a)$$

$$q_1 = \frac{1}{\pi a} \int_0^{2\pi} F(x_c + a \sin \Omega,\ a\, \omega_o \cos \Omega) \cos \Omega \, d\Omega \qquad (3.32b)$$

$$F_c = \frac{1}{2\pi} \int_0^{2\pi} F(x_c + a \sin \Omega,\ a\, \omega_o \cos \Omega) \, d\Omega \qquad (3.32c)$$

where $\Omega = \omega_o t$.

The nonlinear function can be replaced by the expression

$$F(x, \dot{x}) = F_c + \left[q\, x_\pi + (q_1/\omega_o) x_\pi \right] \qquad (3.33)$$

where,

$$x_\pi = a \sin (\omega_o t) \quad ; \quad z_\pi = a_z \sin (\omega_o t + \phi)$$

Substituting expression (3.33) into relationships (3.30), we get

$$\left.\begin{aligned} S(p)\,x &= -R(p)\left\{ F_c + \left[q\,x_\pi + (q_1/\omega_o)x_\pi \right] \right\} \\ x_c + x_\pi &= -z_c - z_\pi \end{aligned}\right\} \qquad (3.34)$$

These may be separated into equations for the periodic components due to self oscillation,

$$\left.\begin{aligned} S(p)\,z_\pi &= R(p)\left[q\,x_\pi + (q_1/\omega_o)x_\pi \right] \\ x_\pi &= -z_\pi \end{aligned}\right\} \qquad (3.35)$$

and equations for the slowly changing mean components,

$$\left.\begin{aligned} S(p)\,z_c &= R(p)\,F_c \\ x_c &= -z_c \end{aligned}\right\} \qquad (3.36)$$

From conditions (3.35) we obtain the characteristic equation for determining the periodic solution as,

$$\Delta = S(p) + R(p)\left[q + (q_1/\omega_o)p \right] = 0 \qquad (3.37)$$

This equation is similar to the one obtained for a system with symmetrical nonlinearity (see equation (3.28)). The nonlinearities in the transistor are known to be asymmetrical junctions. The mechanism of self-oscillation in the transistor oscillator will therefore be similar to that expressed by the conditions (3.35) and (3.36).

The harmonic linearization of a nonlinear function is a general method of obtaining the describing function for more complex nonlinear systems. In this sense the discussions in Chapter 2 can be embraced into Popov's work. Minorsky[15] regards Popov's work as a large scale

attempt to codify the known facts of nonlinear systems with a view to form a comprehensive theory, intended for the analysis and synthesis of nonlinear control systems. However, codification of facts is one thing, implementation of the comprehensive theory is quite another. The nonlinearity present in the complete characterization of the transistor is far too complex to be written down as an explicit function of current and voltage variables. Inevitably one is led to the conclusion that in principle a satisfactory design theory for the transistor oscillator is possible, just as Popov and Paltov[16] have managed to formulate a comprehensive theory for describing self oscillation in control systems. However the elusive nature of the nonlinearity in the transistor oscillator has forced the investigator to look for a departure from established methods. The main requirement from such a departure is that neither the shape nor the explicit function of the nonlinearity is necessary in formulating the design procedure. At this point the investigator has to fall back on his intuition and to re-examine what the essentials for the design basis really are. It is desirable to leave out bits of information which when present, cloud the whole picture and yet can be neglected without jeopardizing the physical mechanism, responsible for the phenomenon of self oscillation. In this connection, the work of Aizerman is extremely relevant. His heuristic treatment of self oscillation provides a surprising depth of insight into the nature of quasi-linear oscillations.

3.5 The Filter Hypothesis of Aizerman

Nonlinear systems often appear in the form,

$$z_1 = \sum_{j=1}^{n} a_{ij}x_j + f(x_k, \dot{x}_k) \tag{3.38a}$$

$$z_i = \sum_{j=1}^{n} a_{ij}x_j \tag{3.38b}$$

when the nonlinearity appears only in one equation of the system. Setting $y = f(x_k, \dot{x}_k)$, and assuming that this is a well behaved (i.e. continuous with a certain number of derivatives) nonlinear function, one can eliminate all variables in equations (3.38a); (3.38b) except y and $x = x_k$. Consequently one obtains,

$$(k_o p^n + k_1 p^{n-1} + \ldots k_n)x = (d_o p^m + d_1 p^{m-1} \ldots + d_m)y \tag{3.39}$$

where $p = \frac{d}{dt}$

The transfer function of the system is,

$$W(p) = K(p)/D(p) \tag{3.40}$$

where,

$$D(p) = d_o p^m + d_1 p^{m-1} + \ldots + d_m$$

$$K(p) = k_o p^n + k_1 p^{n-1} + \ldots + k_n$$

After applying harmonic linearization on y, we obtain

$$W(p) = K(p)/S(p) \tag{3.41}$$

where,

$$S(p) = s_o p^{n+1} + s_1 p^n + \ldots + s_{n+1}$$
$$K(p) = k_o p^m + k_1 p^{m+1} + \ldots + k_m$$

The characteristic amplitude $A = K(j\omega)/S(j\omega)$, where p has been replaced by $j\omega$, permits determination of the ratio in which the various harmonics are present at the input and output of the nonlinearity.

According to Aizerman[14], there are two ways in which quasi-harmonic self-oscillations can occur in such systems:

(1) The linear part of the system may exhibit the property of a filter. Harmonics other than the required frequency of oscillation are suppressed.

(2) The form of oscillation (both at the input and output of the nonlinearity) does not differ much from the sinusoidal waveform.

Aizerman distinguishes the two cases, calling the systems satisfying the first case "filtered systems" and those satisfying the second case "auto-resonance systems". He maintains that these two hypothesis have different physical significance:

(1) The idea of the filter is in fact the method of harmonic balance of Krylov and Bogoluibov, which replaces the Fourier spectrum by the fundamental component. The justification for this is that work done by the higher harmonics during the period of the fundamental is always

zero. The existence of the filter properties will substantiate the justification of Krylov and Bogoluibov's method.

(2) In the method of "auto-resonance", the solution is sought in the form $x = a \sin \left[(\omega + \delta\omega)t \right]$; where "a" and $\delta\omega$ are the quantities to be determined. The methods of Poincare and van der Pol belong to this latter approach.

Aizerman stressed the difference between the concepts of the "filtered system" and that of the "auto resonance" system. He insisted on the point that in control systems, one has nearly always conditions for a "filter" action and very seldom those of an "auto-resonance" action. It should be pointed out that in transistor oscillator circuits, the passive embedding network acts precisely like the "filter" discussed in Aizerman's hypothesis.

3.6 A Short Summary of Discussions in Previous Sections

In Chapter 2, the nature of the transistor oscillator has been discussed. The low frequency Ebers Moll model was used because, under high signal level and high frequency operation conditions, the problem of transistor modelling is still unsatisfactory. It cannot be emphasised too strongly that the high frequency transistor oscillator is a complicated nonlinear system. With the available analytical

techniques it is not possible to give a complete solution to the behaviour of the system. The previous sections in this Chapter have however given indication that approximation methods can be used beneficially. On the other hand the designer should be aware of the limitations imposed on such methods. He must also be sure that, all the relevant factors governing the behaviour of the system, are taken into consideration in the approximation method. Finally he should recognize that his interest is in the steady state solution of the set of nonlinear differential equations describing his system. A subsequent study of the structure of this steady state solution as a function of various constant parameters of the system will reveal the behaviour of the oscillator under different environmental influences. Having established the nature of the transistor oscillator and reviewed the available techniques for nonlinear system analysis, it is now possible to dwell properly *on* the new approach to harmonic oscillator design, proposed in this thesis.

3.7 The Mathematical Interpretation of Large Signal Transistor "Y" Parameters

In earlier sections, it has been shown that after harmonic linearization, the transistor can be characterized by a two-port admittance matrix. If the Ebers Moll equations are employed as the

physical model, then the common-base two-port equations will be of the form,

$$\begin{bmatrix} i_e \\ i_e \end{bmatrix} = \begin{bmatrix} y_{11B}(a,\omega) & y_{12B}(\omega) \\ y_{21B}(a,\omega) & y_{22B}(\omega) \end{bmatrix} \begin{bmatrix} v_e \\ v_c \end{bmatrix} \qquad (3.42)$$

where y_{11B} and y_{21B} are the describing functions discussed in Chapter two.

The matrix elements y_{12B} and y_{22B} are small quantities and they vary negligibly with signal level. At high frequencies, the matrix elements are no longer real quantities but complex. Measurements have shown that y_{12B} and y_{22B} vary little with changes in frequency and signal level. On the other hand y_{11B} and y_{21B} vary appreciably with both frequency and signal level.

The measurement of transistor "y" parameters is normally carried out at small signal levels. Since the proposed procedure is based on these "y" parameters, it will be desirable to examine their derivation a little closer. It has been shown that starting from the Ebers Moll equations, one can go through the process of harmonic linearization and obtain algebraic relationships between the two-port variables. The "y" parameters so obtained, vary with signal levels. Over a limited region at small signal level, these parameters remain constant. These are the small signal parameters of the transistor. This region of operation is essentially linear.

The relationships between the two-port variables can be derived in a more general manner. Consider the two-port shown in Fig. 3.4.

Each of the current variables can be written as general functions of the other three remaining variables.

$$i_I = F(I_1, v_I, v_{II}) \tag{3.42a}$$

$$i_{II} = G(I_{II}, v_I, v_{II}) \tag{3.42b}$$

In principle it is always possible to substitute (3.42b) into (3.42a) and thus eliminate I_{II}; or vice versa for the elimination of I_1 from the functional relationships. This means that, it is only necessary to consider the simplified relationships.

$$I_I = f(v_I, v_{II}); \quad I_{II} = g(v_I, v_{II}) \tag{3.43}$$

It should be pointed out that v_I and v_{II} may have constant components.

$$v_I = V_1 + v_1(t) \; ; \quad v_{II} = V_2 + v_2(t) \tag{3.44}$$

V_1 and V_2 are the constant components and $v_1(t)$; $v_2(t)$ are assumed to be the small excitation signals. The constant terms V_1 and V_2 define an operation point given by

$$I_1 = f(V_1, V_2) \; ; \quad I_2 = g(V_1, V_2) \tag{3.45}$$

as shown in Fig. 3.5. The small signal swings about this operation point will produce excursions in i_I and i_{II} about their corresponding operation points. The magnitude of these swings can be estimated by assuming that the actual surfaces "f" and "g" can be adequately represented by their tangent planes at the points $I_1 = f(V_1, V_2)$ and $I_2 = g(V_1, V_2)$ respectively. This is the case of the small signal approximation.

The mathematical expressions of these geometrical ideas are contained in the Taylor's expansion of a function of two variables.

$$i_I = f(V_1,V_2) + \left[\frac{\partial f}{\partial v_I}\Big|_{V_1,V_2}\right](v_I - V_1) + \left[\frac{\partial f}{\partial v_{II}}\Big|_{V_2,V_1}\right](v_{II} - V_2)$$

$$\text{higher order terms} \qquad (3.46a)$$

$$i_{II} = g(V_1,V_2) + \left[\frac{\partial g}{\partial v_I}\Big|_{V_1,V_2}\right](v_I - V_1) + \left[\frac{\partial g}{\partial v_{II}}\Big|_{V_2,V_1}\right](v_{II} - V_2)$$

$$\text{higher order terms} \qquad (3.46b)$$

If operation is confined to low signal levels, the higher order terms can be neglected. Separating the constant and time varying terms of equation (3.46) we get,

$$i_I = I_1 + i_1(t) \quad ; \quad i_{II} = I_2 + i_2(t) \qquad (3.47)$$

$$I_1 = f(V_1,V_2) \quad ; \quad I_2 = g(V_1,V_2) \qquad (3.48)$$

and also,

$$i_1(t) = \left[\frac{\partial f}{\partial v_I}\Big|_{V_1,V_2}\right] v_1(t) + \left[\frac{\partial f}{\partial v_{II}}\Big|_{V_2,V_1}\right] v_2(t) \qquad (3.49a)$$

$$i_2(t) = \left[\frac{\partial g}{\partial v_I}\Big|_{V_1,V_2}\right] v_1(t) + \left[\frac{\partial g}{\partial v_{II}}\Big|_{V_2,V_1}\right] v_2(t) \qquad (3.49b)$$

The derivatives of f and g with respect to voltage have the dimensions of admittance. We can now define a set of admittance or "y" para-

meters by the relationships,

$$y_{11} = \left.\frac{\partial f}{\partial v_I}\right|_{V_1,V_2} \qquad y_{12} = \left.\frac{\partial f}{\partial v_{II}}\right|_{V_2,V_1}$$

$$y_{21} = \left.\frac{\partial g}{\partial v_I}\right|_{V_1,V_2} \qquad y_{22} = \left.\frac{\partial g}{\partial v_{II}}\right|_{V_2,V_1}$$

Equation (3.49) can be written in the matrix form,

$$\begin{bmatrix} i_1 \\ i_2 \end{bmatrix} = \begin{bmatrix} y_{11} & y_{12} \\ y_{21} & y_{22} \end{bmatrix} \begin{bmatrix} v_1 \\ v_2 \end{bmatrix}$$

The geometrical representation of Fig. 3.5 describes a system with resistive nonlinearity. It has been shown that under normal bias conditions, the nonlinear action appears across the base-emitter junction. Therefore the controlling variable of the nonlinear device is $V_I = V_{eb}$. It has also been pointed out that because of the reverse biasing of the base-collector junction, the values of y_{12B} and y_{22B} are very small.

In practice, one has to take the high frequency effect of the transistor into account. In order to do this, it is necessary to examine the device characterization a little closer. Let it be assumed that the excitation signal be merely periodic and not necessary sinusoidal. The "high frequency effect" can be taken into account by including the time derivatives of the excitation variables into the functional relationships. The relationships (3.42) are now

generalized to

$$i_I = F(v_I, \dot{v}_I, \ddot{v}_I \ \ldots\ , v_{II}, \dot{v}_{II}, \ddot{v}_{II} \ \ldots\ )$$

$$i_{II} = G(v_I, \dot{v}_I, \ddot{v}_I \ \ldots\ , v_{II}, \dot{v}_{II}, \ddot{v}_{II} \ \ldots\ ) \qquad (3.50)$$

The quantities i_I and i_{II} can be treated as hyper-surfaces in n-dimension space. The number "n" depends on the number of derivatives involved in the relationships. Under linear operation conditions (small signal levels), the Superposition Principle can be used. Employing Fourier Analysis techniques, the excitation waveforms can be broken up into their harmonic components and the action of individual component on the device can be treated independently. Therefore it is only necessary to consider the general sinusoidal excitations, $v_I = V_1 + |v_1| \exp(j\omega t)$ and $v_{II} = V_2 + |v_2| \exp(j\omega t + \theta)$. In the Ebers Moll equations there are no interaction between the two voltage variables. For general purposes, it is assumed that any interaction between the part variables are negligibly small. This assumption is supported by experimental evidence and makes it possible to represent the transistor by a two-port. On this assumption relationships (3.50) can be rewritten as,

$$i_I = F_1(v_I, \dot{v}_I, \ddot{v}_I \ \ldots\ ) + F_2(v_{II}, \dot{v}_{II}, \ddot{v}_{II} \ \ldots)$$

$$i_{II} = G_1(v_I, \dot{v}_I, \ddot{v}_I \ \ldots\ ) + G_2(v_{II}, \dot{v}_{II}, \ddot{v}_{II} \ \ldots) \qquad (3.51)$$

The functions F_1, F_2, G_1 and G_2 can now be treated separately. It is noticed that $d^n v_I/dt^n = |v_1|(j\omega)^n \exp(j\omega t)$ and

$d^n v_{II}/dt^n = |v_2|(j\omega)^n \exp(j\omega t + \theta)$. This being the case, it will be sufficient to have V_1, V_2, $|v_1|$, $|v_2|$ and ω as the functional variables. The port-currents and port-voltages are related through these functional variables,

$$\begin{aligned} i_I &= F_1(V_1, |v_1|, \omega) + F_2(V_2, |v_2|, \omega) \\ i_{II} &= G_1(V_1, |v_1|, \omega) + G_2(V_2, |v_2|, \omega) \end{aligned} \tag{3.52}$$

For the linear case, relationships (3.52) can be rewritten as

$$\begin{aligned} i_I &= y_{11}(V_1,\omega)v_1 + y_{12}(V_2,\omega)v_2 + f(V_1,V_2) \\ i_{II} &= y_{21}(V_1,\omega)v_1 + y_{22}(V_2,\omega)v_2 + g(V_1,V_2) \end{aligned} \tag{3.53}$$

where $f(V_1,V_2)$ and $g(V_1,V_2)$ are the d.c. components.

For a particular nonlinear case, relationships (3.52) can be rewritten as

$$\begin{aligned} i_I &= y_{11}(V_1, |v_1|,\omega)v_1 + y_{12}(V_2,\omega)v_2 + f(V_1,V_2, |v_1|) \\ i_{II} &= y_{21}(V_1, |v_1|,\omega)v_1 + y_{22}(V_2,\omega)v_2 + g(V_1,V_2, |v_1|) \end{aligned} \tag{3.54}$$

It should be pointed out that the system represented by relationships (3.54) belongs to Popov's first class and second order. The controlling voltage is v_1. Under normal d.c. bias conditions, the transistor can be represented by such a system.

3.8 Filter Action of the External Embedding Network

It has already been shown that the port currents of the transistor are nonlinear functions of the excitation voltages. For harmonic oscillators, the port voltages are required to be nearly sinusoidal. The requirement of maintaining sinusoidal voltages at the ports of the embedding network in the presence of non-sinusoidal port currents, sets certain constraints on the embedding. There are some embedding networks which will keep port voltages more sinusoidal than others. What then are the features that characterize these preferred embedding networks? In order to answer this question, it is necessary to refer to Fig. 3.6(b). The two-port equations for the embedding network shown in the figure are:-

$$i_I = I_1 + y_{11}^{+} v_1 + y_{12}^{+} v_2 \qquad (3.55a)$$

$$i_{II} = I_2 + y_{21}^{+} v_1 + y_{22}^{+} v_2 \qquad (3.55b)$$

On confining considerations to the oscillatory components and using the two-port impedance matrix, we obtain

$$v_1 = z_{11}^{+} i_1 + z_{12}^{+} i_2 \qquad (3.56a)$$

$$v_2 = z_{21}^{+} i_1 + z_{22}^{+} i_2 \qquad (3.56b)$$

Since the embedding network is passive and linear, the principle of superposition can be used. Relationships (3.56a) and (3.56b) can be separated into their harmonic components. For the ideal case when v_1 and v_2 are sinusoidal voltages, we get

$$\begin{bmatrix} v_1(\omega_o) \\ v_2(\omega_o) \end{bmatrix} = \begin{bmatrix} z^+_{11}(\omega_o) & z^+_{12}(\omega_o) \\ z^+_{21}(\omega_o) & z^+_{22}(\omega_o) \end{bmatrix} \begin{bmatrix} i_1(\omega_o) \\ i_2(\omega_o) \end{bmatrix} \qquad (3.57a)$$

$$\begin{bmatrix} 0 \\ 0 \end{bmatrix} = \begin{bmatrix} z^+_{11}(n\omega_o) & z^+_{12}(n\omega_o) \\ z^+_{22}(n\omega_o) & z^+_{22}(n\omega_o) \end{bmatrix} \begin{bmatrix} i_1(n\omega_o) \\ i_2(n\omega_o) \end{bmatrix} \qquad (3.57b)$$

where $n = 2, 3, 4, 5$ ..... etc.

Equation (3.57a) gives the relationships between the fundamental port currents and voltages. Equation (3.57b) applies to higher harmonic components of the current variables, when the port voltages are required to be zero value. In the practical case $v_1(n\omega)$ and $v_2(n\omega)$ cannot be made to vanish completely, for this would imply the z parameters to be zero valued at these higher harmonic frequencies. However their values can be made insignificantly small by the correct choice of embedding networks. One of the requirements is that the absolute values of the "z^+" parameters decrease rapidly with frequency above the fundamental. This filter action is indicated in Fig. 3.7. However in the filter action, it is not sufficient to know the frequency spectra of $i_1 z^+_{11}$, $i_2 z^+_{12}$, $i_1 z^+_{21}$ and $i_2 z^+_{22}$ alone. Since $v_1(n\omega)$ and $v_2(n\omega)$ are vector sums of the nth. harmonic components of these quantities in pairs, it is also essential to know their relative phase angles.

In order to examine the influence of the phase angles on the filter action, it is necessary to refer to Fig. 3.6. The overall

oscillator system is shown in Fig. 3.6a. This can be separated into a linear part and a nonlinear part. The current and voltage relationships at the ports of the linear part can be treated by the Principle of Superposition. The relative phase angles between port currents and voltages would depend on the mode of operation of the system. This is in turn determined by the state of excitation of the nonlinearity. Therefore one is inevitably forced to identify the controlling variable first of all, and thereafter have the phase angles of other variables referred to it. The controlling variable has already been identified as v_1 (v_1 represents v_{eb}). We can now "measure" the phases of the other variables against v_I. On fixing the amplitude and frequency of v_I, the phase angles of i_I and i_{II} with reference to v_I, will be determined by the embedding network. The phase relationships between v_1 and the harmonic components of i_1 and i_2, are shown pictorially in Fig. 3.8. Multiplication of the impedance and the current can be interpreted geometrically in the complex plane. The current $i_1(\omega)$ is described by a vector rotating in the anti-clockwise direction with angular frequency ω. The impedance function $z^+_{11}(\omega) = r^+_{11}(\omega) + j\, x^+_{11}(\omega)$ can be thought of as an operator function. Its operation on $i_1(\omega)$ is to transform the vector $i_1(\omega)$ into a new one. This new vector rotates in the same direction and the same angular frequency, but with a new amplitude given by $\left| i_1(\omega).\, z^+_{11}(\omega) \right|$ and having a phase difference from $i_1(\omega)$ of ψ_{11}, given by $\tan^{-1}\psi_{11} = x_{11}/r_{11}$. The vector sum, $z^+_{11}(\omega)i_1(\omega) + z^+_{12}(\omega)i_2(\omega)$

is shown in Fig. 3.8k. Similar diagrams can be drawn for each of the higher harmonic components of v_1. It should be pointed out that the phase angles ϕ_1 and ϕ_2 in Fig. 3.8j and Fig. 3.8k are given by

$$\begin{aligned} \phi_1(\omega) &= \theta_1(\omega) + \tan^{-1}\left[x_{11}(\omega)/r_{11}(\omega) \right] \\ \phi_2(\omega) &= \theta_2(\omega) + \tan^{-1}\left[x_{12}(\omega)/r_{12}(\omega) \right] \end{aligned} \qquad (3.58)$$

The phase angles for $i_1(n\omega_o)z^+_{11}(n\omega_o)$ and $i_2(n\omega_o)z^+_{12}(n\omega_o)$ will be of the same form as those given by relationships (3.58), except that the relevant quantities are calculated for the frequency of the higher harmonic frequency concerned. In order for the higher harmonic voltages to be small, it is desirable to have the sum $\phi_1(n\omega_o) + \phi_2(n\omega_o)$ to be as close to π as possible. However the requirement on the frequency characteristic of the "z^+"s is more important. If all the "z^+" parameters have frequency characteristics similar to that shown in Fig. 3.7, then the moduli of vectors $i_1(n\omega_o)z^+_{11}(n\omega_o)$ and $i_2(n\omega_o)z^+_{12}(n\omega_o)$ will be very small compared to those for the fundamental. Therefore the resultant higher harmonic voltages will also be very small compared to that of the fundamental. Provided the existence of a strong filter action is ensured, the effect of the phase angles on the harmonic content will be secondary. In conclusion the designer's attention should be directed firstly to realizing a good filter action. Correction due to phase angle effects can be considered as an unimportant refinement.

3.9 Further Implications of the Filter Action

Aizerman[14] introduced the filter hypothesis to distinguish between the "filtered system" and the "auto-resonance system". In the "auto-resonance system", the input and output waveforms of the active device are nearly sinusoidal. The embedding network need only perform the function of providing "feedback" paths for the oscillatory signal. In the "filtered system", the controlling variable at the input has to be maintained in nearly sinusoidal form. The embedding network in this case performs the function of a filter besides providing the required "feedback" paths. Aizerman discussed the filter hypothesis in terms of control systems, where attention was directed to the study of transfer functions. In circuit theory one is just as interested in the current variable as the voltage variable. Instead of dealing with transfer functions, the designer looks into the circuit transformation matrix.

There are further implications of the filter action which Aizerman had omitted. A strong filter action will not only make possible the production of nearly sinusoidal oscillation in the presence of a strong nonlinear action, but also governs the whole qualitative aspect of the oscillatory solution irrespective of the type of nonlinear element involved. This important aspect is examined briefly below and in more detail later in Section 4.14.

At small signals the transistor parameters are essentially linear. The stability of the initial state of the oscillator circuit can be investigated by studying the roots of the characteristic

equation. The condition for soft excitation to occur is to have at least one pair of characteristic roots possessing a positive real part. On the other hand, a higher order system may have more than one pair of characteristic roots having positive real parts. Does the presence of a strong filter action prevent the establishment of other limit cycles other than the one for the preferred frequency? It is possible to answer this question by a deductive argument. Since the current and voltage variables are related by a fixed immittance matrix, it will be sufficient to solve the characteristic equation for one variable. Let us assume that solutions for the current variable are first found. Those for the voltage variable are obtained by using the impedance matrix transformation. At the initial stages of oscillation "build-up", the current variable i_1 will in general be a sum of complex functions,

$$i_1 = \sum \exp (\sigma_n \pm j\omega_n)t \qquad (3.59)$$

It should be pointed out that the phases are left out. This does not impair the generality of the argument. If the impedance matrix presents a strong filter action, then only the voltage component of the preferred frequency will be allowed to grow into a stable limit cycle. Since the higher harmonic voltages are suppressed it will require a much higher current level to bring the controlling voltage at the higher harmonics into the nonlinear region. As the generative power of the transistor is limited it is unlikely that the controlling voltage can reach into the nonlinear region at frequencies other than

the fundamental. Therefore a strong filter action selects a single steady state oscillation while suppressing other characteristic roots.

The presence of a strong filter action provides the designer with justification to focus attention on the excitation frequency of interest. In such a system, the pair of dominant roots will be of the form exp $(\sigma_o + k\omega_o t)$. Characteristic roots having other complex frequencies will always decay with time. Therefore we should be able to specify this filtered system at a "point" frequency ω_o. If the dominant frequency ω_o is known, it would even be possible to derive a criterion for the initial state to be an unstable focus point. This means that we can avoid constructing the characteristic equation and examining all its roots. Since it requires more quantitative formulation to obtain this criterion, the derivation is given in Section 4.14.

To summarize the qualitative aspects of the filtered system, a pictorial history of the system dynamics are given in Fig. 3.9 and Fig. 3.10. The dynamics of the voltage variable can be decomposed into a dominant root and other roots which exist only for a short period of time after excitation. The time duration of the initial linear state will be symbolized by τ_L, for later reference. There is also another characteristic time interval, starting from when the non-linear action becomes effective and lasting until the steady state of the dominant root has been reached. This time interval is symbolized by τ_N. During the interval τ_L, the dominant root grows exponentially. If the filter action is strong, other excited roots are expected to

decay away rapidly; well within the time interval τ_L. These roots are named here as recessive roots. We can thus mark out a linear region (shaded area in Fig. 3.9 and Fig. 3.10) in the phase planes, within which any excitation will induce "appearance" of roots with complex frequencies. These are the natural frequencies of the system. The number of natural frequencies present will depend on the order of the differential equation involved. It is important to design for all natural frequencies except the dominant pair to decay away with time. In such a case, the initial oscillation will appear as a great profusion of natural frequencies. After the time interval $\tau_L + \tau_N$, only the dominant pair survived. These have then reached the steady state. The dynamical behaviour of all the four circuit variables v_1, v_2, i_1 and i_2 will be of the same form, except that the limit cycles for the current variables may not be as symmetrical as those for the voltage variables. This is due to the distorted shapes of the current waveforms.

3.10 Conclusion for Chapter 3

In this Chapter, the task of decomposing the problem into its bare essentials has been carried out. The exercise has revealed the basic nature of the transistor harmonic oscillator.

The Problem as it appeared before

The designer is faced with a complicated nonlinear system, whose nonlinearities are unknown functions of system variables. He is required to synthesize a steady state solution and to examine the subsequent behaviour of the solution with respect to changes in system environment.

The Problem as it appears now

The transistor oscillator is a higher order nonlinear differential equation belonging to the first class systems under Popov's classification scheme. The presence of a strong filter action in the system suppresses all other natural frequencies except the dominant pair. Therefore the filtered system can be treated as a equivalent second order nonlinear equation. In such a case it will be sufficient to design for steady state oscillation at a "point" frequency and to ensure that soft excitation takes place for the synthesized circuit. The important parameters for synthesis have been identified.

The method of synthesis for such systems is discussed in Chapter 4.

3.11 References

1. H. Poincare, J. des Math., (3), 7, 1881.
2. H. Barkhausen, "The problem of oscillation generation", Doctorate Thesis, Göttingen, 1907.
3. H. Barkhausen, "How far can self-excitation take place in triodes by means of natural capacitances between grid and anode only?" Jahrb. Drahtl. T.U.T., Vol.21, No.4, p.198, 1923.
4. van d. Pol, "The triode as a generator of oscillations", Radio Rev., Vol. 1, pp.701-754, 1920.
5. van d. Pol, "On relaxation oscillations", Phil. Mag., Vol. 2, pp.978-992, 1926.
6. van d. Pol, "Forced oscillations in a circuit with non-linear resistance", Phil. Mag., Vol. 3, p.65, 1927.
7. A. Andronov and A. Witt, "On the mathematical theory of self-oscillation", C. R. Acad. Sci. (Paris). Vol. 190, pp.256-258, 1930.
8. A. Andronov and A. Witt, "On the theory of van der Pol pulling effect", Arch. Elektr., Vol. 24, p.99, 1930.
9. M. A. Liapunov, "Proleine general de la stabilite du movement", Annales de Joulouse, Paris, Vol. 9, 1907. Originally published in Russian in 1892.
10. A. Hurwitz, "Ueber die Bedingungen, unter welchen eine Gleichung nur Wurzeln mit negative reellen Theilen besitzt", Mathematische Annalen, Vol. 46, pp.273-284, 1895.

11. A. Lienard, Rev. Gen. de l'Electricite, 23, 1928.

12. N. Krylov and N. Bogoluibov, Ac. Sc. (USSR) 1945 also "Introduction to nonlinear mechanics", Annals of Mathematics Study, No. 11, Princeton, N. J. Princeton University Press, 1947.

13. E. P. Popov, "The dynamics of automatic control systems", Pergamon Press, 1962.

14. M. A. Aizerman, "Theory of automatic engine regulation", Gostekhizdat, 1952.

15. N. Minorsky, "Investigation of nonlinear control systems", Part 4, "Harmonic Linearization", Office of Naval Research, Department of the Navy, Washington, D.C., March 1962.

16. E. P. Popov and I. P. Paltov, "Approximation methods for the investigation of nonlinear automatic systems", Fizmatgiz, Moscow 1960.

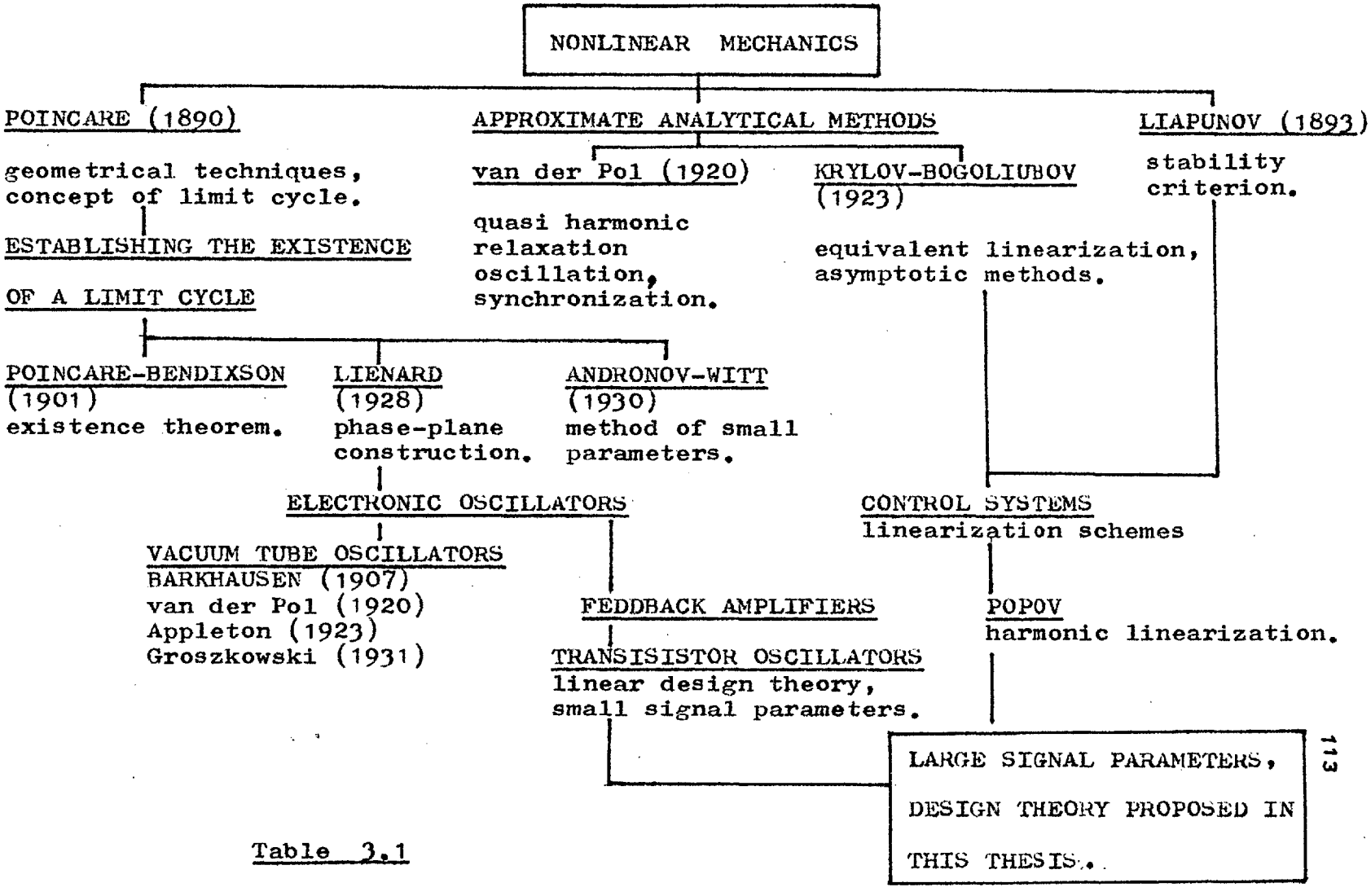
NONLINEAR MECHANICS
POINCARE (1890)
geometrical techniques, concept of limit cycle.
ESTABLISHING THE EXISTENCE OF A LIMIT CYCLE
POINCARE-BENDIXSON (1901) existence theorem.
LIENARD (1928) phase-plane construction.
ANDRONOV-WITT (1930) method of small parameters.
APPROXIMATE ANALYTICAL METHODS
van der Pol (1920)
quasi harmonic relaxation oscillation, synchronization.
KRYLOV-BOGOLIUBOV (1923)
equivalent linearization, asymptotic methods.
LIAPUNOV (1893)
stability criterion.
ELECTRONIC OSCILLATORS
VACUUM TUBE OSCILLATORS
BARKHAUSEN (1907)
van der Pol (1920)
Appleton (1923)
Groszkowski (1931)
FEDDBACK AMPLIFIERS
TRANSISISTOR OSCILLATORS
linear design theory, small signal parameters.
CONTROL SYSTEMS
linearization schemes
POPOV
harmonic linearization.
LARGE SIGNAL PARAMETERS, DESIGN THEORY PROPOSED IN THIS THESIS.

Table 3.1

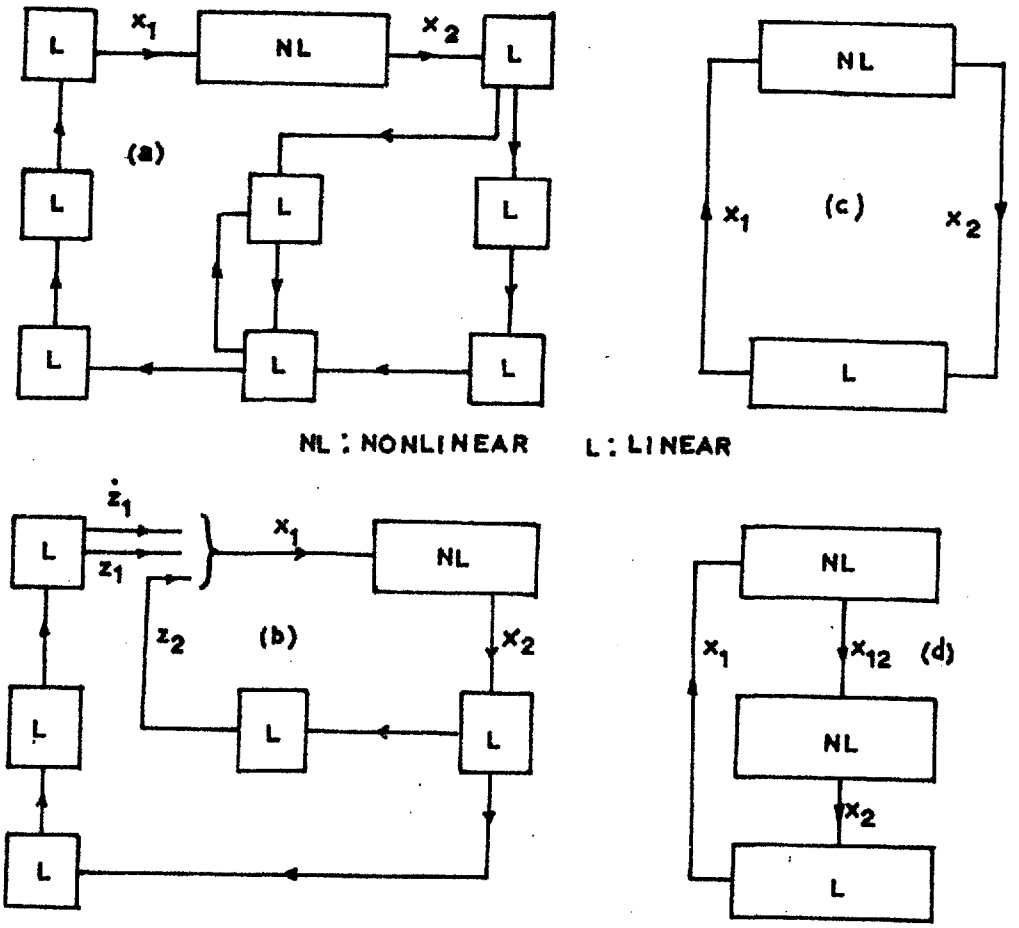

Fig. 3.1 First and second class nonlinear systems

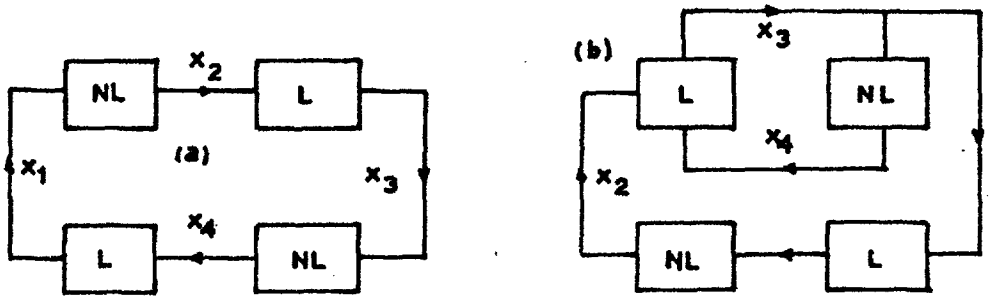

Fig. 3.2 Third class nonlinear systems

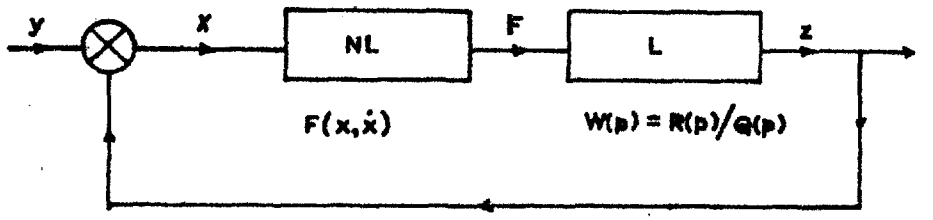

Fig. 3.3 A simple nonlinear feedback system

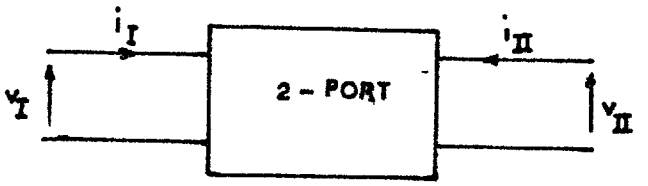

Fig. 3.4 Two-port network with the port variables defined

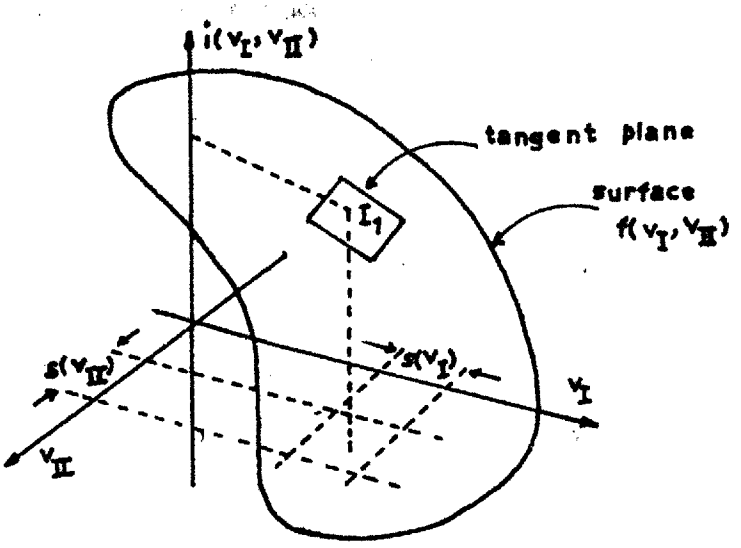

Fig. 3.5 Geometrical illustration of the two-port relationships

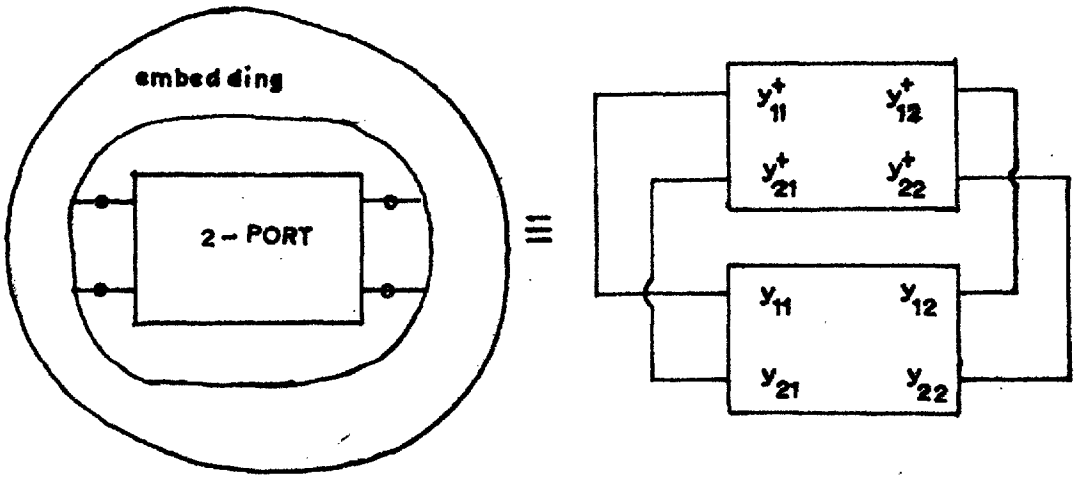

Fig. 3.6.a. Nonlinear active device embedded to produce oscillation

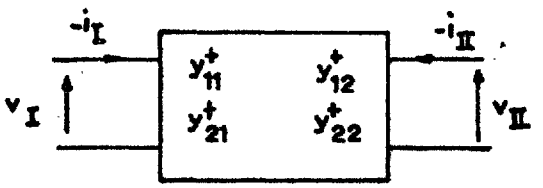

Fig. 3.6.b.

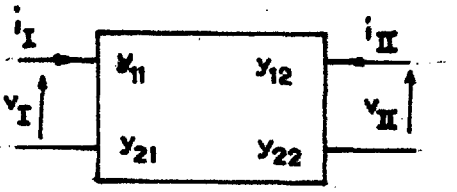

Fig. 3.6.c.

Fig. 3.6.b. Currents and voltages at the ports of the embedding network

Fig. 3.6.c. Currents and voltages at the ports of the nonlinear active device

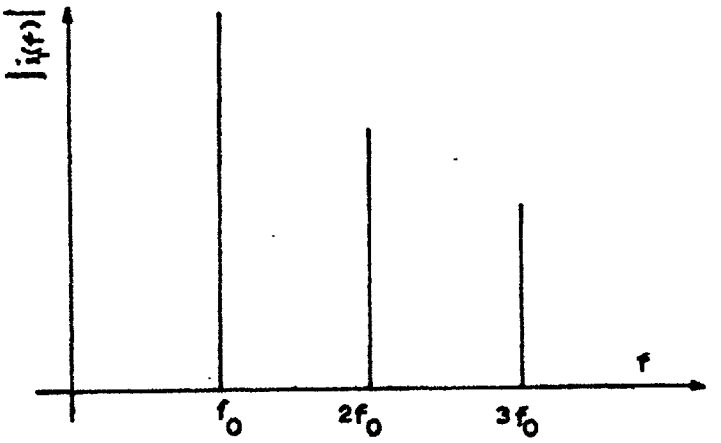

Fig. 3.7.a. Frequency spectrum of port current i_1

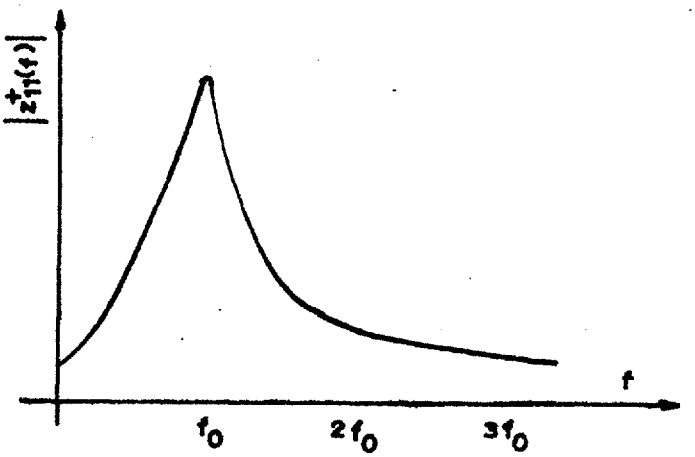

Fig. 3.7.b. Frequency chacteristic of z_{11}^+

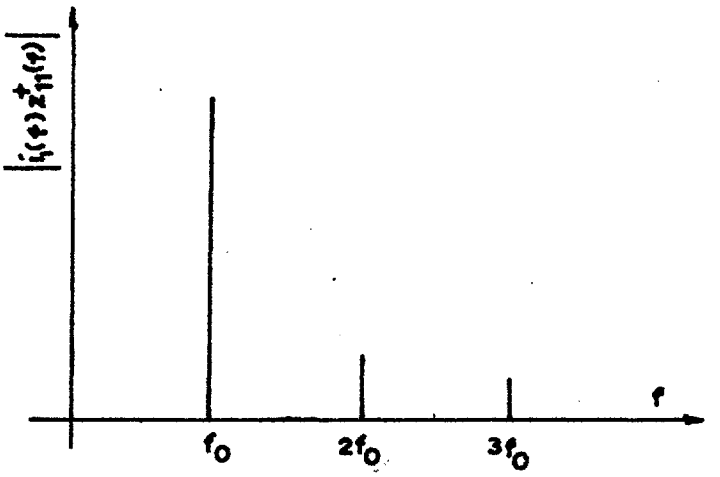

Fig. 3.7.c. Frequency spectrum of $i_1 z_{11}^+$

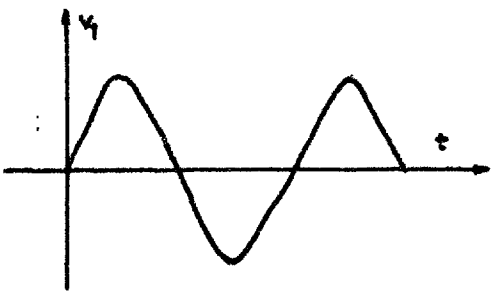

Fig. 3.8.a.

oscillograph of v_1

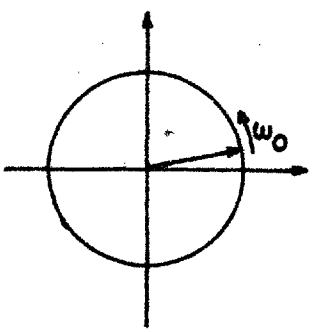

Fig. 3.8.b.

complex plane description of v_1

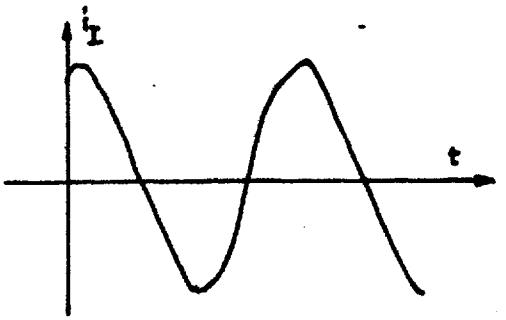

Fig. 3.8.c.

oscillograph of i_1

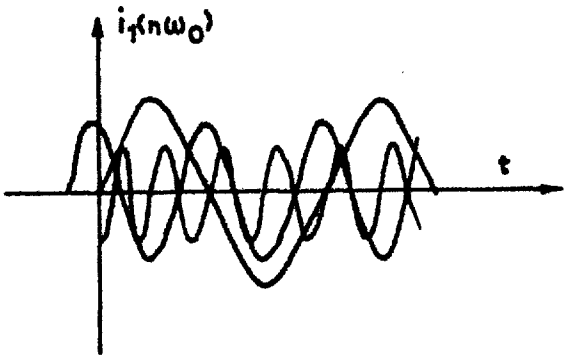

Fig. 3.8.d.

harmonic components of i_1

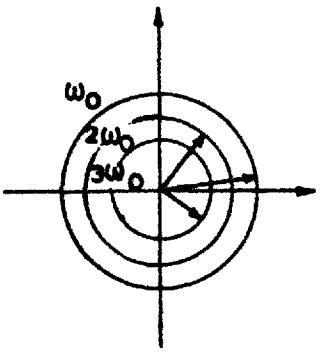

Fig. 3.8.e.

complex plane description of i_1

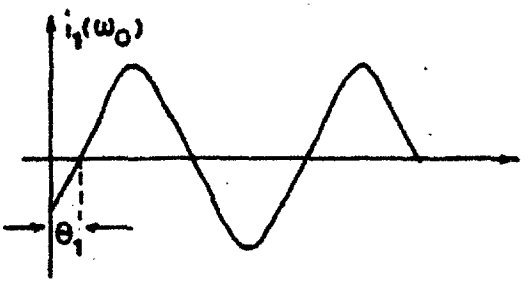

Fig. 3.8.f.

oscillograph of $i_1(\omega_o)$

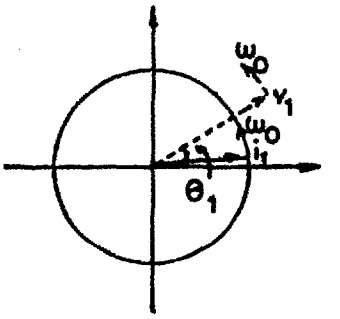

Fig. 3.8.g.

complex plane description of $i_1(\omega_o)$

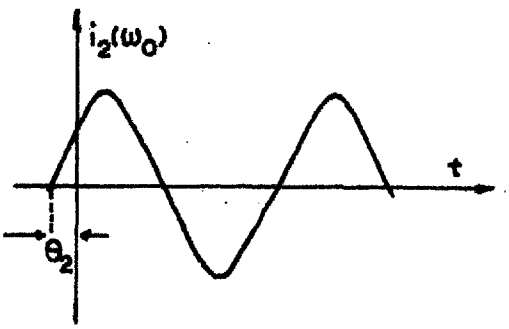

Fig. 3.8.h.

oscillograph of $i_2(\omega_o)$

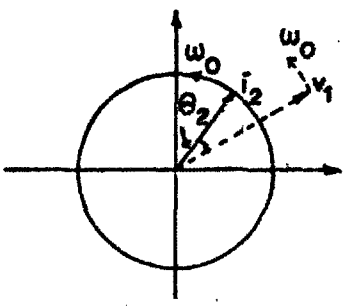

Fig. 3.8.i.

complex plane description of $i_2(\omega_o)$

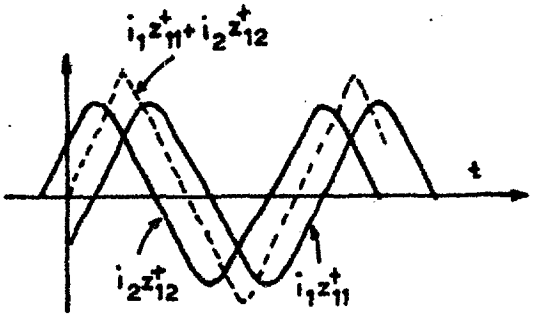

Fig. 3.8.j.

oscillograph of

$i_1z_{11}^+ + i_2z_{12}^+$

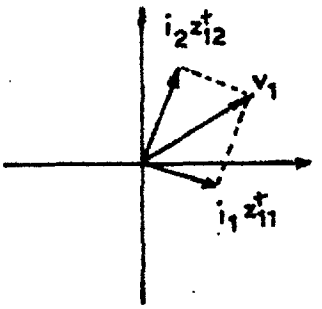

Fig. 3.8.k.

complex plane description

of $i_1z_{11}^+ + i_2z_{12}^+$

	DOMINANT ROOT	RECESSIVE ROOTS		
	$\exp[\sigma_0(t)+j\omega_0]t$	$\exp(-\sigma_1)t$	$\exp(-\sigma_2+j\omega_2)t$	$\exp(-\sigma_3+j\omega_3)t$
trajectories	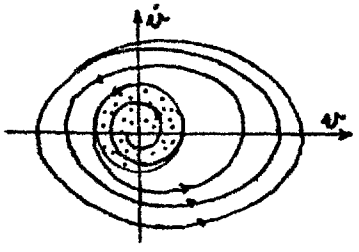	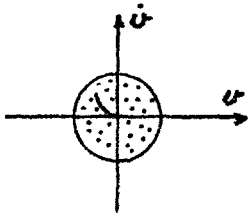	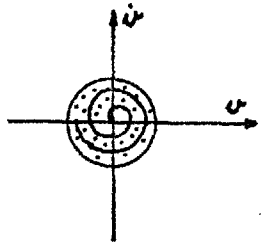	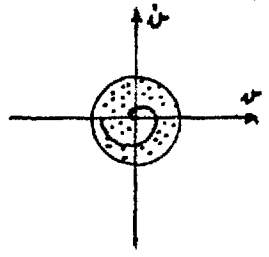
oscillation	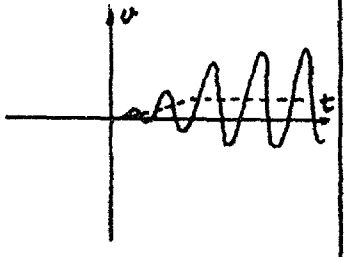	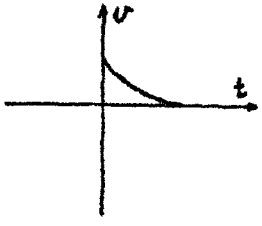	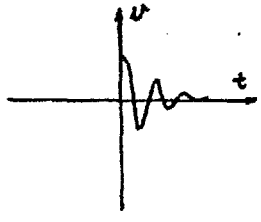	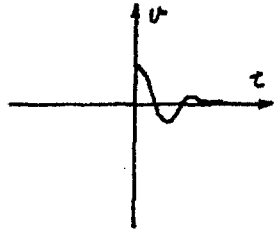
root equatn	$(a_1p^2+b_1p+c_1)v+$ $+\mu_1(v,\dot{v})=0$	$(b_2p+c_2)v=0$	$(a_3p^2+b_3p+c_3)v=0$	$(a_4p^2+b_4p+c_4)v=0$
initial state	$(ap^7+bp^6+cp^5+dp^4+ep^3+fp^2+gp+h)v=0$			
final state	$(a_1p^2+b_1p+c_1)v+\mu(v,\dot{v})=0$			

Fig. 3.9 Dynamics of the voltage variable

	DOMINANT ROOT	RECESSIVE ROOTS		
	$\exp[\alpha_0(t)+j\omega_0]t$	$\exp(-\alpha_1)t$	$\exp(-\alpha_2+j\omega_2)t$	$\exp(-\alpha_3+j\omega_3)t$
trajectories	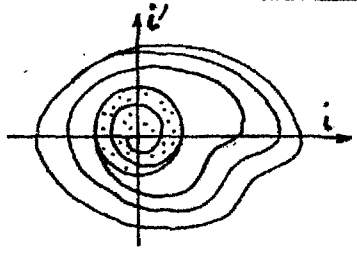	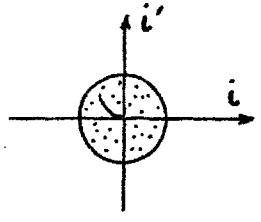	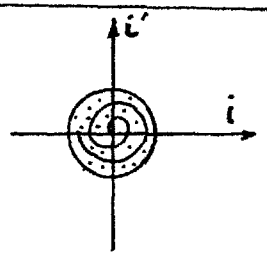	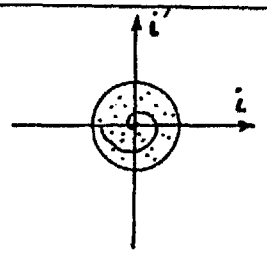
oscillation	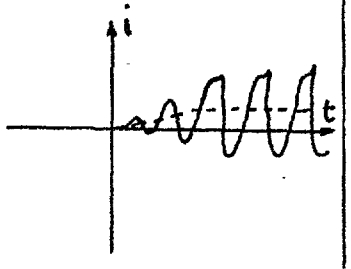	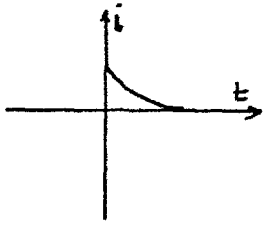	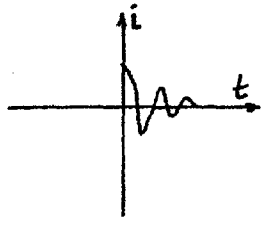	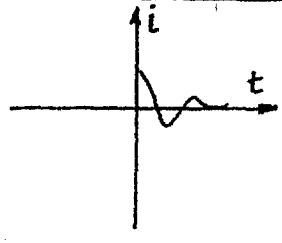
root equatn	$(A_1p^2+B_1p+C_1)i + \mu'_1(i,i') = 0$	$(B_2p+C_2)i = 0$	$(A_3p^2+B_3p+C_3)i = 0$	$(A_4p^2+B_4p+C_4)i = 0$
initial state	$(Ap^7+Bp^6+Cp^5+Dp^4+Ep^3+Fp^2+Gp+H)i = 0$			
final state	$(A_1p^2+B_1p+C_1)i + \mu'(i,i') = 0$			

Fig. 3.10 Dynamics of the current variable

Chapter 4

Quantitative Formulation of the Design Theory

4.1 Introduction

The initial state of the system can be described by a polynomial equation (see Fig. 3.9 and 3.10). To construct such an equation is very time consuming. Besides, there is the disadvantage of having to use equivalent circuits, the accuracy of which one cannot be sure. A more reasonable way to treat the problem, is to discard the recessive roots (since they decay) and focus attention on the pair of dominant roots. These latter roots have complex frequencies with positive real parts. They will appear as growing oscillations at the ports of the active device. If the imaginary part of the complex frequency is known, then the operation of the device will be determined by the set of small signal transistor parameters. Given the set of small signal parameters, their frequency characteristic around the expected frequency of oscillation and the embedding network, one should be able to determine the stability of the initial state of the system. A criterion for initial instability (soft excitation) is given in Section 4.4. In this chapter we are concerned with the new design procedure proposed for transistor harmonic oscillators.

The design procedure starts off with the determination of sets of embedding elements, which satisfy the condition of oscillation

for a given frequency and given controlling voltage v_{eb}. The final choice of a particular embedding network will be made on the basis of two considerations: (1) To achieve a strong filter action in the system. (2) To ensure initial instability or soft excitation, these two considerations are basic in the operation of the transistor oscillator. The first consideration will contribute towards suppressing the unwanted natural frequencies. Requirements on the performance of the oscillator will narrow the choice of embedding elements even further. In order to characterize the transistor for such a design procedure, we need two sets of measurements: (1) small signal parameters and (2) large signal parameters.

The measurements of the transistor parameters and the actual construction of the oscillator circuits are discussed in Chapter 5. In the present chapter, it is assumed that the means of measuring the required quantities are available.

4.2 The Condition for Steady State Oscillation

In Section 1.2 it has been pointed out that the criterion for oscillation in the earlier design theories is,

$$\Delta(j\omega) = 0 \qquad (4.1)$$

where Δ represents the circuit determinant. Equation (4.1) can

mean only one thing i.e. the condition for sustaining steady state oscillation in a given electrical network. This interpretation of the above equation can be explained with the aid of Fig. 4.1. The transistor is embedded with admittances Y_b^+, Y_e^+ and Y_c^+. The subscript indicates the position of the admittance e.g. Y_b^+ means the embedding element opposite the base terminal. In order to facilitate discussion, the network is redrawn in the form of a two-port with a direct feedback path from 'output' port to 'input' port. In the initial linear region of operation the oscillation is a growing sinusoid (ignoring the effects of the recessive roots). This applies to all the four port variables. No single one of them can be looked upon as the control variable and thus it is impossible to distinguish between an input and an output port. Therefore the three possible feedback paths shown in Fig. 4.1 are equally valid. In fact the best description of such a system is to write down the relevant mathematical expressions in symmetrical form. More will be said about symmetry later. Meanwhile, Fig. 4.1(a) is referred to for the following discussion. The subscript 'b' indicating common base configuration is dropped, on the understanding that such a configuration is considered. The termination of the two-port with admittances Y_c^+ and Y_e^+, will modify the original two-port admittance matrix to,

$$[Y] \equiv \begin{bmatrix} y_{11}+Y_c^+ & y_{12} \\ y_{21} & y_{22}+Y_e^+ \end{bmatrix} \qquad (4.2)$$

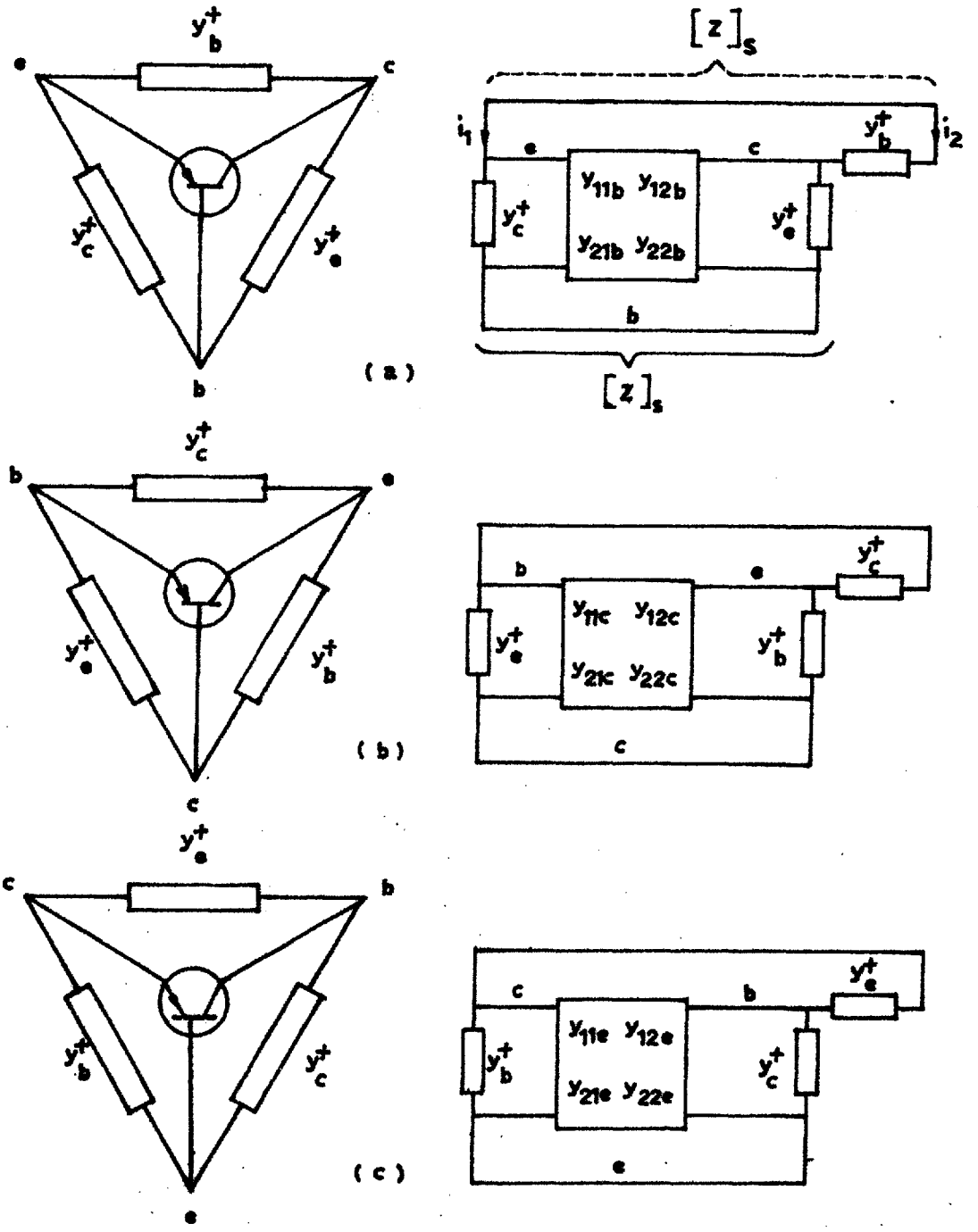

Fig. 4.1 Sustaining steady state oscillation in a transistor circuit

Transforming this to impedance form one gets,

$$[Z]_s \equiv \begin{bmatrix} (y_{22}+Y_e^+)/\Delta_s & (-y_{12})/\Delta_s \\ (-y_{21})/\Delta_s & (y_{11}+Y_c^+)/\Delta_s \end{bmatrix} \qquad (4.3)$$

where $\Delta_s = (y_{11}+Y_c^+)(y_{22}+Y_e^+) - y_{12}y_{21}$.

On terminating $[Z]_s$ with the impedance $1/Y_b^+$, a new overall impedance matrix is obtained,

$$[Z]_s \equiv \begin{bmatrix} (y_{22}+Y_e^+)/\Delta_s & (-y_{12})/\Delta_s \\ (-y_{21})/\Delta_s & (y_{11}+Y_c^+)/\Delta_s)+(1/Y_b^+) \end{bmatrix} \qquad (4.4)$$

Expression (4.4) refers to the overall system marked out by the broken outline in Fig. 4.1(a). The relationships between the port currents and voltages are given below,

$$\begin{bmatrix} v_1 \\ v_2 \end{bmatrix} = \begin{bmatrix} z_{11S} & z_{12S} \\ z_{21S} & z_{22S} \end{bmatrix} \begin{bmatrix} i_1 \\ i_2 \end{bmatrix} \qquad (4.5)$$

When steady state oscillation is reached one has $i_1 = -i_2$ and $v_1 = v_2$. Using these conditions in relationships (4.5), one gets

$$(z_{11S} + z_{22S}) - (z_{12S} + z_{21S}) = 0 \qquad (4.6)$$

Expression (4.4) can be used to rewrite condition (4.6) in terms of

the original y parameters. The reformulated condition is,

$$(y_{11} + y_{22} + y_{12} + y_{21} + Y_e^+ + Y_c^+)Y_b^+ + \Delta_s = 0 \qquad (4.7)$$

condition (4.7) is in fact equivalent to having a singular admittance matrix for the overall network. This singular matrix can be obtained by inspecting Fig. 4.2.

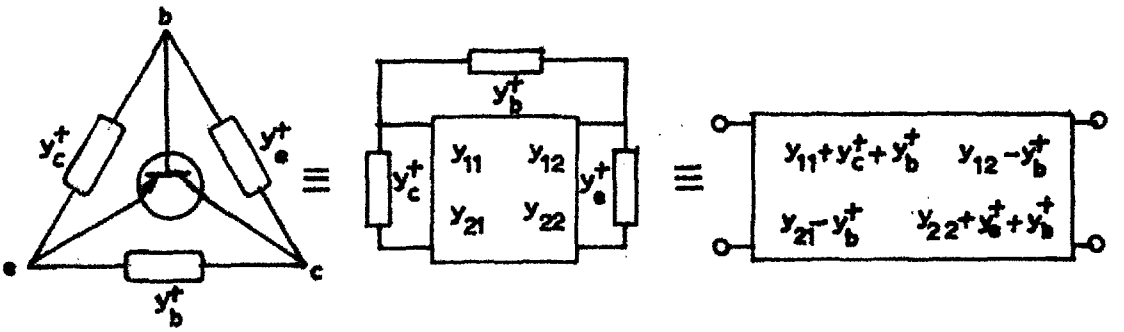

Fig. 4.2 Overall admittance matrix of the embedded transistor

On setting the determinant to zero we get,

$$\Delta = (y_{11} + y_{22} + y_{12} + y_{21} + Y_e^+ + Y_c^+)Y_b^+ + \Delta_s = 0 \qquad (4.8)$$

Condition (4.8) and (4.7) are identical. Therefore $\Delta = 0$ means the condition for sustaining steady state oscillation. It should be pointed out that there is an anomaly in the above discussion. In

earlier chapters, it has been emphasized that stable steady state oscillation can only occur in nonlinear systems. How can one discuss self sustained steady state oscillation of a linear system? In linear design theories, condition (4.8) is interpreted incorrectly as the condition for initial oscillation. This cannot be the case because this would require examination of the system in the complex frequency domain, whereas quantities involved in the above equation are measured on the $j\omega$ axis of the complex plane. Therefore it is not surprising that earlier design theories, which use condition (4.8) as the design basis have not been very successful. A simple way out of this difficulty is to employ the large signal transistor parameters. These are measured at the chosen signal level of the control voltage v_{eb}. In this case, it is valid to use condition (4.8) as a condition for sustaining steady state oscillation.

In this chapter the upper case "Y"s will be used to represent large signal "y" parameters and the lower case "y"s for the small signal ones. To be correct according to this notation, condition (4.8) should be written as,

$$\Delta = (Y_{11}+ Y_{22}+ Y_{12}+ Y_{21} + Y_e^+ + Y_c^+)Y_b^+ + \Delta_s = 0 \qquad (4.9)$$

where $\Delta_s = (Y_{11}+ Y_c^+)(Y_{22}+ Y_e^+) - Y_{12}Y_{21}$.

4.3 Symmetry and the Complex Gyrator Representation

One very marked feature of the transistor oscillator is its symmetry with respect to the terminals of the transistor. Provided that the sinusoidal form of the controlling voltage v_{eb} is assured, the transistor can be characterized by a set of measured parameters. Using the three sets of parameters (common base, common emitter or common collector), three basic feedback systems can be formed. However these are just three different ways of representing the same three terminals oscillator. Why then do we not use a single representation which avoid the need to identify any feedback path? Another argument for doing so is that symmetry schemes always throw up invariant quantities of special significance.

The basis for such a symmetric representation is the indefinite admittance matrix proposed by Tellegen[1] and Shekel[2]. The three sets of two-port admittance matrices are combined into a single 3X3 indefinite admittance matrix. In Fig. 4.5, is shown how the three basic sets of two-port matrices can be extracted from the more embracing indefinite admittance matrix. An important property of the indefinite matrix is that all the columns and rows add up to zero value. Therefore knowing any four of its elements, the whole matrix can be constructed.

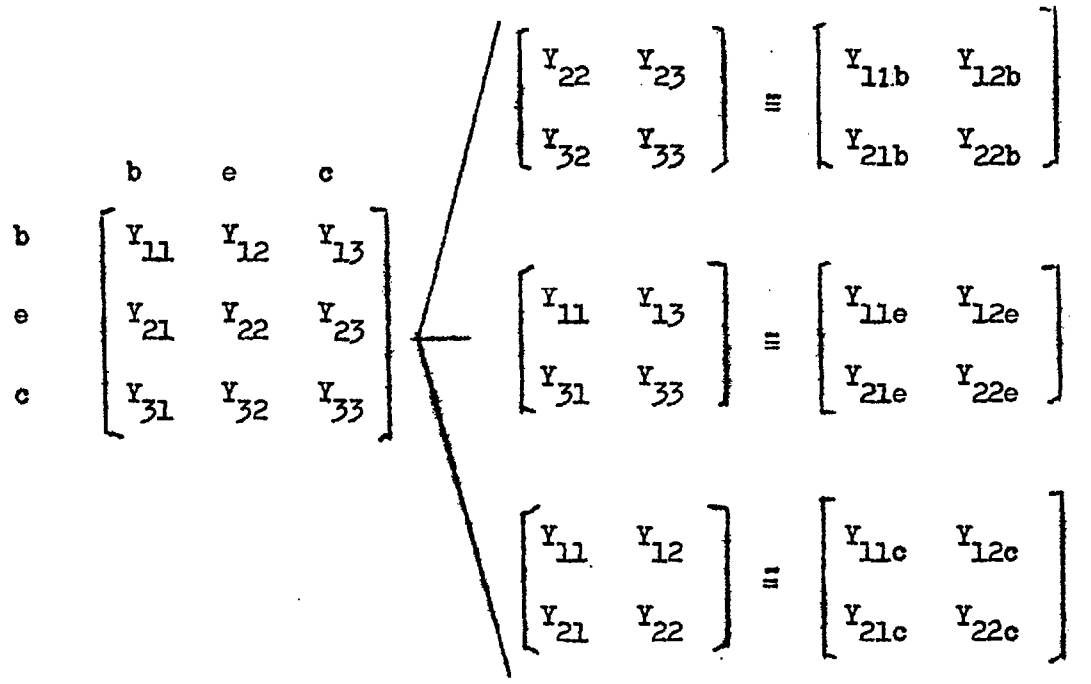

Fig. 4.5 Extracting the two-port matrices from the indefinite matrix

The indefinite admittance matrix can always be partitioned into a symmetric part and a skew symmetric part as shown in relationship (4.10).

$$\begin{bmatrix} Y_{11} & Y_{12} & Y_{13} \\ Y_{21} & Y_{22} & Y_{23} \\ Y_{31} & Y_{32} & Y_{33} \end{bmatrix} \equiv \begin{bmatrix} Y_{11} & \frac{1}{2}(Y_{21}+Y_{12}) & \frac{1}{2}(Y_{31}+Y_{13}) \\ \frac{1}{2}(Y_{21}+Y_{12}) & Y_{22} & \frac{1}{2}(Y_{32}+Y_{23}) \\ \frac{1}{2}(Y_{31}+Y_{13}) & \frac{1}{2}(Y_{32}+Y_{23}) & Y_{33} \end{bmatrix}$$

$$+ \begin{bmatrix} 0 & -\frac{1}{2}(Y_{21}-Y_{12}) & -\frac{1}{2}(Y_{31}-Y_{13}) \\ \frac{1}{2}(Y_{21}+Y_{12}) & 0 & -\frac{1}{2}(Y_{32}-Y_{23}) \\ \frac{1}{2}(Y_{31}-Y_{13}) & \frac{1}{2}(Y_{32}-Y_{23}) & 0 \end{bmatrix} \qquad (4.10)$$

The symmetric matrix can be realized by a Δ network. This is shown in Fig. 4.6.

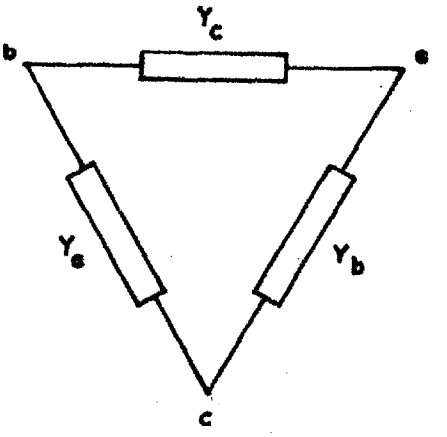

$$\begin{bmatrix} Y_a+Y_c & -Y_c & -Y_a \\ -Y_c & Y_c+Y_b & -Y_b \\ -Y_a & -Y_b & Y_b+Y_a \end{bmatrix}$$

Fig. 4.6 A network and its indefinite matrix

On comparing this matrix with the symmetric matrix in relationship (4.10), one gets

$$\begin{aligned} Y_c &= -\tfrac{1}{2}(Y_{21} + Y_{12}) \\ Y_b &= -\tfrac{1}{2}(Y_{32} + Y_{23}) \\ Y_a &= -\tfrac{1}{2}(Y_{31} + Y_{13}) \end{aligned} \qquad (4.11a)$$

The skew symmetric matrix cannot be realized in simple form. It will simply be represented by the circuit element called "GYRATOR". Using the property of the indefinite matrix it is easy to show that

$$(Y_{21} - Y_{12}) = (Y_{32} - Y_{23}) = -(Y_{31} - Y_{13})$$

The quantities inside the brackets will be defined as Y_0,

$$Y_0 = (Y_{31} - Y_{13}) = -(Y_{21} - Y_{12}) = -(Y_{32} - Y_{23}) \qquad (4.11b)$$

One can now characterize the gyrator by Y_0. However a sign convention is needed to indicate the order of permutation of the y parameters. This is indicated by an arrow drawn onto the gyrator symbol (see Fig. 4.7). In network synthesis, the gyrator considered has always been real i.e. Y_0 is a real quantity. Here Y_0 is a complex quantity: $Y_0=G_0+jB_0$. Y_0 will be called the "GYRATANCE" in this thesis. G_0 and B_0 are normally known as the gyration conductance and gyration susceptance respectively.

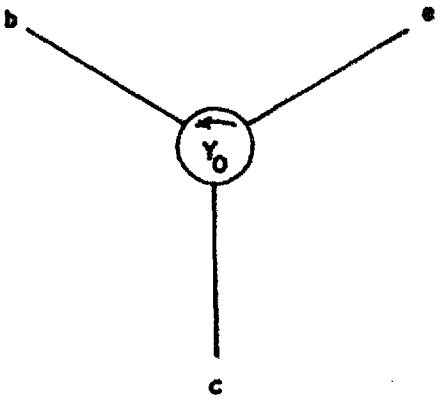

$$\begin{bmatrix} 0 & -Y_0 & Y_0 \\ Y_0 & 0 & -Y_0 \\ -Y_0 & Y_0 & 0 \end{bmatrix}$$

Fig. 4.7 The gyrator and its gyration matrix

Thus the transistor can be represented by a gyrator embedded in network as shown in Fig. 4.8. Its indefinite admittance matrix,

expressed in terms of the new circuit elements is also shown in Fig. 4.8.

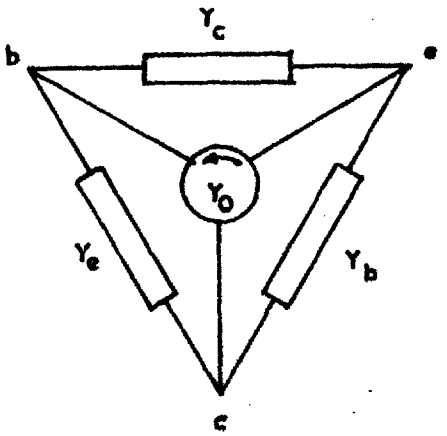

$$\begin{bmatrix} Y_e+Y_c & -Y_0-Y_c & +Y_0-Y_e \\ Y_0-Y_c & Y_c+Y_b & -Y_0-Y_b \\ -Y_0-Y_e & Y_0-Y_b & Y_b+Y_e \end{bmatrix}$$

Fig. 4.8 Symmetrical representation of the three terminal device

4.4 The Geometrical Representation of the Condition for Steady State Oscillation

In this section a geometrical model of the condition for steady state oscillation is constructed. In order to do this, condition (4.9) is first rewritten in terms of the gyrator representation. Fig. 4.2 is redrawn in the symmetrical form shown in Fig. 4.9. It should be pointed out that the external embedding elements can be lumped with the Δ network of the gyrator representation conveniently On setting the determinant of the two-port matrix given in Fig. 4.9 to

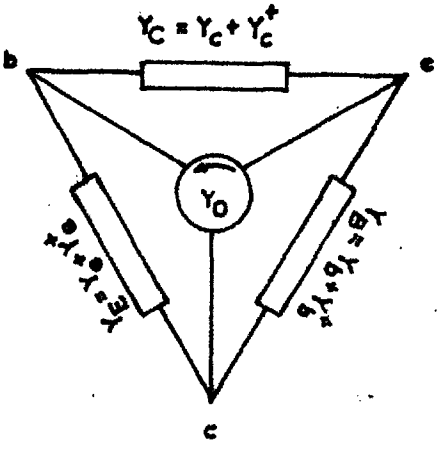

$$\begin{array}{c} \\ b \\ e \end{array} \begin{array}{c} \begin{array}{cc} b & e \end{array} \\ \begin{bmatrix} Y_E + Y_C & -Y_O - Y_C \\ Y_O - Y_C & Y_C + Y_B \end{bmatrix} \end{array}$$

Fig. 4.9 The embedded three terminal active device

zero one obtains

$$Y_B Y_E + Y_E Y_C + Y_C Y_B + Y_O^2 = 0 \qquad (4.12)$$

This new formulation is symmetrical in form, and as one expects no feedback path needs to be identified. Before proceeding further, the reader is reminded that the admittances consist of real parts and imaginary parts e.g. Y=G+jB. Equating the real and imaginary parts of equation (4.12) separately, the following equations are obtained:

$$B_B B_E + B_E B_C + B_C B_B = G_B G_E + G_E G_C + G_C G_B + G_O^2 - B_O^2 \qquad (4.13a)$$

$$(G_E+G_C)B_B+(G_C+G_B)B_E+(G_B+G_E)B_C = -2G_O B_O \qquad (4.13b)$$

These two equations can be interpreted geometrically. In order to do this, the quantities B_B, B_E and B_C are alloted values x, y and z

respectively along the axes of a rectangular coordinate system. The above equations may now be rewritten as:

$$xy + yz + zx = P \qquad (4.14a)$$

$$ax + by + cz = p \qquad (4.14b)$$

where, $P = G_B G_E + G_E G_C + G_C G_B + G_0^2 - B_0^2$

$$p = -2G_0 B_0 \qquad (4.15)$$

$$a = G_E + G_C, \quad b = G_C + G_B, \quad c = G_B + G_E$$

The condition for steady state oscillation requires equations (4.14a) and (4.14b) to be satisfied simultaneously.

Equation (4.14a) represents a hyperboloid system. If P is positive, we have the hyperboloid of two sheets and if P is negative we have the hyperboloid of one sheet. The axis of these hyperboloids is given by a line, equally inclined to the three co-ordinate axes. Any plane perpendicular to this line and cutting the hyperboloid will produce a circular locus of intersection. For the hyperboloid of two sheets, the two nearest points of its surface to the origin are given by the co-ordinates, $(\sqrt{P/3}, \sqrt{P/3}, \sqrt{P/3})$ and $(-\sqrt{P/3}, -\sqrt{P/3}, -\sqrt{P/3})$. This system of hyperboloids is fixed in a rectangular co-ordinate system as shown in Fig. 4.10a.

Equation 4.14b represents a plane in three dimensional space. It is inclined to each of the three co-ordinate axes, intersecting them at the points X(p/a, 0,0), Y(0,p/b,0) and Z(0,0,p/c). We shall call this the "ASSOCIATED PLANE" (see Fig. 4.11b).

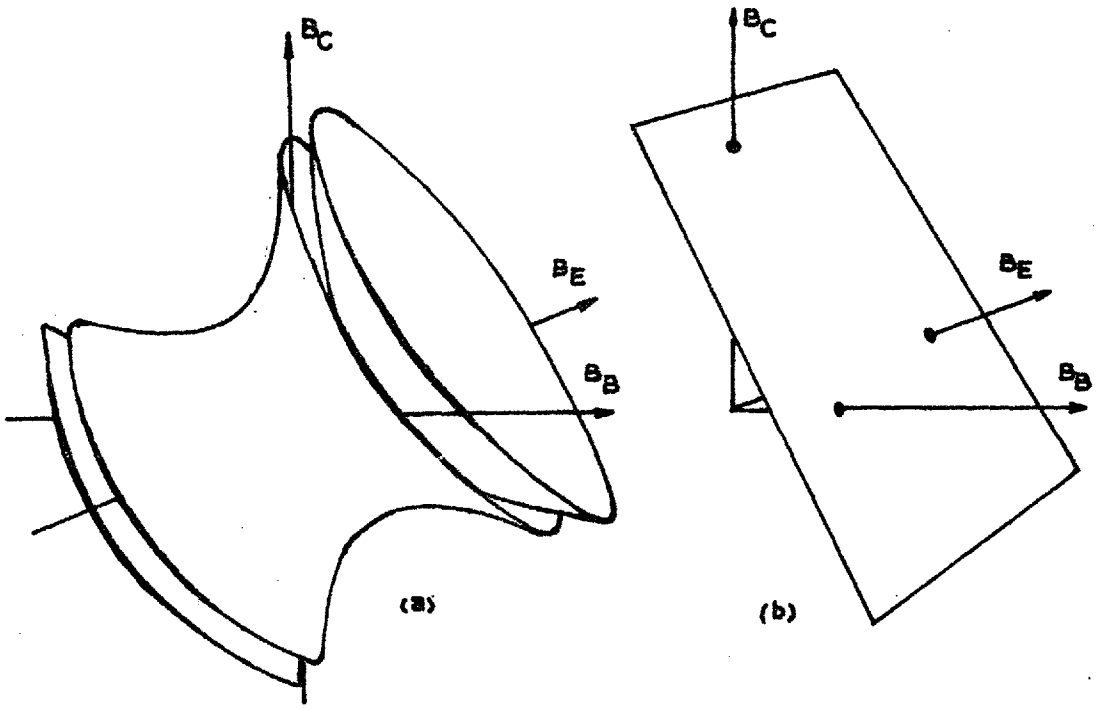

Fig. 4.10 (a) the hyperboloid (b) the associated plane

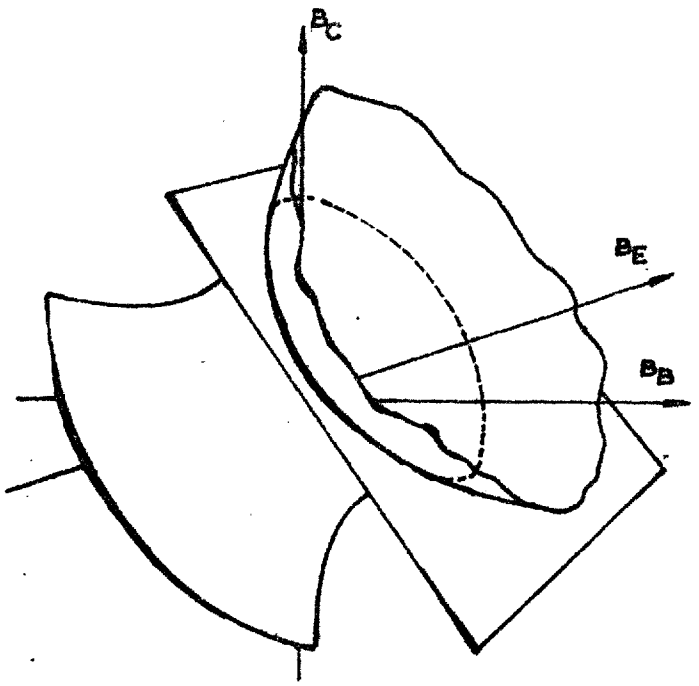

Fig. 4.11 The hyperboloid of one sheet cut by its associated plane

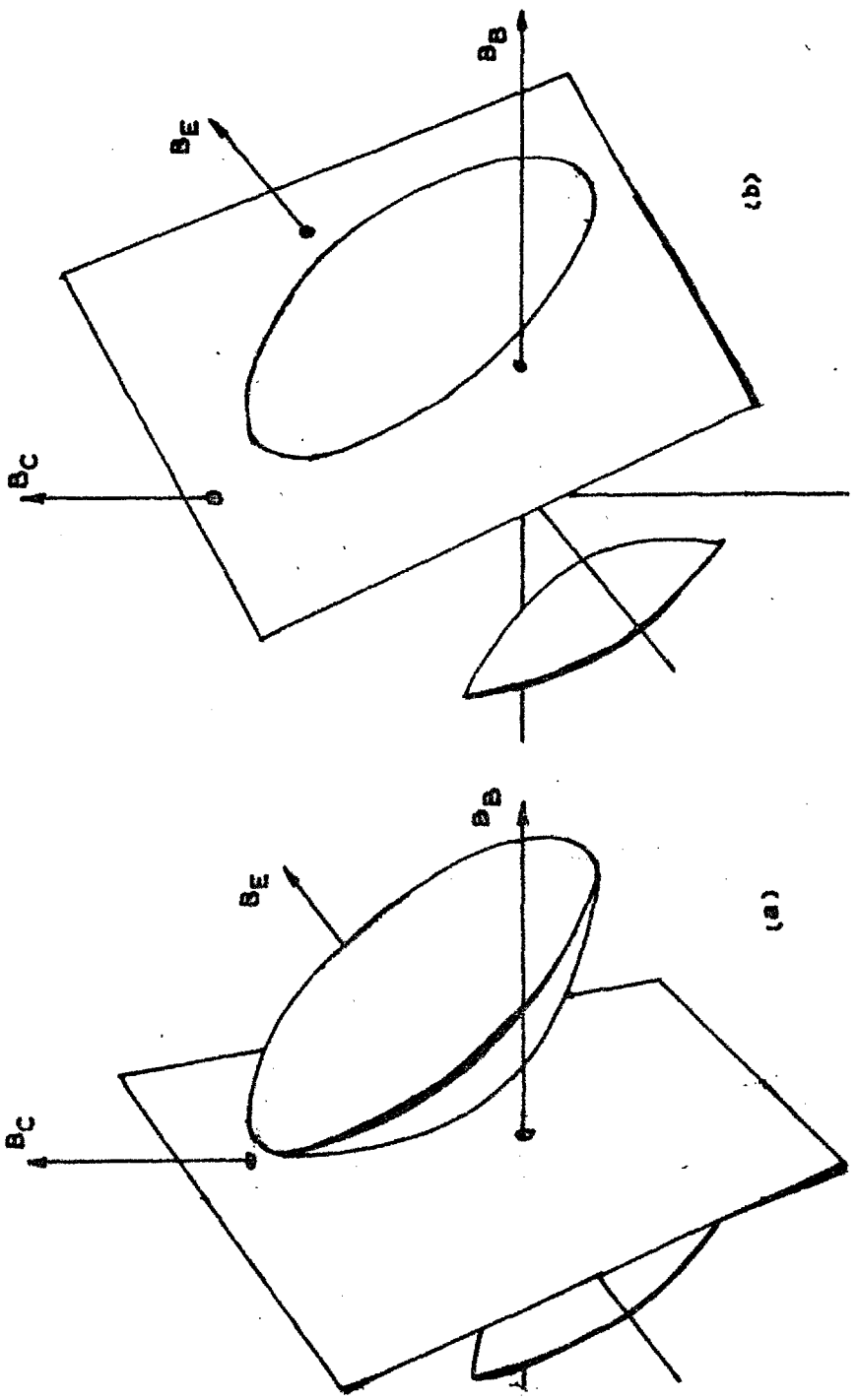

Fig. 4.12 (a) the associated plane not touching the hyperboloid
(b) the associated plane cutting the hyperboloid

The condition for steady state oscillation will be satisfied by points along the intersection of the hyperboloid and its associated plant. (see Fig. 4.11). For the hyperboloid of one sheet a lossless embedding can always be found such that the associated plane cuts the hyperboloid. However with the hyperboloid of two sheets, this is not the case. Fig. 4.12a shows the associated plane lying between the two hyperboloids, but not actually cutting any of the surfaces. To obtain oscillation (limit cycle), it is necessary to make the hyperboloid touch or cut its associated plane. Given the conductances G_B, G_E, G_C and the gyratance Y_0 of the transistor, the locus of intersection between the hyperboloid and its associated plane is fixed in space. Each point along this locus will define an embedding necessary to bring about oscillation. This is so because the co-ordinates of these points are specified by the three values B_B, B_E and B_C. Subsequently the embedding elements B_b^+, B_e^+ and B_c^+ can be calculated from the relationships $B_b^+ = B_B - B_b$ etc. The effect of loading the transistor with any dissipative elements e.g. conductances is to move the hyperboloid along its axis and also to tilt the associated plane. We can also alter the system from a hyperboloid of one sheet to that of two sheets by loading. Lastly, it should be pointed out that not every point on the locus will give stable oscillation. The question of stability is discussed in a later section.

4.5 Embedding for the Maximally Loaded Oscillator

In equation (4.14a), if P is negative, we will be dealing with the hyperboloid of one sheet. The hyperboloid will always be cut by its associated plane. But if P is positive, there will be a boundary case. The associated plane will be tangential to the hyperboloid at only one point. This special case is that of the maximum load.

Consider a load G_C^+ added to the active device so that the expression for P is modified.

$$P = (G_b G_e + G_e G_c + G_c G_b) + G_0^2 - B_0^2 + G_c^+(G_b + G_e) \qquad (4.16)$$

This has the effect of moving the hyperboloid up or down the axis of rotation depending on whether the sign of $G_c^+(G_b + G_e)$ is positive or negative. The tip of the hyperboloid is given by the co-ordinates

$$x = y = z = \sqrt{P/3} \qquad (4.17)$$

Provided $G_b + G_e$ is positive, increasing the load conductance will move this point away from the origin. The maximum value of G_c^+, for which the condition of oscillation can still be satisfied will be that for which the hyperboloid just touches its associated plane. Using three dimensional co-ordinate geometry, the point of tangency can be found. This point fixes the values of B_B, B_E and B_C and gives the expression for the maximum load conductance, $\hat{G}_c^+$. The "cap" placed on top of the symbol is meant to indicate maximum value. The

design expressions are derived in Appendix 1. They are presented below:

$$\begin{aligned} \hat{G}_c^+ &= (B_0^2 - \textstyle\sum G_b G_e)/(G_b + G_e) \\ B_b^+(\hat{G}_c^+) &= -(G_0/B_0)G_b - B_b \\ B_e^+(\hat{G}_c^+) &= -(G_0/B_0)G_e - B_e \\ B_c^+(\hat{G}_c^+) &= -(G_0/B_0)(G_c^+ + G_c) - B_c \end{aligned} \qquad (4.18)$$

where, $\sum G_b G_e = G_b G_e + G_e G_c + G_c G_b$

$B_b^+(\hat{G}_c^+)$ etc. indicate external susceptances, associated with $\hat{G}_c^+$

If the load is placed in one of the other two ports, the expressions will be of the same form and can be written down accordingly using symmetry.

A special note is required here. Since large signal parameters are used throughout the discussion, the maximum load actually means that calculated to sustain oscillation at the measured amplitude of the control voltage v_{eb}. The genuine maximum load is one calculated from the transistor parameters which are measured a signal level just above the upper bound for small signal measurements. Only in this case will the oscillation die down on increasing the load above its maximum value. In the other cases an increase in the load will cause readjustment of both the amplitude and frequency of oscillation.

4.6 Bounds of the Lossless Embeddings Required to Sustain Oscillation

The locus of intersection between the hyperboloid and its associated plane will be fixed given the transistor parameters and the external load. By considering the points at which the locus of intersection touches planes parallel to xoy, yoz and zox, it should be possible to find the extreme values of z, x and y respectively (see Fig. 4.13). Hence the upper and lower bounds on the values of the lossless elements B_b^+, B_e^+ and B_c^+ can be calculated. The derivation is given in Appendix 2. The derived expressions are given below:

$$\hat{B}_C \text{ or } \overset{\vee}{B}_C = \frac{G_O B_O G_C \pm \sqrt{(\Sigma G_B G_E + G_C^2)(B_O^2 - \Sigma G_B G_E)(\Sigma G_B G_E + G_O^2)}}{\Sigma G_B G_E} \qquad (4.19a)$$

where the "cap" and the "inverted-cap" over the symbol indicate upper and lower bound values respectively.

The external embedding elements can be calculated using the relationships $B_c^+ = B_C - B_c$ etc. In association with each of the above boundary values are the values of the other two co-ordinates. Expressions for these are given below:

$$B_B(\overset{\wedge\vee}{B}_C) = (-G_O B_O + \overset{\wedge\vee}{B}_C G_E)/(G_E + G_C)$$
$$B_E(\overset{\wedge\vee}{B}_C) = (-G_O B_O + \overset{\wedge\vee}{B}_C G_B)/(G_C + G_B) \qquad (4.19b)$$

Design expressions for the other two pairs of variables are of the same

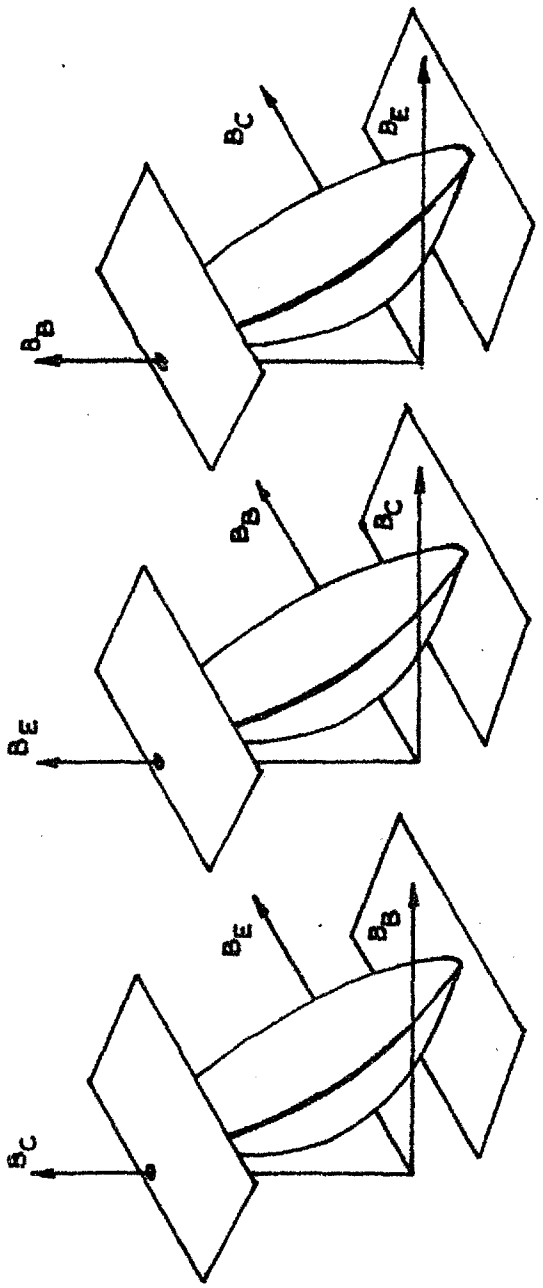

Fig. 4.13 Bounds on the locus of intersection

form and can be written down accordingly using symmetry.

4.7 Stability

4.7.1 Introduction

In chapter 3, it has already been pointed out that two stability criteria are required in the proposed design theory. The first criterion is connected with the stability of the limit cycle. Only when a stable limit cycle exists for the system, will there be any steady state oscillation. Unstable limit cycles have no physical interpretation. The second criterion is connected with initial instability, which is necessary for soft excitation. The transistor which we aim to synthesize must have the following properties:

(1) Criterion 1 is satisfied.

(2) Criterion 2 is satisfied.

(3) A strong filter action exists.

(4) Only one controlling variable exists.

Such a system is equivalent to a second order nonlinear differential equation. Oscillation will grow from the unstable centre and eventually asymptote into the stable limit cycle.

4.7.2 The design for a particular stable limit cycle

Investigations discussed in earlier sections have revealed the basic nature of the higher order differential equation system, which we know as the transistor harmonic oscillator. Therefore the design of a transistor oscillator when translated into mathematical terms, means the construction of a higher order system with a stable elliptical limit cycle for the controlling variable v_{eb}. The geometrical model of the condition for oscillation provides a means of synthesizing the embedding network. However the oscillation condition (4.12) is only a necessary condition. By it alone steady state oscillation cannot be guaranteed to appear. An additional requirement is that the synthesized system should possess a stable cycle. This is criterion 1 mentioned in section 4.7.1. and in fact this has already been derived earlier in section 2.7. It only remains to elaborate the derivation a little. In the vicinity of the stable limit cycle, the phase trajectory spirals into its final orbit. In the time domain this means that the amplitude of oscillation approaches steady state. If the trajectory approaches its final orbit slowly as shown in Fig. 4.14, then it is valid to approximate the oscillation by the complex frequency $\sigma + j\omega$. The real part σ is simply the decrement δ derived in section 2.7. Its expression is

$$\sigma = \frac{\left[(\partial M/\partial a)(\partial N/\partial \omega) - (\partial M/\partial \omega)(\partial N/\partial a) \right] \Delta a}{(\partial M/\partial \omega)^2 + (\partial N/\partial \omega)^2} \qquad (4.20)$$

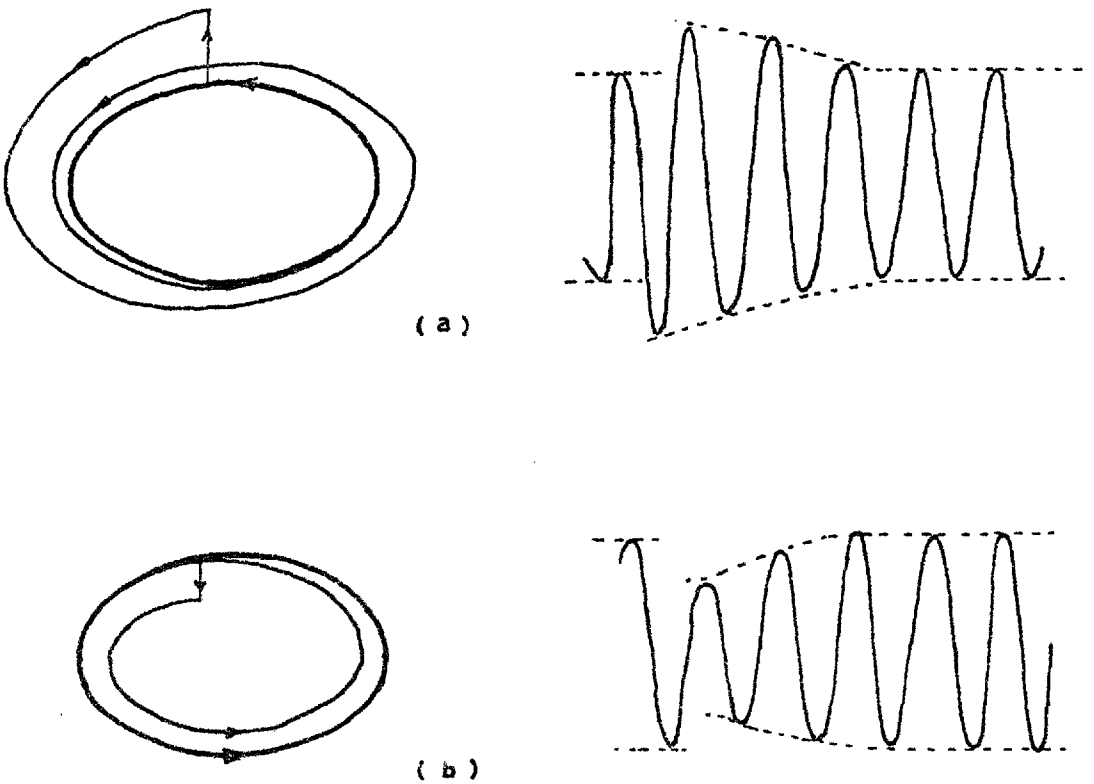

Fig. 4.14 Small perturbation of the stable limit cycle

where $M = \sum B_B B_E - G_O^2 - \sum G_B G_E + B_O^2$

$$N = (G_E+G_C)B_B+(G_C+G_B)B_E+(G_B+G_E)B_C+2G_OB_O$$

From expression (4.20) we notice that the a-posteri condition for the complex frequency approximation to be valid is for both the quantities $(\partial M/\partial\omega)^2$ and $(\partial N/\partial\omega)^2$ to be large. This is automatically satisfied in the presence of a strong filter action. Therefore the stability criterion derived earlier is indeed applicable to the transistor oscillator, which complies to the properties stated in section 4.7.1. This criterion for a stable limit cycle (or criterion 1) is re-stated below:

$$(\partial M/\partial a)(\partial N/\partial\omega) - (\partial M/\partial\omega)(\partial N/\partial a) > 0 \qquad (4.21)$$

Thus the designer is required to measure the transistor parameters for a small range of frequency and amplitude variation about the steady state operation point.

4.7.3 The design for initial instability or soft excitation

The geometrical model together with criterion 1 provide a means of synthesizing systems with stable limit cycles. The next obvious question is, how to find a set of embedding elements that will ensure initial instability. The geometrical model discussed above can be modified for this purpose by replacing all admittance functions

involved e.g. $Y(a,j\omega)$ with linear admittance functions expressed in terms of the complex frequency variable $(\sigma + j\omega)$ e.g. $y(\sigma + j\omega)=g(\sigma + j\omega)+jb(\sigma + j\omega)$. We obtain,

$$b_B b_E + b_E b_C + b_C b_B = \sum g_B g_E + g_0^2 - b_0^2 \qquad (4.22a)$$

$$(g_E + g_C)b_B + (g_C + g_B)b_E + (g_B + g_E)b_C = -2g_0 b_0 \qquad (4.22b)$$

The real and imaginary parts of the admittance functions $g(\sigma + j\omega)$, $b(\sigma + j\omega)$ can be obtained directly from $y(j\omega)$ and its frequency characteristic about the designed frequency:

$$g(\sigma + j\omega) = g(j\omega) + (\partial g/\partial \sigma)\,\sigma$$

$$b(\sigma + j\omega) = b(j\omega) + (\partial b/\partial \sigma)\,\sigma$$

It should be pointed out that the above relationships are only valid for $\sigma \ll \omega$. Using the Cauchy-Riemann relationships we get

$$\partial g/\partial \sigma = \partial b/\partial \omega; \quad \partial b/\partial \sigma = -\partial g/\partial \omega$$

Therefore $$g(\sigma + j\omega) = g(j\omega) + (\partial b/\partial \omega)\sigma$$

$$b(\sigma + j\omega) = b(j\omega) - (\partial g/\partial \omega)\sigma$$

Thus a set of small signal measurements are sufficient to define the geometry represented by the equations (4.22a) and (4.22b). They represent the intersection of a hyperboloid with its associated plane. The locus so obtained will be called the "generative locus".

Both σ and ω of the growing oscillation $\exp(\sigma + j\omega)t$ are determined uniquely by equation (4.22a) and (4.22b). The basis of

choosing a point on the "generative locus" to represent the set of desired embedding elements is given in section 4.10. Meanwhile the procedure for constructing the locus is given: the first step is to fix σ as a fraction of ω ($2\pi/\omega = \tau$, period of oscillation). Let $\sigma = k\omega$. Take for an example a growing oscillation which takes ten periods to double its amplitude. This means $\exp(20\pi k)=2$ or $k \cong 0.011$. It is seen that k is normally a small fraction. Next it is necessary to find the set of transistor parameters expressed in terms of complex frequency. Measurements have shown that for the common base configuration, only y_{11b} and y_{21b} varies appreciably with frequencies. Therefore we find,

(1) $$y_{11b}(\sigma + j\omega) = g_{11b}(\sigma + j\omega) + jb_{11b}(\sigma + j\omega)$$
$$= g_{11b}(j\omega) + (\partial b_{11b}/\partial\omega)k\omega + j\, b_{11b}(j\omega) - (\partial g_{11b}/\partial\omega)k\omega$$

(2) $$y_{21b}(\sigma + j\omega) = g_{21b}(\sigma + j\omega) + jb_{21b}(\sigma + j\omega)$$
$$= g_{21b}(j\omega) + (\partial b_{21b}/\partial\omega)k\omega + j\, b_{21b}(j\omega) - (\partial g_{21b}/\partial\omega)k\omega$$

(3) $$y_{11}(\sigma + j\omega) \cong y_{11b}(j\omega), \qquad y_{12b}(\sigma + j\omega) \cong y_{12b}(j\omega)$$

(4) The required set of two-port parameters is

$$\begin{bmatrix} y_{11b}(\sigma + j\omega) & y_{12b}(j\omega) \\ y_{21b}(\sigma + j\omega) & y_{22b}(j\omega) \end{bmatrix}$$

From this set of parameters we can construct the "generative" locus

and thus relate the lossless embedding elements to the condition for soft excitation.

4.8 Power Dissipation in the Transistor Oscillator

In oscillator design we are exploiting the circuit properties of an active device. One of the important aspects of active network theory is the derivation of power formulae; so that given a device we know its output power available to the load. A convenient approach to investigate power dissipation in the oscillator is to partition the circuit representation of the transistor into two constituent states.

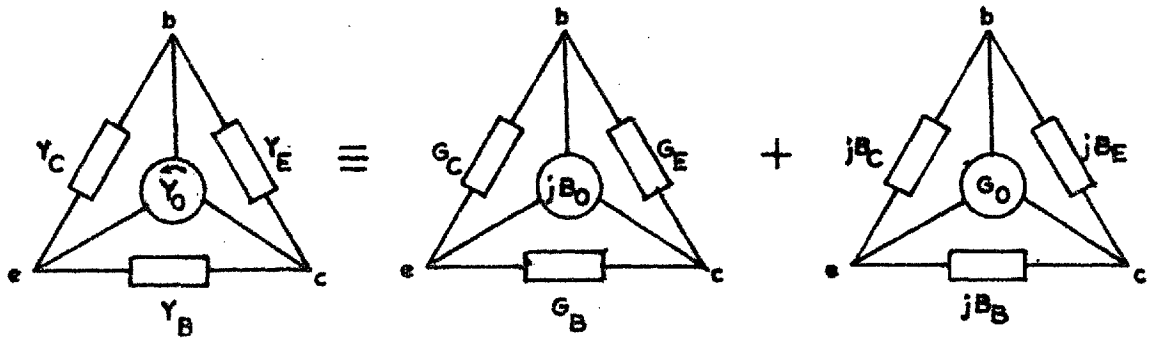

Fig. 4.15 The two constituent energy states of the oscillator

It is well known in circuit theory that the real gyrator comprising G_0, is a lossless element and that the imaginary gyrator comprising B_0 is a dissipative element. Therefore in the above partitioning, we have separated the embedded transistor into a "conductive state" and a "susceptive state". We shall symbolize these by $S_g(G_B, G_E, G_C, jB_0)$ and $S_b(jB_B, jB_E, jB_C, G_0)$ respectively. During steady state oscillation, energy equilibrium is reached. Therefore the total power dissipation in both states must be zero.

Power dissipation is an additive quantity. The total power dissipation in S_g can be written as the sum of dissipation in the separate elements.

$$P(S_g) = P(G_B) + P(G_E) + P(G_C) + P(jB_0) \tag{4.23}$$

Terms $P(G_B)$, $P(G_E)$ and $P(G_C)$ can either be positive or negative depending on the sign of G_B, G_E and G_C respectively. The term $P(jB_0)$ can either be positive or negative depending on the relative phases of its port voltages. In order to derive an expression for $P(jB_0)$ it is necessary to refer to Fig. 4.16. We have

$$P(jB_0) = v_c^* i_1 + v_e^* i_2 \tag{4.24}$$

In matrix notation, (4.24) becomes

$$P(jB_0) = \begin{bmatrix} v_c^* & v_e^* \end{bmatrix} \begin{bmatrix} 0 & -jB_0 \\ jB_0 & 0 \end{bmatrix} \begin{bmatrix} v_c \\ v_e \end{bmatrix} \tag{4.25}$$

On evaluating the quadratic form of expression (4.25) we get

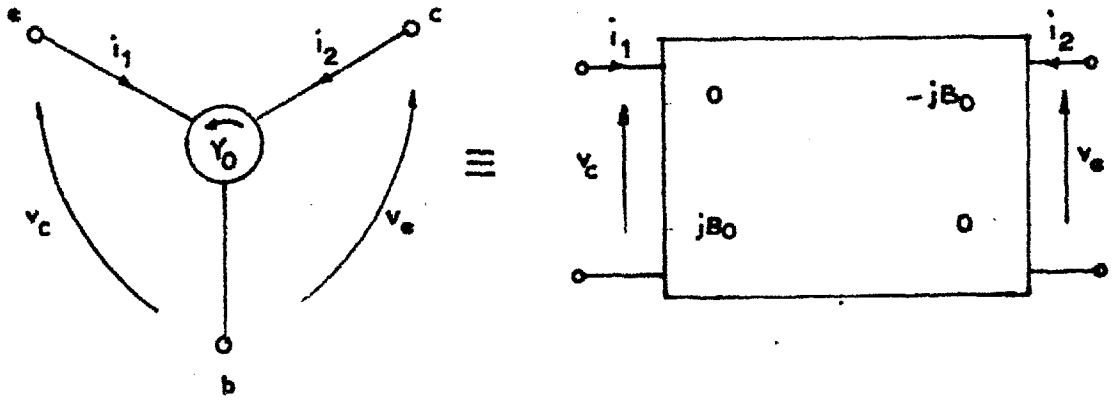

Fig. 4.16 The port currents and voltages of the gyrator

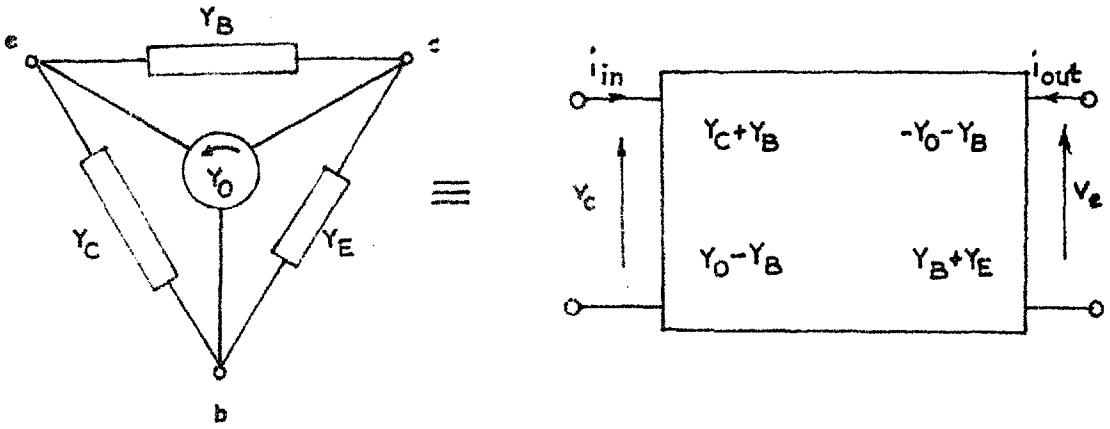

Fig. 4.17 The two-port matrix of the embedded transistor

$$P(jB_0) = 2B_0 \, \mathrm{Im}(v_c v_e^*) \tag{4.26}$$

The next step is to find v_e in terms of the controlling voltage v_c. Once the embedding network is chosen for steady state oscillation, the ratios between the port voltages v_b, v_e and v_c will be determined. For example in the case of the common base configuration shown in Fig. 4.17 we have

$$i_{in} = (Y_C + Y_B)v_c + (-Y_O - Y_B)v_e = 0$$

$$i_{out} = (Y_O - Y_B)v_c + (Y_B + Y_E)v_e = 0$$

Therefore

$$v_e/v_c = (Y_C + Y_B)/(Y_O + Y_B) = -(Y_O - Y_B)/(Y_B + Y_E) \tag{4.27a}$$

Similarly the other ratios are:

$$v_c/v_b = (Y_B + Y_E)/(Y_O + Y_E) = -(Y_O - Y_E)/(Y_E + Y_C) \tag{4.27b}$$

$$v_b/v_e = (Y_E + Y_C)/(Y_O + Y_C) = -(Y_O - Y_C)/(Y_C + Y_B) \tag{4.27c}$$

Using relationship (4.27b) in expression (4.26) we obtain

$$P(jB_0) = 2B_0 |v_c|^2 \, \mathrm{Im}\left(\frac{Y_B - Y_O}{Y_B + Y_E}\right)^* = 2B_0 |v_c|^2 \, \mathrm{Im}\left(\frac{Y_C + Y_B}{Y_O + Y_B}\right)^* \tag{4.28}$$

The expressions for $P(G_B)$, $P(G_E)$ and $P(G_C)$ are

$$P(G_C) = G_C |v_c|^2 \tag{4.29a}$$

$$P(G_B) = G_B \left| \frac{Y_E + Y_B}{Y_O - Y_E} \right|^2 |v_c|^2 = G_B \left| \frac{Y_O + Y_E}{Y_B + Y_E} \right|^2 |v_c|^2 \quad (4.29b)$$

$$P(G_E) = G_E \left| \frac{Y_C + Y_B}{Y_O + Y_B} \right|^2 |v_c|^2 = G_E \left| \frac{Y_O - Y_B}{Y_B + Y_E} \right|^2 |v_c|^2 \quad (4.29c)$$

On examining expression (4.28) and (4.29) the following properties are noticed:

(1)

$P(jB_O)$ can either be dissipative (positive value) or generative (negative value) depending on the relative phases of the port voltages. These are fixed by the embedding network.

(2)

$P(G_B)$, $P(G_E)$ and $P(G_C)$ can either be dissipative or generative depending on whether the corresponding values of G_B, G_E and G_C are positive or negative.

Given any set of embedding elements, the available power can be calculated by evaluating the expressions of (4.28) and (4.29). Normally one would expect $P(jB_O)$ and possibly one of the expressions of (4.29) say $P(G_C)$ to be negative. The generative power of the system is then given by

$$P_{gen} = P(jB_O) + P(G_c) \quad (4.30)$$

The power dissipated will be

$$P_{dis} = P(G_b) + P(G_e) \quad (4.31)$$

Attention is drawn to the lower case letters used for subscripts of the 'G's to indicate the absence of external embedding. Consider the case when the external load is G_e^+, then equation (4.31) becomes

$$P_{dis} = P(G_b) + P(G_e) + P(G_e^+) \tag{4.32}$$

For energy equilibrium we must have

$$P_{gen} = P_{dis}$$

The efficiency of d.c. to a.c. power conversion is

$$\eta_c = P_{gen}/P_{d.c.} \tag{4.33}$$

where $P_{d.c.} = I_e(d.c.)V_e(d.c.) + I_c(d.c.)V_c(d.c.)$

The efficiency of operation is

$$\eta_o = P(G_e^+)/P_{gen} \tag{4.34}$$

In terms of economics it is desirable to have high efficiencies. However other considerations like actual power available to the load and frequency sensitivity of the system must also be taken into account. These different demands on the system might require different embedding networks to fulfil. A unified treatment of these demands is not attempted in this thesis.

4.9 Power Dissipation of a Maximally Loaded Oscillator

Consider the case of a maximally loaded oscillator. From Section 4.5 we have the following data:

Quantities characterizing the transistor,

$$G_b,\ G_e,\ G_c,\ G_0$$
$$B_b,\ B_e,\ B_c,\ B_0$$

Quantities making up the embedding network,

$$\hat{G}_e^+ = (B_0^2 - \sum G_b G_e)/(G_c + G_b)$$
$$B_b^+(\hat{G}_e^+) = -mG_b - B_b$$
$$B_e^+(\hat{G}_e^+) = -m(G_e + G_e^+) - B_e \qquad \text{where } m = G_0/B_0$$
$$B_c^+(\hat{G}_e^+) = -mG_c - B_c$$

and susceptances

The synthesized system will have arm conductances, given by,

$$G_B = G_b, \qquad B_B = -mG_b$$
$$G_E = G_e + G_e^+, \qquad B_E = -m(G_e + G_e^+)$$
$$G_C = G_c, \qquad B_C = -mG_c$$

It is noticed that

(1) $B_B/G_B = B_E/B_E = B_C/B_C = -m$

(2) $\sum G_B G_E - B_0^2 = 0\ , \quad \sum B_B B_E - G_0^2 = 0$

The two constituent states of the oscillator are given in Fig. 4.18.

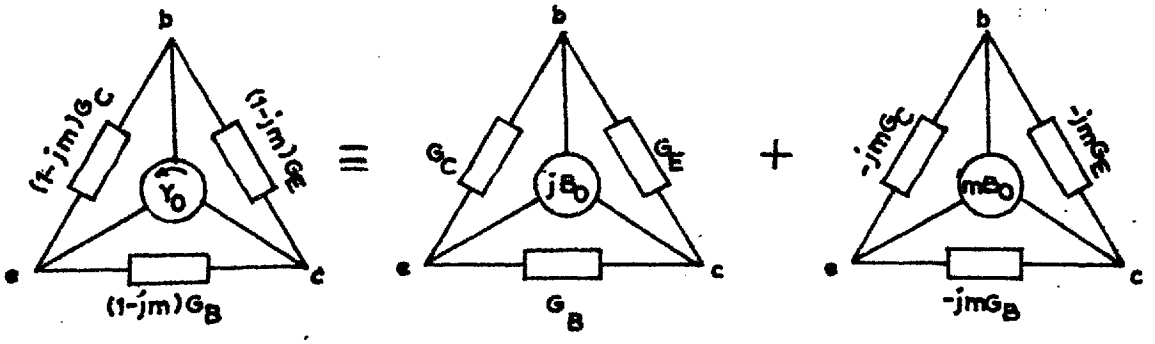

Fig. 4.18 The constituent states of the maximally loaded transistor

On substituting the arm admittances into relationship (4.27) we get,

$$v_e/v_c = (G_c + G_b)/(jB_0 + G_b) = -(jB_0 - G_b)/(G_b + G_E) \quad (4.35a)$$

$$v_c/v_b = (G_b + G_E)/(jB_0 + G_E) = -(jB_0 - G_E)/(G_E + G_c) \quad (4.35b)$$

$$v_b/v_e = (G_E + G_c)/(jB_0 + G_c) = -(jB_0 - G_c)/(G_c + G_b) \quad (4.35c)$$

Substituting the relevant voltage ratios into expressions (4.28) and (4.29) we obtain

$$P(jB_0) = \left[-2B_0^2/(G_b + G_E)\right]|v_c|^2 = \left[-2\sum G_b G_E/(G_b + G_E)\right]|v_c|^2 \quad (4.36)$$

$$P(G_b) = G_b |v_c|^2 \frac{(G_E+G_c)^2}{G_E^2 + B_0^2} = G_b |v_c|^2 \frac{(G_E+G_c)}{G_b+G_E} \quad (4.37a)$$

$$P(G_E) = G_E |v_c|^2 \frac{(G_c+G_b)^2}{G_b^2 + B_0^2} = G_E |v_c|^2 \frac{(G_c+G_b)}{(G_b+G_E)} \qquad (4.37b)$$

$$P(G_c) = G_c |v_c|^2 = G_c |v_c|^2 \frac{(G_b+G_E)}{(G_b+G_E)} \qquad (4.37c)$$

It should be pointed out that in deriving the relationships given by (4.37), the identities below were used

$$B_0^2 = \sum G_b G_E \quad \text{and} \quad G_E^2 + \sum G_b G_E = (G_b + G_E)(G_E + G_c)$$

The total power dissipation in the arm conductances is:

$$P(G_b) + P(G_E) + P(G_c) = \left[2\sum G_b G_E/(G_b + G_E) \right] |v_c|^2 \qquad (4.38)$$

From expression (4.37b) we find the power dissipated in the maximum load to be

$$P(G_e^+) = G_e^+ |v_c|^2 \frac{(G_c + G_b)}{(G_b+G_e+G_e^+)} \qquad (4.39)$$

The maximally loaded oscillator is a particular configuration. As a result of its unique position in the "geometry" of the oscillation condition, design expressions derived for this special case appear in simple forms.

4.10 Frequency and Amplitude Sensitivity with Respect to Small Parameter Variations

Oscillators are often used in electronic equipment as frequency references. As such they are called "clocks" or "master oscillators". In such operations, constancy of frequency is demanded. Temperature and mechanical agitation are two environmental factors which can induce frequency changes. The study of frequency sensitivity with respect to a general environmental variation is beyond the scope of this thesis. Instead, attention is focussed on how the amplitude and frequency vary when there is an incremental change in a pre-selected circuit element. Such a study should reveal the circuit parameters which are important in controlling the frequency of oscillation, and thus pave the way for a broader study later.

At present the following problem is considered:

Given data

A transistor is embedded to oscillate.

Amplitude of the control variable: $v_c = a_0$; (note: $v_{eb} \equiv v_c$).

Frequency of steady state oscillation: $\omega = \omega_0$

Transistor parameters:

$$\begin{bmatrix} y_{bb} & y_{be} & y_{bc} \\ y_{eb} & y_{eb} & y_{ec} \\ y_{cb} & y_{ce} & y_{cc} \end{bmatrix}$$

Embedding elements: jB_b^+, jB_e^+, jB_c^+ and load G_e^+.

Problem

What is the change in frequency or amplitude of v_c, if say jB_e^+

has undergone an incremental change of $j\Delta B_e^+$? $j\Delta B_e^+$ is assumed to be due to ΔC_e^+.

Approach to problem

In terms of the geometrical model, the set of embedding elements together with the transistor parameters, are represented by a point P_1 on the locus of steady state oscillation as shown in Fig. 4.19(a). On altering jB_e^+ to $j(B_e^+ + B_e^+)$, the operation of the oscillator can assume one of the following new states:

(1) No oscillation

(2) Squegging or self oscillation

(3) A new steady state, $(a_0 + \Delta a) \exp(j(\omega_0 + \Delta \omega)t)$

Which of these new states the oscillator assumes, will depend on the stability of the operation point P_1. In a well designed oscillator P_1 represents a well stabilized limit cycle. Points in the vicinity of P_1 will lie on other loci of oscillation. Each of these other loci is the result of the intersection of a new hyperboloid with its new associated plane. The actual positions of these loci depends on the incremental changes Δa and $\Delta \omega$. As ΔB_e^+ is small, Δa and $\Delta \omega$ are expected to be small. Therefore the new operation point P_2 resulting from the addition of ΔB_e^+, is expected to be in the vicinity of P_1.

The criterion of stability for a limit cycle is

$$K = (\partial M/\partial a)(\partial N/\partial \omega) - (\partial N/\partial \omega)(\partial M/\partial a) > 0$$

where expressions for M and N are given in Section 4.7.2. Since

(a) P_1 and P_2 are close to each other and (b) the incremental change ΔC_e^+ does not change the frequency characteristic of the embedding network significantly, we expect K_1 and K_2 calculated for P_1 and P_2 to differ only slightly. We have

$$K_2 = K_1 \pm \delta K$$

Since P_1 is well stabilized, K_1 is a significant positive quantity and also since δK is small, we expect

$$K_2 > 0$$

This means that for a well designed oscillator, a small variation in the circuit environment will cause the system to oscillate at a new steady state $(a_0+\Delta a)\exp(j(\omega_0+\Delta\omega)t)$. We can disregard the other two possibilities of "no oscillation" and "squegging".

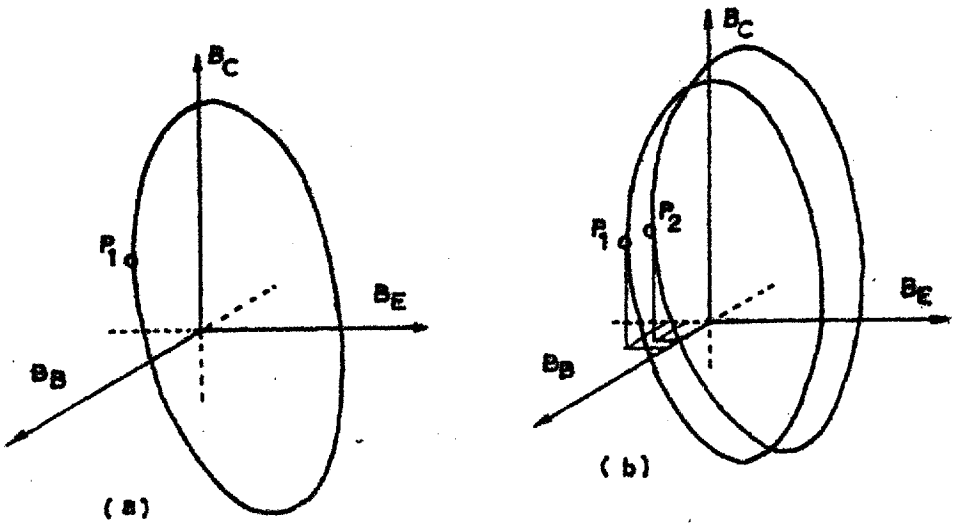

Fig. 4.19 Properties of the embedding space around a well stabilized limit cycle represents by P_1

Solution to the problem

Associated with the limit cycle P_1 we have

$$M(a_0, j\omega_0) + jN(a_0, j\omega_0) = 0 \tag{4.40}$$

and associated with the limit cycle P_2

$$M\left[(a_0+\Delta a),\ j(\omega_0+\Delta\omega),\ j(B_e+\Delta B_e)\right] + jN\left[(a_0+\Delta a), j(\omega+\Delta\omega), j(B_e+\Delta B_e)\right]=0 \tag{4.41}$$

Limiting the Taylor expansion of M and N in expression (4.41) to the first order terms and then using relationship (4.40), we get

$$\begin{aligned}(\partial M/\partial a)\Delta a + (\partial M/\partial\omega)\Delta\omega + (\partial M/\partial B_E)\Delta B_e^+ = 0\\ (\partial N/\partial a)\Delta a + (\partial N/\partial\omega)\Delta\omega + (\partial N/\partial B_E)\Delta B_e^+ = 0\end{aligned} \tag{4.42}$$

On evaluating $(\partial M/\partial B_E)$, $(\partial N/\partial B_E)$ and substituting their expressions into relationship (4.42) we obtain

$$\begin{aligned}(\partial M/\partial a)\Delta a + (\partial M/\partial\omega)\Delta\omega = -(B_C+B_B)\Delta B_E^+\\ (\partial N/\partial a)\Delta a + (\partial N/\partial\omega)\Delta\omega = -(G_C+G_B)\Delta B_E^+\end{aligned} \tag{4.43}$$

Solving these simultaneous equations for Δa and $\Delta\omega$ we get

$$\Delta a = \frac{-\left[(B_C+B_B)(\partial N/\partial\omega)-(G_C+G_B)(\partial M/\partial\omega)\right]\Delta B_e^+}{(\partial M/\partial a)(\partial N/\partial\omega)-(\partial M/\partial\omega)(\partial N/\partial a)} \tag{4.44a}$$

$$\Delta\omega = \frac{\left[(B_C+B_B)(\partial N/\partial a)-(G_C+G_B)(\partial M/\partial a)\right]\Delta B_e^+}{(\partial M/\partial a)(\partial N/\partial\omega)-(\partial M/\partial\omega)(\partial N/\partial a)} \tag{4.44b}$$

It should be pointed out that the quantities above are calculated at ω_0

and a_0, Therefore knowing the amplitude and frequency characteristics of the transistor parameters about the original steady state values (a_0, ω_0), the amplitude and frequency sensitivity of the oscillator can be predicted. These are normally defined as

$$(\Delta a/a_0)/(\Delta B_e^+/B_e^+) \ , \quad (\Delta\omega/\omega_0)/(\Delta B_e^+/B_e^+)$$

respectively.

Evaluation of the expressions (4.44a) and (4.44b)

These expressions are derived on the basis of local linearization. The partial differential terms are carried out at $a=a_0$ and $\omega=\omega_0$. A direct approach will be to differentiate the constituent terms of M and N individually and in places where the terms involve transistor parameters, we use the slope of the tangent to the characteristic curves, obtained by measurements. This approach is very time consuming. A more reasonable approach is as follows:

At the steady state, $(a_0, j\omega_0)$ we have $M+jN=0$. M and N are the real and imaginary parts of the circuit determinant

$$\Delta = \begin{vmatrix} Y_{11b}^+ + Y_c^+ + Y_b^+ & Y_{12b}^- - Y_b^+ \\ Y_{21b}^- - Y_b^+ & Y_{22b}^+ + Y_e^+ + Y_b^+ \end{vmatrix}$$

As an approximation let us assume that the characteristic curves of the transistor parameters are linear for increments up to 5 % from the point of reference $(a_0, j\omega_0)$. This is illustrated in Fig. 4.20.

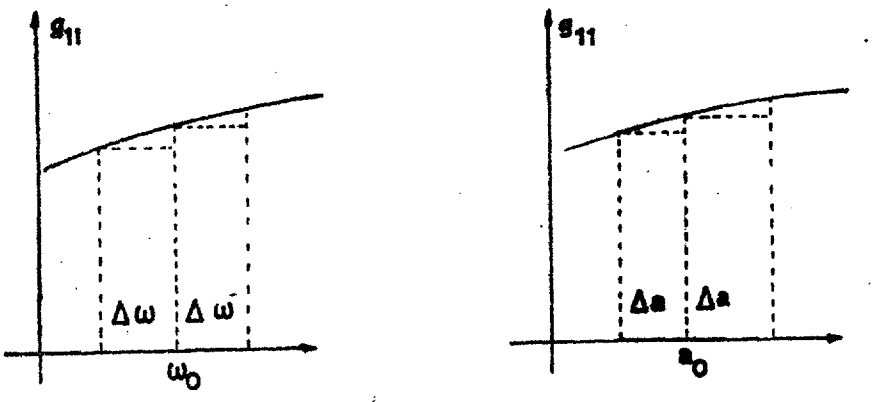

Fig. 4.20 Local linearization at the steady state $(a_0, j\omega_0)$

We can now measure the transistor parameters at $a=a_0+\Delta a$ and $\omega=\omega_0+\Delta\omega$. The embedding network is recalculated for the new frequency (keeping amplitude constant) or for the new amplitude (keeping frequency constant) e.g.

$jB_e^+=j(\omega_0+\Delta\omega)C_c^+$; $jB_e=jB_e\left[(\omega_0+\Delta\omega), a_0\right]$ keeping "a_0" constant

$jB_e^+=j(\omega_0)C_c^+$; $jB_e=jB_e\left[(a_0+\Delta a), \omega_0\right]$ keeping "ω_0" constant

A new circuit determinant can be constructed for the state $(a_0+\Delta a, \omega_0)$

$$\Delta = \begin{vmatrix} Y'_{11b}+Y_c^{+'}+Y_b^{+'} & Y'_{12b}-Y_b^{+'} \\ Y'_{21b}-Y_b^{+'} & Y'_{22b}+Y_e^{+'}+Y_b^{+'} \end{vmatrix}$$

The real and imaginary parts of this new circuit determinant will not

be zero value in general. They are:-

$$M' = \Delta M$$

$$N' = \Delta N$$

Since these increments are due to the increments in "a", we have the relationships

$$\partial M/\partial a = \Delta M/\Delta a\Big|_{a_0,\omega_0} = M'/0.005a_0$$

$$\partial N/\partial a = \Delta N/\Delta a\Big|_{a_0,\omega_0} = N'/0.005a_0$$

The values of $\partial M/\partial \omega$ and $\partial N/\partial a$ can be evaluated in a similar way. As expressions (4.44a) and (4.44b) are of an approximate nature (relying on the validity of local linearization), the proposed method of approximation is compatible to the degree of accuracy required. Substituting these values of the partial differential terms into expressions (4.44a) and (4.44b), we will be able to find numerical values for the amplitude and frequency sensitivity of the oscillator.

4.11 A High "Q" Oscillator

Consider the case when one of the external arm admittance is given by the series connection shown in Fig. 4.21a, where "r" is very small compared to $\omega_0 L$ or $1/\omega_0 C$.

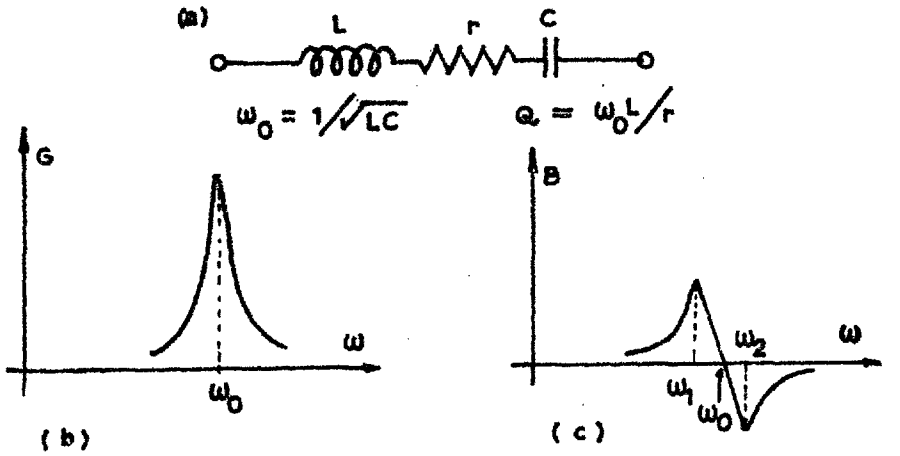

Fig. 4.21 A series-resonant arm and its frequency characteristics

We have Y = G+jB where

$$G = \frac{r}{r^2 + \left[\omega L - (1/\omega C)\right]^2}$$

$$B = \frac{1/\omega C - \omega L}{r^2 + \left[\omega L - (1/\omega C)\right]^2}$$

The frequency characteristics of G and B are given in Figs. 4.22b and 4.22c respectively. At the resonant frequency we get G=1/r and B = 0. Differentiating B with respect to ω and assuming $r \ll \omega L$, we find

$$B_{max} = 1/2r \; ; \qquad B_{min} = -1/2r$$

$$\omega_1 = \omega_0\left[(1-1/2Q)\right] \; ; \; \omega_2 = \omega_0\left[1+(1/2Q)\right]$$

In the vicinity of $\omega=\omega_0$, G can be rewritten as

$$G = \frac{1}{r}\left[\frac{1}{1+(q\,\delta\omega)^2}\right] \qquad (4.45a)$$

where $q = 2Q/\omega_0$

We can now move the origin of the co-ordinate system to $\omega=\omega_0$ and let the frequency variable be $\delta\omega=\omega-\omega_0$ i.e. considering only small variations of frequency about $\omega=\omega_0$. On differentiating G with respect to $\delta\omega$, we obtain

$$\frac{\partial G}{\partial(\delta\omega)} = \frac{\partial G}{\partial\omega} = -\frac{1}{r}\,\frac{2q^2\delta\omega}{\left[1+(q\,\delta\omega)^2\right]^2} \qquad (4.45b)$$

Similarly we find

$$B = -\frac{1}{r}\left[\frac{q\delta\omega}{1+(q\delta\omega)^2}\right] \qquad (4.46a)$$

$$\frac{\partial B}{\partial\omega} = +\frac{1}{r}\,\frac{q\left[1-(q\delta\omega)^2\right]}{\left[1+(q\delta\omega)^2\right]^2} \qquad (4.46b)$$

From expressions (4.45b) and (4.46b), we find

$$\mu = (\partial G/\partial\omega)/(\partial B/\partial\omega) = \frac{-2(q\delta\omega)}{1-(q\delta\omega)^2} \qquad (4.47)$$

Let the resonance arm be inserted in the port opposite the emitter terminal as shown in Fig. 4.22.

For a high "Q" oscillator e.g. crystal oscillator, the frequency of oscillation $\omega=\omega_0+\delta\omega$ is known to deviate only slightly from the resonant frequency ω_0. $\delta\omega/\omega_0$ is of the same order of magnitude as Q. Consider

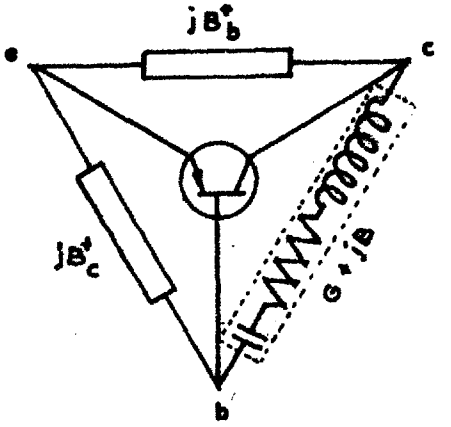

Fig. 4.22 Transistor oscillator having a high "Q" resonant arm admittance

the simplest example, when the frequency of operation is in fact the resonant frequency ω_0. We find

$$\partial M/\partial\omega = (B_B + B_E)(\partial B_e^+/\partial\omega) = +(q/r)(B_B + B_E) \qquad (4.48)$$

$$\partial N/\partial\omega = (G_B + G_E)(\partial B_e^+/\partial\omega) = +(q/r)(G_B + G_E) \qquad (4.49)$$

Using these relationships in expressions (4.44a) and (4.44b) we find

$$\frac{\Delta a}{\Delta B_e^+} = \frac{(B_C + B_B)(G_B + G_E) - (G_C + G_B)(B_B + B_E)}{(\partial M/\partial a)(G_B + G_E) - (\partial N/\partial a)(B_B + B_E)}$$

$$\frac{\Delta \omega}{\Delta B_e^+} = \frac{(G_C + G_B)(\partial M/\partial a) - (B_C + B_B)(\partial N/\partial a)}{(G_B + G_E)(\partial M/\partial a) - (B_B + B_E)(\partial N/\partial a)} \left(\frac{r}{q}\right)$$

In practice it is not possible to have things perfect and the frequency of oscillation will be slightly different from ω_0. This

deviation from the resonant frequency is often known as frequency pulling. In this more general case we find

$$\partial M/\partial\omega = (B_B + B_E) + \mu (G_B + G_E)(\partial B_e^+/\partial\omega) \qquad (4.50a)$$

$$\partial N/\partial\omega = (G_B + G_E) + \mu (B_B + B_E)(\partial B_e^+/\partial\omega) \qquad (4.50b)$$

where $(\partial B_e^+/\partial\omega)$ is given by expression (4.46b). It is seen that in these new relationships the frequency deviation $\delta\omega$ plays a part. It should also be remembered that it is an experimental fact that $\delta\omega/\omega_0$ is the same order of magnitude as Q for high Q oscillators. Further operations directed to the evaluation of the sensitivity expressions are best done numerically.

4.12 Crystal Oscillator Design

The high "Q" external admittance can be realized by a quartz crystal. The design of crystal oscillator is considered to an art by established workers[3,4,5,6] in the field. A survey of the available literature indicates that there is yet no single well defined procedure for crystal oscillator design. The design theory proposed in this thesis provides a straight forward method, which is an improvement over the earlier treatments of crystal oscillator design.

The typical equivalent circuit of a quartz crystal is given in Fig. 4.23.

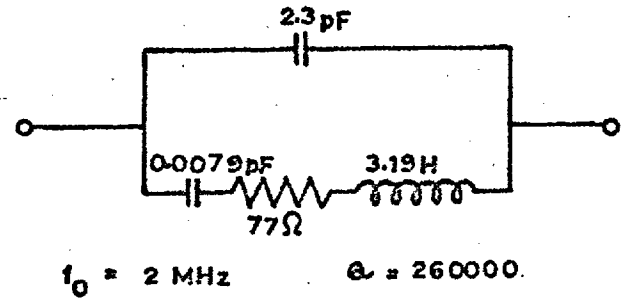

Fig. 4.23 Equivalent circuit of a typical quartz crystal

Discussions in Section 4.11 has shown that frequency sensitivity is lowest when the resonance arm is operated at its resonant frequency, ω_0. At the resonant frequency the admittance of the crystal is given by $Y^+_{res} = G^+_{res} + jB^+_{res}$ where

$$G^+_{res} = 1/r \qquad (4.51)$$

$$B^+_{res} = \omega_0 C_0 \qquad (4.52)$$

The dissipative conductance G^+_{res} must be less than the maximum load calculated for the port to which the crystal is inserted.

At this stage the question of selecting the amplitude of operation for the controlling voltage v_c arises. To be able to answer this question, it is necessary to know the nature of the nonlinearity governing the operation of the system. It has already been shown in chapter two that an analytical treatment of the nonlinearity can only be carried out for very idealized cases. In face of the elusive nature of the nonlinearities, the above question cannot yet be answered categorically. However we are helped in our choice by the following considerations:

(1) The amplitude $|v_c|$ should be large enough to tolerate small swings of amplitude without being forced into the linear region. Let the critical amplitude be $|v_c|_{crit}$, then we must ensure $|v_c| + \delta|v_c| < |v_c|_{crit}$. For practical reasons the allowable swing is 10 per cent.

(2) The amplitude should not be larger than sufficient. This is to avoid other unexpected nonlinear effects.

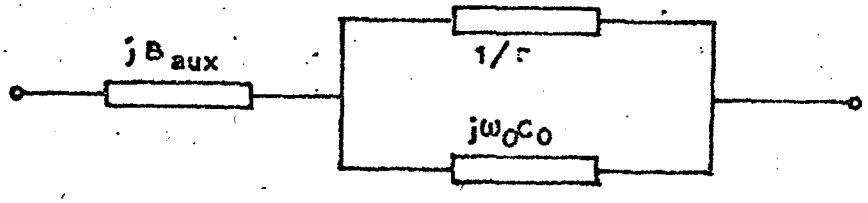

Fig. 4.24 Auxiliary susceptance added to crystal arm

Using these two considerations as a guide, the amplitude chosen is $|v_c| = 1.2\ |v_{crit}|$, where v_{crit} is the critical voltage at which nonlinear action begins. Another consideration is the rate of change of parameters with respect to variations in $|v_c|$. This has to be considered individually for individual devices.

Given the amplitude $|v_c|$ and the frequency ω_0, the transistor can now be measured and the indefinite admittance matrix for the device constructed. Knowing the load G^+_{res} together with any other load say G^+_e and the transistor parameters, we can construct the locus of steady state oscillation. The insertion of the crystal susceptance $B^+_{res} = \omega_0 C_0$ fixes one co-ordinate of the operation point in the geometry. The other two co-ordinates can be calculated. We thus have a straight forward procedure of synthesizing the crystal oscillator.

An improvement can be made by the addition of either an auxiliary capacitance or an auxiliary inductance to the resonant circuit, as shown in Fig. 4.24.

Since $1/r \ll \omega_0 C_0$, the new arm admittance is given by $Y^{+'}_{res} = G^{+'}_{res} + jB^{+'}_{res}$ where

$$G^{+'}_{res} = 1/r \tag{4.53}$$

$$B^{+'}_{res} = 1/r^2 B^+_{aux} \tag{4.54}$$

where $B^{+'}_{aux}$ is either $\omega_0 C^+_{aux}$ or $-1/\omega_0 L^+_{aux}$. The modified susceptance of the resonant arm gives the designer an additional degree of freedom by making the value of B^+_{res} controllable. Since the "Q" value of B^+_{aux} is much smaller than that for the series resonant arm of the crystal,

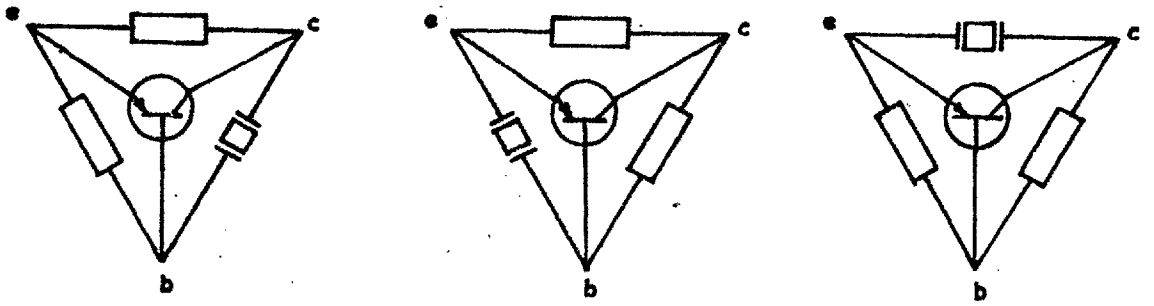

Fig. 4.25 The possible positions for inserting the crystal

the values of $\partial M/\partial\omega$ and $\partial N/\partial\omega$ will not be modified by the additional susceptance. The same procedure described earlier can then be used to find the necessary embedding network for steady state oscillation. The question now arises as where to insert the crystal. This depends on three considerations:-

(1) Crystal is inserted at the port where power dissipation in the crystal is lowest.

(2) Crystal is inserted at the port whereby the resulting limit cycle for the system so produced will be most stable.

(3) Crystal is inserted at the port where as a result the embedding elements required are most easily realized.

It is therefore necessary to calculate the performances of all three possible cases and then on the basis of the above considerations choose the most suitable port for insertion.

4.13 The "Y" and "Z" Oscillator

In the earlier sections, the embedding network of the transistor was always transformed into a network comprising three admittances, Y_b^+, Y_e^+ and Y_c^+. Transistors amenable to such an analysis shall be called a "Y" oscillator. The dual to this configuration is the "Z" oscillator. In the "Z" oscillator case it is more convenient to

(a)

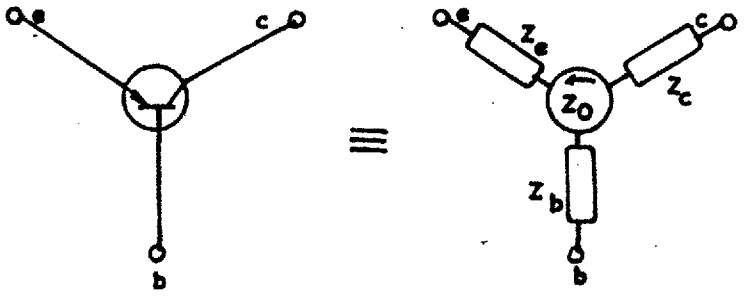

(b)

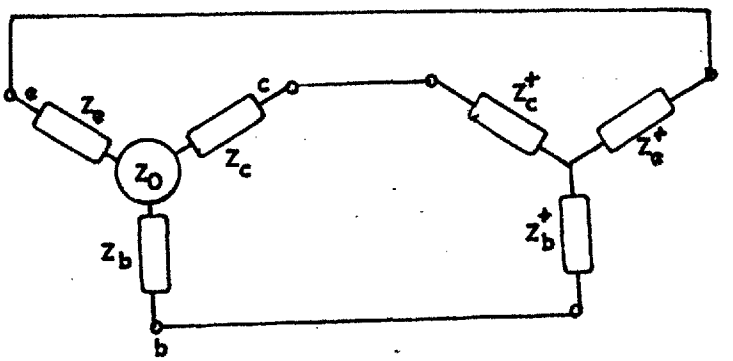

Fig. 4.26 Construction of the "Z" mode oscillator

transform the embedding network into a star network comprising three impedances, Z_b^+, Z_e^+ and Z_c^+. Instead of the indefinite admittance matrix, the indefinite impedance matrix of the transistor is used. The design expressions derived for the "Z" oscillator will be of the same form as those derived for the "Y" oscillator, with the admittances being replaced by the corresponding impedances of the network. The construction of the "Z" oscillator model is shown in Fig. 4.26. The condition for oscillation is:-

$$Z_B Z_E + Z_E Z_C + Z_C Z_B + Z_0^2 = 0 \qquad (4.55)$$

All the discussions presented earlier in connection with the "Y" oscillator will hold for the "Z" oscillator if we make the necessary translation of circuit parameters.

4.14 Soft Excitation and the Suppression of Unwanted Natural Frequencies

In Section 3.4 it was indicated that in the linear region of operation, the oscillator can be looked upon as a higher order linear differential equation. In order to solve for the characteristic roots (or natural frequencies of such a system, it is necessary to construct the circuit determinant for the network. As an example consider the CR oscillator shown in Fig. 4.27.

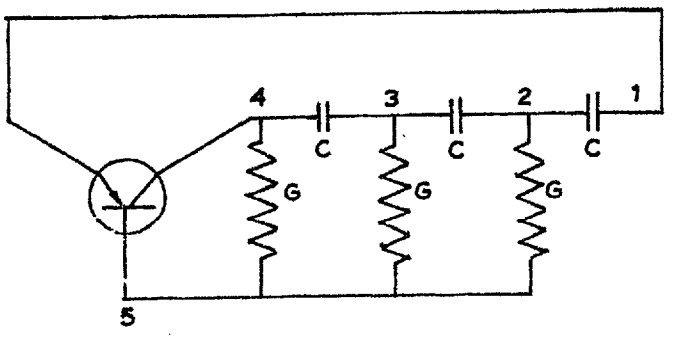

Fig. 4.27a Schematic diagram of a CR oscillator

In the initial linear region of operation (see Section 3.4) the circuit matrix for the above network is:-

$$\begin{bmatrix} i_1 \\ i_2 \\ i_3 \\ i_4 \end{bmatrix} = \begin{bmatrix} y_{11}(s)+sC & -sC & 0 & y_{12}(s) \\ -sC & G+2sC & -sC & 0 \\ 0 & -sC & g+2sC & -sC \\ y_{21}(s) & 0 & -sC & y_{22}(s)+G+sC \end{bmatrix} \begin{bmatrix} v_1 \\ v_2 \\ v_3 \\ v_4 \end{bmatrix} \qquad (4.56)$$

The subscripts of the current variables indicate the relevant nodes of the network, and the subscripts of the voltage variables refer to the voltage between the relevant node and the common node 5. In order to solve equation (4.56) for its natural frequencies, it is necessary to know the polynomial functions y_{11}, y_{12}, y_{21} and y_{22} explicitly in terms

of the complex frequency variable "s". This in turn requires knowledge of the transistor equivalent circuit. A simple transistor equivalent circuit is shown in Fig. 4.27b. The circuit matrix for this equivalent circuit is:-

$$\begin{bmatrix} i_1 \\ i_6 \\ i_4 \end{bmatrix} = \begin{bmatrix} g_e & -g_e & 0 \\ -g_e + \alpha g_e & g_e + g_b - \alpha g_e + sC_c & -sC_c \\ -\alpha g_e & -sC_c + \alpha g_e & sC_c \end{bmatrix} \begin{bmatrix} v_1 \\ v_6 \\ v_4 \end{bmatrix} \qquad (4.57)$$

The circuit matrix for the embedded transistor circuit as shown in Fig. 4.27c is:-

$$\begin{bmatrix} i_1 \\ i_2 \\ i_3 \\ i_4 \\ i_6 \end{bmatrix} = \begin{bmatrix} g_e + sC_c & -sC & 0 & 0 & -g_e \\ -sC_c & G + 2sC & -sC & 0 & 0 \\ 0 & -sC & G + 2sC & -sC & 0 \\ -+g_e & 0 & -sC_c & sC_c + G + sC & -sC_c + \alpha g_e \\ -g_e + \alpha g_e & 0 & 0 & -sC & -sC_c - \alpha g_e \end{bmatrix} \begin{bmatrix} v_1 \\ v_2 \\ v_3 \\ v_4 \\ v_6 \end{bmatrix}$$

(4.58)

On setting the determinant of the circuit matrix to zero, we obtain a polynomial equation in "s". The roots of this polynomial will define the initial stability of the system.

It is important for the oscillator to have only one pair of characteristic roots which will eventually grow into a stable limit cycle. In a well designed oscillator, all other roots decay away

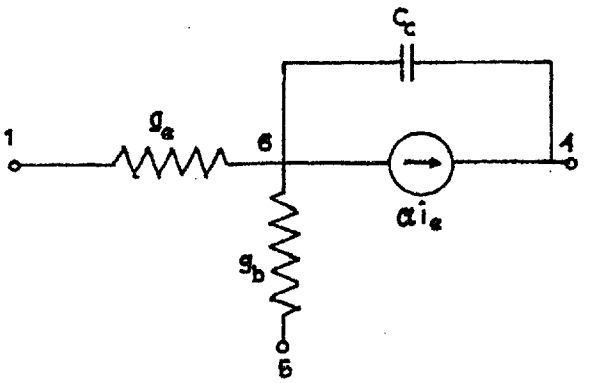

Fig. 4.27.b. Transistor equivalent circuit

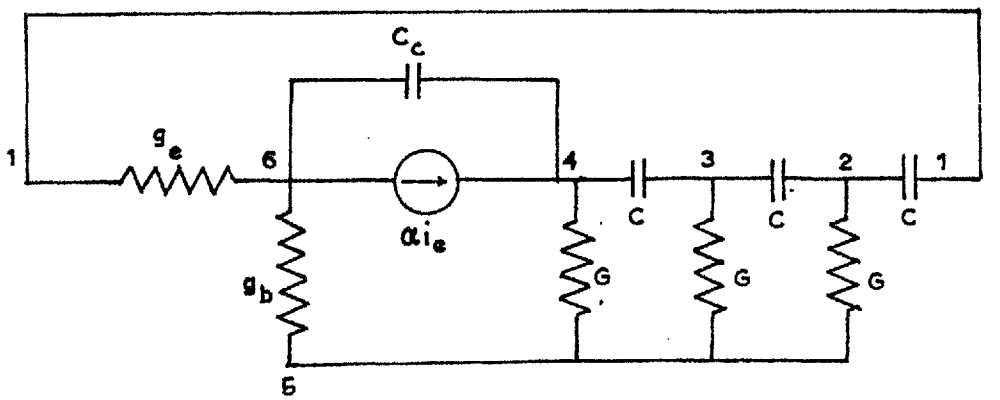

Fig. 4.27.c. Network representation of a CR oscillator in the linear region of operation

after a short time of their excitation. As an example assume the characteristic polynomial to be of 5th. order. The desired zero pattern of the determinant in the complex frequency plane is as shown in Fig. 4.28.

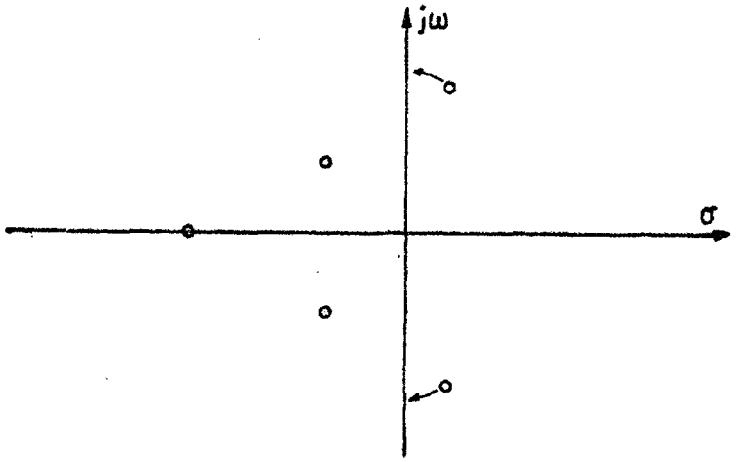

Fig. 4.28 A desired "complex frequency portrait" of the oscillator

As indicated in Section 2.8 there exist established methods for investigating the stability of linear systems. Examples of these are: (1) the algebraic methods of Routh and Hurwitz (2) The graphical methods of Nyquist and Mikhailov. However it is not easy to apply these methods to the design of transistor oscillators. An intuitive approach to stability investigation is presented in this section.

Consider the simple transistor oscillator shown in Fig. 4.29a.

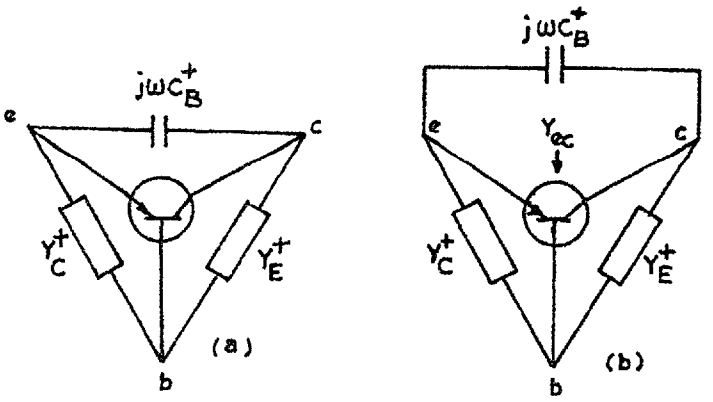

Fig. 4.29 Driving point admittance of the embedded transistor as "seen" by the element C_b^+

Let us extract the capacitor C_b^+ from the rest of the network. The condition of oscillation is:-

$$(Y_b + j\omega C_b^+)(Y_E + Y_C) + Y_E Y_C + Y_0^2 = 0 \qquad (4.59)$$

Relationship (4.58) can be rewritten as

$$j\omega C_b^+ = - \frac{Y_b Y_E + Y_E Y_C + Y_C Y_B + Y_0^2}{Y_E + Y_C} \qquad (4.60)$$

The quantity on the right hand side of equation (4.60) is in fact the driving point admittance Y_{ec} of the network as "seen" by the capacitor

C_b^+.

$$Y_{ec} = G_{ec}^+ + jB_{ec} = \frac{Y_b Y_E^+ Y_E Y_C^+ Y_C Y_B^+ Y_O^2}{Y_E + Y_C} \qquad (4.61)$$

The instantaneous power dissipation in the capacitor is:-

$$P(C_b^+) = (j\omega C_b^+)(|v_b|^2/2)(1-\cos(2\omega t)) \qquad (4.62)$$

The instantaneous power dissipation in the rest of the network is:-

$$P(G_{ec}^+ + jB_{ec}) = -(j\omega C_b^+)(|v_b|^2/2)(1-\cos(2\omega t)) \qquad (4.63)$$

From expressions (4.62), (4.63) and relationship (4.60) we find that the total instantaneous power of the oscillator is zero value, $P_T(j\omega) = 0$. In the case of the network oscillating with complex frequency $s = \sigma + j\omega$, we get

$$sC_b^+ = - G_{ec}(s) + jB_{ec}(s) \qquad (4.64)$$

The instantaneous power dissipated in the capacitor C_b^+ and the rest of the network are respectively:-

$$P(sC_b^+) = (sC_b^+)(|v_b|^2/2)\exp(2\sigma t)(1-\cos(2\omega t)) \qquad (4.65)$$

$$P(G_{ec}(s)+jB_{ec}(s)) = \left[(G_{ec}(s)+jB_{ec}(s))(|v_b|^2/2)\exp(2\sigma t)\right] \times (1-\cos(2\omega t)) \qquad (4.66)$$

The total instantaneous power of the network is again zero value. In the case of exponentially growing oscillation, the "generative" elements in the transistor will have to generate excess power so that energy in the storage elements (capacitances or inductances) can be

maintained at a constant exponential growth rate. It is found that energy consideration does not lead to a convenient criterion for soft excitation.

Consider now a passive CR embedding network, whose characteristic equation is a 4th order polynomial in "s". The circuit determinant Δ^+ can be written in terms of its characteristic roots.

$$\Delta^+ = [s-(-\sigma_0+j\omega_0)][s-(-\sigma_1+j\omega_1)][s-(-\sigma_1-j\omega_1)][s-(-\sigma_0-j\omega_0)] \tag{4.67}$$

The "zeros" pattern of this network is shown in Fig. 4.30. The modulus $|\Delta^+|$ will vary with frequency in a manner shown in Fig. 4.31. It is seen that the network exhibits a frequency selective effect. Its characteristic frequency is ω_0. In principle this passive network can always be transformed into a Δ or a star network at a given frequency. In order to shift the "zeros" to the right half plane and thus produce oscillation, a transistor is embedded into the passive network. On examining equation (4.58), it is seen that the transistor introduces an additional fifth root into the modified characteristic equation. One of this characteristic roots always lies on the negative σ axis. This is because of the following reason. The original d.c. bias point of the transistor is stable i.e. power generated by the active elements is not sufficient to produce a "build up" of stored d.c. energy in the capacitance of the transistor equivalent circuit. If more dissipative and storage elements are connected to the transistor, it will require even more

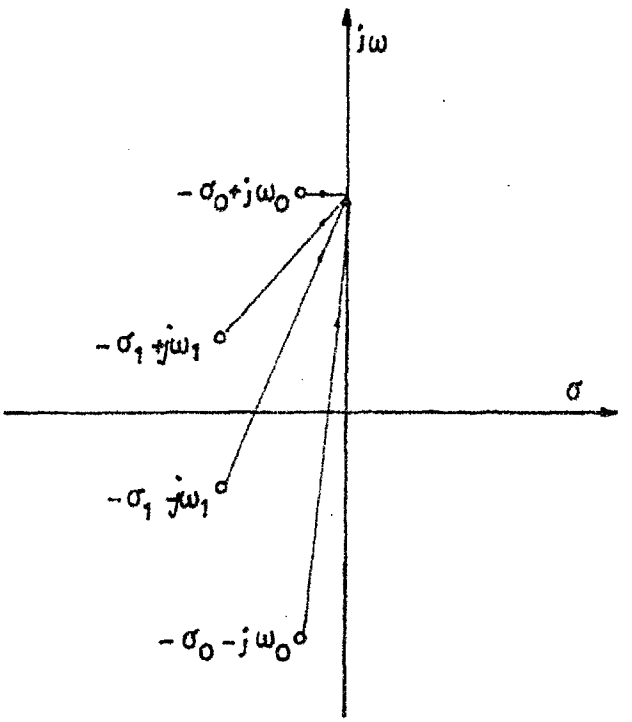

Fig. 4.30 The "zeros" pattern of a CR embedding network

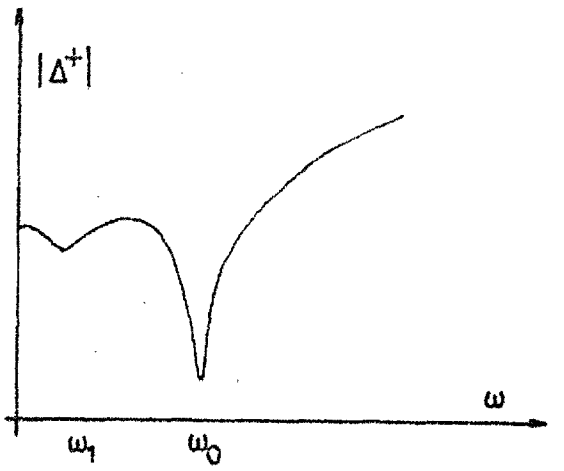

Fig. 4.31 The frequency characteristic of $|\Delta^+|$

energy from the active device to sustain a "build up" of d.c. stored energy. Therefore the single root must always be on the negative axis. It is only necessary to focus attention on the pairs of complex roots. In order to avoid the possibility of moving more than one pair of complex roots into the right half plane, it is desirable to have a pair of complex roots very near the jω axis and the other roots to be both far away from the point $j\omega_0$ and from the jω axis itself. This means that a notch filter effect is a desirable characteristic of the CR embedding network. Since the activity of the transistor increases with decreasing frequencies, it is most important to have roots with frequencies lower than ω_0, to be far off the jω axis. This will lessen the chance of producing unwanted natural frequencies with positive real parts. Also since the transistor parameters are known to be monotonic functions of frequency, the embedded transistor will preserve the same notch effect of the CR embedding. This means that the roots $(-\sigma_0 \pm j\omega_0)$ undergoes insignificant modification of its real frequency and any movement of its position will be along a line parallel to the line $j\omega = j\omega_0$. As the pair of roots $(-\sigma_0 \pm j\omega)$ are near to the jω axis, they will be easily moved into the right half plane by the addition of generative elements. The hypothetical movement of the "zeros" are shown in Fig. 4.32.

Let M+jn be the evaluated value of the circuit determinant for the embedded transistor. (note: lower case letters are used for "m" and "n" to indicate linear operation).

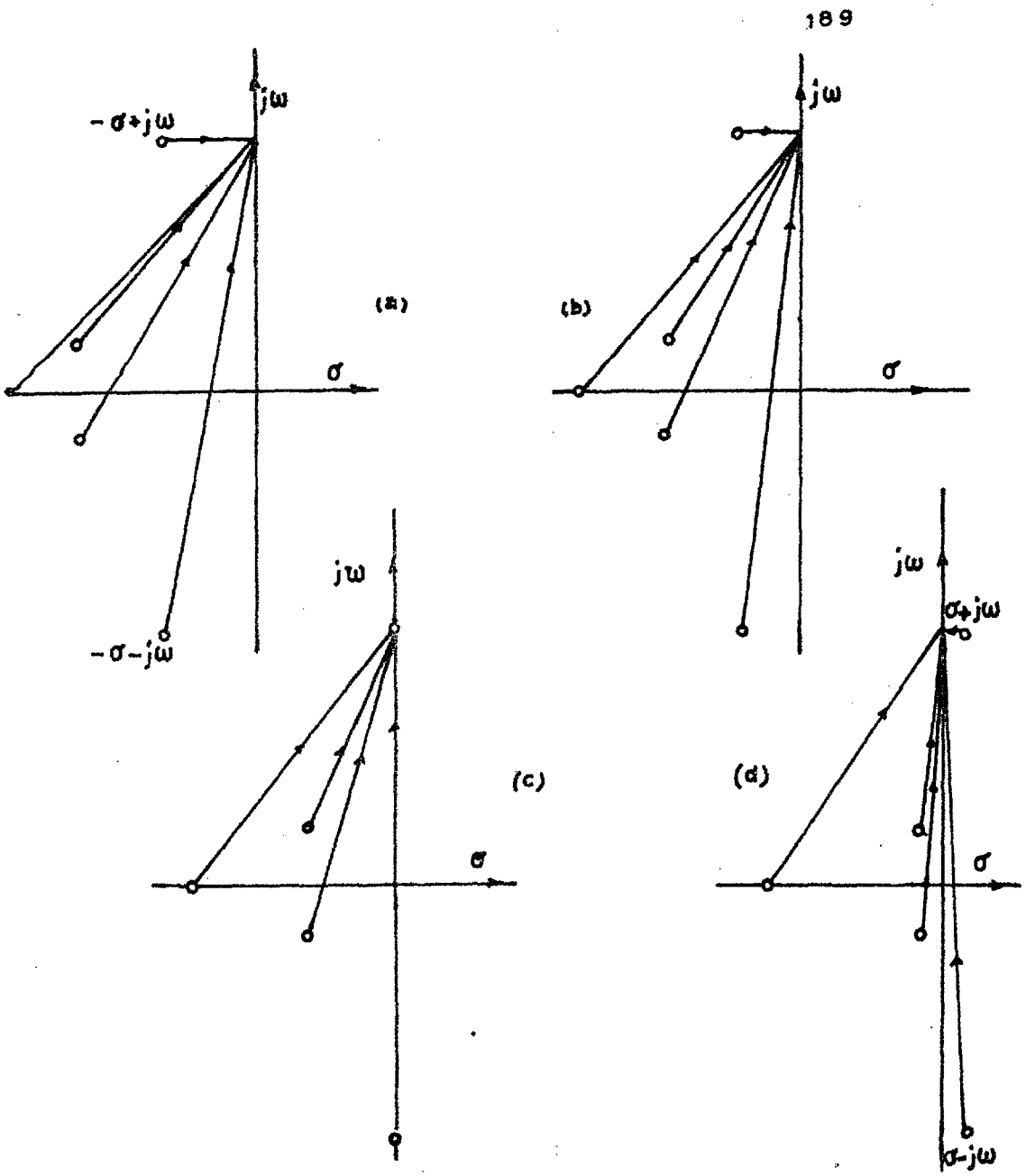

Fig. 4.32 The "zeros" pattern of the CR network embedded with a transistor. The progressive movement of a pair of roots into the right half plane is shown.

The condition for the existence of a pair of characteristic roots at frequency ω_0 can be written as

$$m + \left.\frac{\partial n}{\partial \omega}\right|_{\omega_0} \sigma = 0 \qquad (4.68a)$$

$$n - \left.\frac{\partial m}{\partial \omega}\right|_{\omega_0} \sigma = 0 \qquad (4.68b)$$

where $\sigma \ll \omega$

From these expressions we obtain

$$\sigma = - m/(\partial n/\partial \omega) = n/(\partial m/\partial \omega) \qquad (4.69)$$

Given any embedding network and knowing the real frequency of the characteristic root of interest, expression (4.69) can be used to predict initial instability. A more accurate approach will be the calculation of $-m/(\partial n/\partial \omega)$ and $n/(\partial m/\partial \omega)$ for a small range of frequencies around $\omega=\omega_0$. On plotting these quantities against frequency, we should obtain two intersecting curves as shown in Fig. 4.33. The frequency ω_1 at which the two curves intersect will be slightly different from ω_0, the characteristic frequency of the passive embedding network. Thus the problem of CR oscillator design, is simply one of filter synthesis. The designer is required to realize a passive network with the required "zero" pattern and then embed a transistor of sufficient activity into the passive network. A general synthesis method is beyond the scope of this thesis. It should be stated that the aim of this section is to clarify

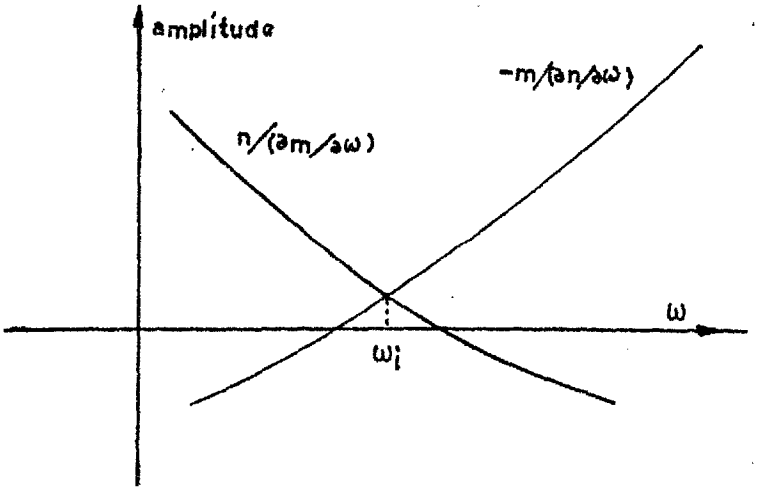

Fig. 4.33 The locating of a pair of characteristic roots slightly off the $j\omega$ axis in the right half plane

the mechanism underlying the soft excitation of a selected frequency. The strong filter action as a means of suppressing unwanted natural frequencies, follows from the discussion in this section.

4.15 Conclusion

In this chapter the condition for oscillation was examined. A geometrical model was constructed for the oscillation condition. Design expressions were derived for the maximally loaded oscillator. For the more general case the embedding network was found to be not unique. There

will be a choice of possible embedding networks. The choice is narrowed down by the requirements for good performance. These requirements are:-

(1) The criterion for stability of the steady oscillation to be satisfied (see Section 4.72).

(2) The criterion for soft excitation to be satisfied (see Section 4.13).

(3) The presence of a strong filter action to be ensured.

The expressions for frequency and amplitude sensitivity of a given oscillator were derived. The mechanism of frequency control in a crystal oscillator was discussed. The expressions for power dissipation of an oscillator were derived.

4.16 References and Bibliography

References

1. B. D. H. Tellegen, "The gyrator, a new electric network element", Philips Research Reports, 3, 2, p.81, April, 1948.

2. J. Shekel, "The gyrator as a three-terminal element", Proc. IRE, 41, p.1014, August 1953.

3. E. Hafner, "Analysis and design of crystal oscillators". Technical Report, U.S. Army Electronics Laboratories, Fort Monmouth, New Jersey, May 1964.

4. P. J. Baxandall, "Transistor crystal oscillators and the design of a 1-Mc/s oscillator circuit capable of good frequency stability", Radio and Electronic Engineer, Vol. 29, No. 4, April 1965.

5. E. P. Felch and J.O. Israel, "A simple circuit for frequency standards employing overtone crystals", Proc. IRE, pp.596-603, May 1955.

6. E. A. Gerber and R. A. Sykes, "State of the Art - Quartz Crystal units and oscillators", Proc. IEEE, Vol. 54, No.2, pp.103-116, February 1966.

Bibliography

1. R. Spence, "Linear active networks", post graduate lecture notes. Imperial College, 1967.

2. D. F. Page, "Instability in transistor circuits with passive feedback, with special reference to tuned oscillators and super-regenerative applications",Ph.D.thesis,Imperial College,London, 1959.

3. A. Singhakowinta, "Gain, sensitivity and stability of linear two-port amplifiers", Ph.D. thesis, Imperial College, London, 1964.

4. P. d. v.d. Puije, "Gain sensitivity of linear active networks", Ph.D. thesis, Imperial College, London, 1966.

5. E. A. Guillemin, "Introductory Circuit Theory", John Wiley & Sons, Book Co., 1953.

6. M. E. van Valkenberg, "Modern network synthesis", John Wiley & Sons, Book Co., 1964.

7. L. D. Pian, "Linear active network theory", Prentice-Hall Book Co., 1962.

8. J. M. Rollett, "Stability and power-gain invariants of linear two-ports", IRE Trans. on Ct. Th., CT-9, p.29, March 1962.

9. T. Fijallbrant, "Activity and stability of linear networks", Trans. IEEE on Ct. Th., CT-12, p.12, March 1965.

10. J. O. Scanlan and J. S. Singleton, "A linear theory of three-pole oscillators", Proc. IEE, Vol. 110, p.271, February 1963.

Chapter 5

Experimental Verification of the Proposed Design Theory

5.1 Measurements on the Transistor

In the proposed theory, the transistor is characterized by two sets of parameters. For the "Y" configuration, these are the small signal "y" parameters and the large signal "Y" parameters. We shall denote the initial state (focus point) by $S(\omega_s)$ and the steady state by $S(a_0,\omega_0)$. In order to predict the instability of $S(\omega_s)$ and the stability of $S(a_0,\omega_0)$, it is necessary to know the changes in transistor parameters with respect to small variations of frequency and amplitude about $S(\omega_s)$ and $S(a_0,\omega_0)$. Since we are dealing with small variations, the method of local linearization which was discussed in Section 4.10 can be used. Therefore the measured quantities characterizing the transistor are:

(1) For $S(\omega_s)$

$$\left[y_{ij}(\omega_s)\right] \quad ; \quad \left[y_{ij}(\omega_s + \Delta\omega).\right]$$

(2) For $S(a_0,\omega_0)$

$$\left[Y_{ij}(a_0,\omega_0)\right] \quad ; \left[Y_{ij}(a_0,\omega_0+\Delta\omega)\right] \quad ; \left[Y_{ij}(a_0+\Delta a,\omega_0)\right].$$

The square brackets above indicate the transistor indefinite admittance matrix. y_{ij} or Y_{ij} indicates the element in the ith. row and jth. column.

5.2 The Transformer Ratio-Arm Bridge

The small signal two-port parameters of the transistor can be measured on a standard transformer ratio-arm bridge. By monitoring the applied signal, the large signal parameters can also be measured. The essential features of a transformer ratio-arm bridge are shown in Fig. 5.1. The two halves of the secondary side of the input transformer are closed coupled, with equal voltages across them which are independent of loads. Balance is achieved by adjusting the current through Y_S (which usually consists of a parallel combination of variable resistance and capacitance) such that it cancels out the current through the unknown entering the detecting transformer at "D". When cancellation is complete, null voltage appears across the detecting transformer. The bridge used for the measurements in this thesis is the WAYNE KERR B601. For more detailed descriptions of this bridge, two monographs can be consulted, these are:

(1) "The transformer ratio-arm bridge", by R. Calvert, WAYNE KERR MONOGRAPH No. 1.

(2) "Semiconductor parameter measurements using transformer ratio-arm bridge", by B. Rogal, WAYNE KERR REPRINT.

In Section 2.3, it was shown that the d.c. bias point of the transistor readjust itself to large signal operation. This means that the biasing resistors of the transistor has to be taken into consideration. The simplest solution to this problem is to measure the parameters of the transistor together with its biasing resistors. These same biasing resistors are then used in the oscillator circuit. In this way any

change in the measured "Y" parameters due to readjustment of the d.c. bias point will be automatically taken care of and we shall have an accurate set of design parameters for large signal operation. The level of the controlling voltage v_c is monitored on a valve voltmeter. There will be a critical value of $|v_c|$ above which nonlinear action becomes appreciable. This value is called $|v_c|_{crit}$ for later reference. For values of $|v_c|$ such that $|v_c| < |v_c|_{crit}$, the transistor parameters are essentially linear. These are the small signal "y" parameters. For $|v_c| > |v_c|_{crit}$, the transistor parameters are nonlinear. These are the large signal "Y" parameters.

In order to construct the indefinite admittance matrix of the transistor, it is necessary to measure at least four of the matrix elements. The ones measured are shown in the "skeleton" matrix below:

$$\begin{array}{c} \\ b \\ e \\ c \end{array} \begin{array}{c} \begin{array}{ccc} b & e & c \end{array} \\ \begin{bmatrix} Y_{11} & & \\ & & Y_{23} \\ & Y_{32} & Y_{33} \end{bmatrix} \end{array}$$

From these four parameters the rest of the parameters are calculated using the property of "indefiniteness" of the matrix i.e. all rows and all columns add up to zero value. The schematic diagrams of the arrangements for measuring these four parameters are shown in Fig. 5.2.

A word of caution should be made in connection with large signal "Y" parameter measurements. It was explained in Chapter 2, that the

describing function method can be used in oscillator design, provided the excitation voltage is nearly sinusoidal. As the level of the applied voltage v_c is increased, the emitter current becomes increasingly nonsinusoidal. This current flows through the input transformer of the bridge, producing the excitation voltage. The bridge is basically designed for small signal parameter measurements, thus the impedance function of the input transformer is not designed for the suppression of unwanted higher harmonics. Because of this difficulty, the operation level of $|v_c|$ is chosen to be around $1.2\,|v_c|_{crit}$. For values of $|v_c|$ much higher than this, special arrangements would have to be made for the measurements. The design of a special bridge, having an input transformer with a frequency selective impedance function will be very welcome. This will aid further investigations of harmonic oscillators operating at very high emitter current levels. Such investigations are beyond the scope of this thesis. Finally the voltage v_c can be monitored on an oscilloscope to ensure nearly sinusoidal waveform during measurements.

5.3 The Scale of the Geometrical Model for Steady State Oscillation

In Chapter 4, the construction of a geometrical model for the oscillation condition was presented. Such a model provides a means of studying the limit cycle of the nonlinear process in terms of circuit parameters. By evaluating the values of the characteristic quantities

governing the form of the "geometry", we can see more clearly what sort of scale is involved. For this purpose a Germanium pnp transistor (OC 44) is chosen. It should be pointed out that no two transistors can have exactly the same set of parameters. Therefore the examples presented in this chapter are valid only for the individual transistor, whose parameters are used. A study of the spread in performance for different transistors using the same embedding network has not been undertaken in this thesis.

From a set of four measured "Y" parameters, the indefinite admittance matrix of the transistor can be constructed. The gyrator representation of the transistor can be constructed from the elements of the indefinite admittance matrix in turn. A set of typical values for the elements of the gyrator representation is shown in Fig. 5.3 and Fig. 5.4. These are calculated from "Y" parameters of an OC 44 transistor operated at $V_{cb} = 5v$, $I_e = 5$ mA, $a_o = |v_c| = 100$ mV (r.m.s.) and $\omega_o = 4\pi 10^6$ rad/s.

The circuit representation is shown in Fig. 5.5. From these values the characteristic quantities of the "geometry" can be calculated. They are:

$$\begin{aligned} P &= \sum G_b G_e + G_0^2 - B_0^2 &&= -228.69 \\ p &= -2\, G_0 B_0 &&= 136.20 \\ \alpha &= p/(G_e + G_c) &&= 17.73 \\ \beta &= p/(G_c + G_b) &&= 7.96 \\ \gamma &= p/(G_b + G_e) &&= 243.21 \end{aligned} \qquad (5.1)$$

(all values are in m$\mho$ or related units).

The "geometry" is shown in Fig. 5.6a. Since P is a negative quantity, the hyperboloid involved in the "geometry" is the hyperboloid of one sheet. The three intercepts of the associated plane are widely different in their values. In order to avoid the uncertainty of any dissipation that might be present in high frequency chokes, these are not used in the experimental circuits. Instead the transistor is biased through two biasing resistors (each of 3.3 kΩ). The values of the biasing resistors can be lumped onto the appropriate arm of the gyrator representation. The modified design parameters of the biased transistor are given in Fig. 5.5b. The modified characteristic quantities are:

$$\begin{aligned} P &= -223.30 \\ p &= 136.20 \\ \alpha &= 16.45 \\ \beta &= 7.82 \\ \gamma &= 158.37 \end{aligned} \qquad (5.2)$$

It is noticed that the inclination of the associated plane is changed by the introduction of the biasing resistors. The "geometry" is shown in Fig. 5.6b.

5.4 The Locus of Steady State Oscillation

The condition for steady state oscillation is:

$$B_B B_E + B_E B_C + B_C B_B = P \tag{5.3}$$

$$(G_e + G_c)B_B + (G_c + G_b)B_E + (G_b + G_e)B_C = p \tag{5.4}$$

For the biased transistor shown in Fig. 5.5b, we have

$$B_B B_E + B_E B_C + B_C B_E = 223.30 \tag{5.5}$$

$$(G_e + G_c)B_B + (G_c + G_b)B_E + (G_b + G_e)B_C = 136.20 \tag{5.6}$$

The intersection of the plane (5.6) with the hyperboloid (5.5) produces the locus of steady state oscillation. The locus of intersection can take the form of a closed curve, "quasi ellipse" or an open ended curve, "quasi hyperbola". The qualifying adjective "quasi" is used because the locus is not a perfect ellipse or a perfect hyperbola. The modification is due to the surface being not a cone but a hyperboloid. Which of these two forms, the locus takes will be dependent on the inclination of the associated plane. The case of a "quasi hyperbolic" locus is shown in Fig. 5.7 and that of a "quasi elliptical" locus is shown in Fig. 5.8. We shall now define the asymptote angle of the hyperboloid. Consider the "associated" right angle cone of the hyperboloid surface as shown in Fig. 5.9. The circular cross section A E D F is made by a plane of equal inclination cutting the cone. E O F is a right angle triangle with OE = OF. OE = OF = OD. OC is the median of triangle EOF. Produce OC to the point B. Raise a perpendicular at point B to intersect the cone at point A. Angle AOB

will be defined as the asymptote angle θ_H of the hyperboloid surface, associated with the condition of oscillation. θ_H is found to be:

$$\theta_H = \tan^{-1}(2\sqrt{2} / 5) = \tan^{-1} 0.56 \qquad (5.7)$$

Similarly the angles of inclination θ_B, θ_E and θ_C of the associated plane can be defined. The associated plane is shown in Fig. 5.10. It intersects the three axes at points α, β and γ. OM is the median of the triangle $O\gamma\beta$. The angle of inclination to the B_C axis is called θ_C. The other two angles of inclination θ_B and θ_E are similarly defined.

We find

$$\theta_B = \tan^{-1} 2\alpha/\sqrt{\beta^2 + \gamma^2} \qquad (5.8a)$$

$$\theta_E = \tan^{-1} 2\beta/\sqrt{\gamma^2 + \alpha^2} \qquad (5.8b)$$

$$\theta_C = \tan^{-1} 2\gamma/\sqrt{\alpha^2 + \beta^2} \qquad (5.8c)$$

In order to produce a "quasi elliptical" locus of steady state oscillation, all these three angles must be larger than θ_H. Failing this we will have the case of a "quasi hyperbolic" locus of steady state oscillation. The angles of inclination θ_B, θ_E and θ_C for the set of values given in (5.2) are:-

$$\begin{aligned} \theta_B &= \tan^{-1} 0.21 \\ \theta_E &= \tan^{-1} 0.10 \\ \theta_C &= \tan^{-1} 17.39 \end{aligned} \qquad (5.9)$$

Comparing these angles with θ_H, we find that the criterion for the existence of a "quasi elliptical" locus is not satisfied. It is noticed that the associated plane can be tilted by the addition of a

conductive load to any of the "arms" of the gyrator representation. Consider the addition of $G_e^+ = 12$ m℧ to the "arm" Y_e of the gyrator representation shown in Fig. 5.5b. We obtain a new set of design parameters:

$$\begin{aligned} Y_b &= 5.00 - j15.07 \\ Y_E &= 7.86 + j15.33 \\ Y_C &= 12.42 - j12.86 \\ Y_O &= 4.46 - j15.27 \end{aligned} \tag{5.10}$$

The angles of inclination θ_B, θ_E and θ_C for this modified set of values are:

$$\begin{aligned} \theta_B &= \tan^{-1} 1.02 \\ \theta_E &= \tan^{-1} 1.25 \\ \theta_C &= \tan^{-1} 2.05 \end{aligned} \tag{5.11}$$

The criterion for a close locus is satisfied for this modified system. The extreme values of the co-ordinates contained in the locus are given by expressions of the form (see Section 4.6),

$$\overset{\wedge\vee}{B}_C = \frac{G_O B_O G_c \pm \sqrt{(\Sigma G_b G_E + G_c^2)(B_O^2 - \Sigma G_b G_E)(\Sigma G_b G_E + G_O^2)}}{\Sigma G_b G_E} \tag{5.12}$$

On evaluating the expressions for B_B, B_E and B_C we obtain

$$\begin{aligned} \hat{B}_B &= 8.21 & \check{B}_B &= -4.79 \\ \hat{B}_E &= 9.71 & \check{B}_E &= -4.33 \\ \hat{B}_C &= 12.41 & \check{B}_C &= -3.92 \end{aligned}$$

(all quantities are in m ℧ units)

Knowing the bounds on the locus and the pair of simultaneous equations (5.5) and (5.6) we can calculate the points constituting the whole locus. This is done by setting a value for one of the co-ordinates and then solving the pair of simultaneous equations for the other two. On doing this for the set of design parameters (5.10), we obtain the locus shown in Fig. 5.11. It is noticed that the whole locus lies

(1) to right hand side of the ordinate $B_b = -15.07$ m℧
(or $\check{B}_B > B_b$)

(2) to the left hand side of the ordinate $B_e = 15.33$ m℧
(or $\hat{B}_E < B_e$)

(3) to the right hand side of the ordinate $B_c = -12.86$ m℧
(or $\check{B}_C > B_c$).

Therefore any set of external embedding (B_b^+, B_e^+, B_c^+), which satisfies the condition for steady state oscillation, must always comprise one negative susceptance and two positive susceptances. In this case, B_b^+ and B_c^+ have to be capacitive and B_e^+ inductive. This means that for the "conductive state" given by the real parts of the admittances in data (5.10), the oscillator circuit assumes the Colpitts configuration. However, this need not always be the case. For other "conductive states" we may well have the following geometrical feature:

(1) $\check{B}_B > B_b$
(B_b being negative)

(2) $\hat{B}_E < B_e$
(B_e being positive)

(3) $\hat{B}_C > B_c > \check{B}_C$

In this case we find: (a) Those points of the locus, which lie between $\hat{B}_C$ and B_c, will have B_b^+ capacitive; B_e^+ inductive and B_c^+ capacitive. These points will correspond to embeddings belonging to the basic Colpitts configuration. (b) Those points of the locus which lie between $\check{B}_C$ and B_c, will have B_b^+ capacitive; B_e^+ inductive and B_c^+ inductive. These points will correspond to embeddings belonging to the basic Hartley configuration. For the case of the "quasi hyperbolic" locus, there will be less restriction on the values of the co-ordinates corresponding to points on the locus. Therefore the types of configurations possible are also increased. However, not all points on the locus (either "quasi hyperbolic" or "quasi elliptical") will represent systems with stable oscillation. The criteria of stability (see Section 4.7.2 and Section 4.14) can be used to investigate individual cases of embeddings.

5.5 A Test Oscillator

5.5.1 Synthesis of an oscillator circuit which corresponds to a selected point on the locus of steady state oscillation

Given the "conductance state" of the biased and conductively loaded transistor, the embedding network required to produce steady state oscillation will correspond to any point on the locus of oscillation (see Fig. 11.), which satisfy the stability criteria

(see Section 4.7.2 and Section 4.14). In this section we shall consider a simple delta embedding network. Each of the arms of the delta network comprises of a single circuit element; either a capacitor or an inductor.

In the discussions on the filter action of the embedding network, it was stated that a strong filter action enhances stability of the steady state oscillation and that it is also a pre-requisite for the Describing Function Method. It has been stated that a necessary condition for the existence of a strong filter action, is to have $|\Delta^+|$, (the circuit determinant of the embedding network) to be a minimum and very close to zero value at the frequency of oscillation. Any point on the locus of Fig. 5.11 will be determined by the co-ordinates (B_B, B_E, B_C). Knowing the "susceptance state" of the transistor i.e. the values of B_b, B_e, B_c and B_0, we can calculate the embedding elements corresponding to the point (B_B, B_E, B_C) on the locus of oscillation. We find:

$$\begin{aligned} B_b^+ &= B_B - B_b \\ B_e^+ &= B_E - B_e \\ B_c^+ &= B_C - B_c \end{aligned} \qquad (5.13)$$

The determinant of the lossless embedding is:

$$\Delta^+ = B_b^+B_e^+ + B_e^+B_c^+ + B_c^+B_b^+ \qquad (5.14)$$

In Fig. 5.12, Δ^+ is plotted against the co-ordinates of points lying on the locus of Fig. 5.11. It is seen that Δ^+ reaches a minimum *modulus* near the point P_1 where $B_B = 0\,m\mho$, $B_E = 8.97\,m\mho$, $B_C = -1.59\,m\mho$.

The set of embedding elements is found to be $B_b^+ = 15.07$ m$\mho$, $B_e^+ = -6.36$ m$\mho$, $B_c^+ = 11.27$ m$\mho$. The corresponding circuit elements are:

$$\begin{aligned} C_b^+ &= 1199 \text{ pF} \\ L_e^+ &= 13 \ \mu\text{H} \\ C_c^+ &= 897 \text{ pF} \end{aligned} \tag{5.15}$$

The synthesized oscillator circuit corresponding to the set of embedding values (5.15) is shown in Fig. 5.13. The calculated and the measured performances are given in Table 5.1a.

TABLE 5.1a

Quantities	Designed Performance	Measured Performance
v_c	100.00mV (r.m.s.)	95.00 mV (r.m.s.)
v_e	97.00mV (r.m.s.)	100.00 mV (r.m.s.)
f_o	2.00 MHz	1.92 MHz
η_o	42 %	unable to measure directly
η_c	0.7 %	

(The expressions for $|v_e|$, η_o and η_c are given in Section 4.8).

Three important features of this circuit are noticed. They are:

(1) η_c (i.e. the d.c. to a.c. conversion efficiency) is very small.

(2) η_o (i.e. the efficiency of channelling the a.c. energy generated in the system to the load), is only 42% . The rest of the

energy is dissipated in the transistor itself.

(3) On setting $\Delta^+ = 0$, we find the resonant frequency of the lossless embedding to be $f_0^+ = \omega_0^+/2\pi = 1.96$ MHz. In this case f_0^+ is very close to the actual frequency of oscillation (designed to be $f_0 = 2.0$ MHz).

In order to complete the table of performance, it is necessary to have some indications of the frequency and amplitude sensitivity of the steady state oscillation with respect to small variations in circuit parameters. To fascilitate experimental investigation we shall consider the effect of the small changes $\Delta C_b^+ = 50$ pF, $\Delta C_c^+ = 50$ pF and $\Delta G_e^+ = 0.1$ m$\mho$ respectively. The corresponding susceptances will be given by $\Delta B_b^+ = \omega_0 \Delta C_b^+$, $\Delta B_c^+ = \omega_0 \Delta C_c^+$. The expressions for the incremental changes in amplitude and frequency are given in Section 4.10. In the case where the change in performance is due to a small change in arm conductance, we find expressions of the form,

$$\Delta a = \frac{\left[(B_C+B_B)(\partial M/\partial\omega)-(G_C+G_B)(\partial N/\partial\omega) \right] \Delta G_e^+}{(\partial M/\partial a)(\partial N/\partial\omega)-(\partial M/\partial\omega)(\partial N/\partial a)} \qquad (5.16)$$

$$\Delta\omega = \frac{-\left[(B_C+B_B)(\partial M/\partial a)-(G_C+G_B)(\partial N/\partial a) \right] \Delta G_e^+}{(\partial M/\partial a)(\partial N/\partial\omega)-(\partial M/\partial\omega)(\partial N/\partial a)} \qquad (5.17)$$

As recommended in Section 4.10, we shall evaluate the quantities $S_G^a(\Delta a, \Delta G_e^+) = (\Delta a/a)/(\Delta G_e^+/G_e^+)$ $S_G^\omega(\Delta\omega, \Delta G_e^+) = (\Delta\omega/\omega)/(G_e^+/G_e^+)$ etc. from three sets of design parameters. These are:

(1) design parameters for the steady state $S(a_0, \omega_0)$; where $a_0 = 100$ mV, $\omega_0 = 4\pi 10^6$ rad./s.

(2) design parameters for the adjascent state $S(a_0+\Delta a, \omega_0)$;

where $a = -5mV$,

(3) design parameters for the adjascent state $S(a_0, \omega_0+\Delta\omega)$;

where $\Delta\omega = -0.05\ \omega_0 = -0.63 \times 10^6$ rad./s. For the set of embedding elements given in data (15.15) and the loaded transistor characterized by data (5.10), we obtain the following design data: (all admittances are in m$\mho$ units).

Design parameters for $S(a_0, \omega_0)$

$$\begin{aligned} Y_B &= 5.00 + j\ 0.00 \\ Y_E &= 7.86 + j\ 8.97 \\ Y_C &= 12.42 - j\ 1.59 \\ Y_0 &= 4.46 - j15.27 \end{aligned} \tag{5.18}$$

Design parameters for $S(a_0 + \Delta a, \omega_0)$

$$\begin{aligned} Y_B &= 4.90 - j\ 0.13 \\ Y_E &= 7.91 + j\ 9.40 \\ Y_C &= 12.34 - j\ 1.73 \\ Y_0 &= 4.38 - j15.40 \end{aligned} \tag{5.19}$$

Design parameters for $S(a_0, \omega_0 + \Delta\omega)$

$$\begin{aligned} Y_B &= 5.50 - j\ 0.97 \\ Y_E &= 7.35 + j\ 9.25 \\ Y_C &= 12.77 - j\ 2.26 \\ Y_0 &= 4.92 - j15.51 \end{aligned} \tag{5.20}$$

The circuit determinant Δ for the set of values (5.18) is

$\Delta = M + jN = 0$. The circuit determinant for the set of values (5.19) is $\Delta = M^{*} + jN^{*} = -3.88 + j\,2.37$. Therefore,

$$\partial M/\partial a = (-3.88)/(-5.00) = 0.78 \quad [m\mho]^2\,[mV]^{-1} \tag{5.21a}$$

$$\partial N/\partial a = 2.37/(-5.00) = -0.47\,[m\mho]^2\,[mV]^{-1} \tag{5.21b}$$

The circuit determinant for the set of values (5.20) is $\Delta = M' + jN' = -39.52 - j\,32.39$. Therefore,

$$\partial M/\partial \omega = (-39.52)/(0.63 \times 10^{6}) = 65.87 \times 10^{-6}\,[m\mho]^2\,[\text{rad./s.}]^{-1} \tag{5.22a}$$

$$\partial N/\partial \omega = (-32.39)/(0.63 \times 10^{6}) = 53.98 \times 10^{-6}\,[m\mho]^2\,[\text{rad./s.}]^{-1} \tag{5.22b}$$

From data (5.21) and (5.22) we obtain,

$$(\partial M/\partial a)(\partial N/\partial \omega) - (\partial M/\partial \omega)(\partial N/\partial a) = 67.47 \times 10^{-6}\,[mV]\,[\text{rad./s.}]^{-1} \tag{5.23}$$

Expression (5.23) is a positive quantity, therefore the limit cycle corresponding to the steady state $S(a_0,\omega_0)$ is stable (see Section 4.7.2). From data (5.18), (5.21), (5.23) and the relevant expressions (5.16), (5.17) etc., we obtain the calculated values given in Table 5.1b. The measured values are obtained by monitoring $|v_c|$ on a valve voltmeter and measuring the frequency on a Hewlett Packard Electronic Counter (model 524c) connected to the output of the Marconi Valve Voltmeter (TF 2600). Knowing the small additional circuit element, which induce the change in performance we can obtain the measured sensitivity ratios S_G^a, S_G^ω etc. On comparing these measured ratios to the calculated ones, we find that they agree reasonably well. There are two factors, which make close agreement difficult. These are:

(1) In the computation we have to deal with differences of pairs of nearly equal quantities.

(2) The method of local linearization used, is an approximate method.

TABLE 5.1b

Quantities	Calculated	Measured
$S_B^a(\Delta a, \Delta B_b^+)$	2.09	2.75
$S_G^a(\Delta a, \Delta G_e^+)$	-1.86	-3.00
$S_B^a(\Delta a, \Delta B_c^+)$	0.61	1.78
$S_B^\omega(\Delta \omega, \Delta B_b^+)$	-0.33	-0.44
$S_G^\omega(\Delta \omega, \Delta G_e^+)$	-0.10	-0.06
$S_B^\omega(\Delta \omega, \Delta B_c^+)$	-0.19	-0.24

As the accuracy of the method is not very good, the calculated sensitivity measures should be treated as an order of magnitude measure rather than an absolute measure. The values in the above table should be rounded up to the nearest significant figure.

5.5.2 Soft excitation in the test oscillator

The test oscillator considered in this section is designed to sustain steady state oscillation at a specific frequency f_o. If the initial state is unstable, then the frequency of initial oscillation f_i, is expected to be close to f_o. Therefore we can apply the method

discussed in Section 4.14, to investigate if soft excitation occurs.

The small signal "y" parameters of the transistor were measured over a small interval of frequencies centred round f_o. The set of embedding elements is given in data (5.15). From these quantities, the set of design parameters e.g. $y_B(\omega) = y_b(\omega) + \omega C_b^+$ etc. were calculated for frequencies within the interval of measurements. From the set of design parameters $y_B(\omega)$, $y_E(\omega)$, $y_c(\omega)$ and $y_0(\omega)$, the corresponding circuit determinant $\Delta(\omega) = y_B y_E + y_E y_C + y_C y_B + y_0^2 = m + jn$ was evaluated. The frequency plots of $|\Delta|$, m and n are shown in Fig. 5.14. From these curves, the values for $-m/(\partial n/\partial\omega)$ and $n/(\partial m/\partial\omega)$ were evaluated. Their frequency plots are shown in Fig. 5.15. From Fig. 5.15 it is found that the natural frequency of the test oscillator responsible for soft excitation is $\sigma_i + j\omega_i$, where $\sigma_i \simeq 0.1 \times 10^6$ nepers/s. and $\omega_i/2\pi = 1.98$ MHz. These values indicate that soft excitation occurs and that the frequency of initial oscillation is close to the design frequency of $f_o = 2.0$ MHz.

In order for the circuit to sustain steady state oscillation, it must have a stable limit cycle. It is therefore more important to test for stability of the steady state oscillation. When there is any doubt on the occurrence of soft excitation or if the knowledge of σ_i is required, then the method discussed above can be used to investigate the initial state, otherwise the designed embedding network can be constructed and the circuit tested experimentally.

5.6 The Performance of Two Synthesized Oscillator Configurations

Two other points P_2 and P_3 on the locus of Fig. 5.11 have been investigated. Both these points correspond to realizable oscillator circuits generating stable oscillations. The designed values and measured values are listed below:

Point P_2: $B_B = 2.00$ m℧ $B_E = -2.78$ m℧ $B_C = 11.18$ m℧

Designed values: $C_b^+ = 1357$pF, $L_e^+ = 4.39$ μH, $C_c^+ = 1919$pF

Experimental values: $C_b^+ = 1350$pF, $L_e^+ = 4.40$ μH, $C_c^+ = 1910$pF

Designed performance: $v_c = 100$ mV, $v_e = 134$ mV, $f_o = 2.00$ MHz

Measured performance: $v_c = 93$ mV, $v_e = 125$ mV, $f_o = 1.93$ MHz

Point P_3: $B_B = -2.00$ m℧ $B_E = 1.01$ m℧ $B_C = 12.35$ m℧

Designed values: $C_b^+ = 1039$pF, $L_e^+ = 5.55$ μH, $C_e^+ = 2005$pF

Experimental values: $C_b^+ = 1040$pF, $L_e^+ = 5.20$ μH, $C_c^+ = 2050$pF

Designed performance: $v_c = 100$ mV, $v_e = 103$ mV, $f_o = 2.00$ MHz

Measured performance: $v_c = 93$ mV, $v_e = 105$ mV, $f_o = 1.94$ MHz

The experimental values listed are measured on the Wayne Kerr B601 bridge. It is seen that the agreement between designed values and measured values is reasonably good.

5.7 Experimental Verification of the Maximum Loads

The expressions for the maximum load and its associated lossless embedding elements are given in expressions (4.18). For the calculations of these expressions the small signal transistor parameters are used. For the calculations carried out in this section, the "y" parameters measured at $|v_c|$ = 80 mV,* f = 2.00 MHz were used. The elements of the gyrator representation corresponding to these "y" parameters are shown in Fig. 5.4(a), (b), (c) and (d).

The schematic diagram for the experimental verification of the maximum load is shown in Fig. 5.16. The transistor was embedded with the lossless circuit elements associated with the maximum load. A load resistance $R_b^+ + r_b^+$ was inserted into the port opposite the base terminal. The trimming resistor r_b^+ was varied until oscillation just ceased. The value of r_b^+ at which this happened is recorded as r_b^+. The frequency of the last detectable oscillation was recorded. $R_b^+ + r_b^+$ was measured on the Wayne Kerr Bridge. Similar measurements were made on the maximum load conductances $G_e^+ = 1/(R_e^+ + r_e^+)$ and $G_c^+ = 1/(R_c^+ + r_c^+)$.

The results of these experiments are:

(1) Maximum load G_b^+

Designed Quantities:

$1/G_e^+ = 71.07$, $C_b^+ = 1332$ pF, $L_e^+ = 6.1$ μH, $C_c^+ = 1339$ pF

Embedding used in test circuit:

$C_b^+ = 1300$ pF, $L_e^+ = 6.3$ μH, $C_c^+ = 1340$ pF

* see Fig. 5.4 ; below 80 mV we get small signal "y" parameter values.

Measured values:

$$1/G_e^+ = 78\,\Omega \quad , \qquad f = 1.92 \text{ MHz.}$$

(2) Maximum load G_c^+

Designed Quantities:

$1/G_c^+ = 3.42\,\Omega$, $C_b^+ = 1332$ pF, $L_e^+ = 4.74$ μH, $C_c^+ = 7621$ pF

Embedding used:

$$C_b^+ = 1300 \text{ pF}, \quad L_e^+ = 4.9 \text{ μH}, \quad C_c^+ = 7600 \text{ pF}$$

Measured values:

$$3.3 < 1/G_c^+ < 4.7 \quad , \qquad f = 1.93 \text{ MHz}$$

(3) Maximum load G_b^+

Designed Quantities:

$1/G_b^+ = 35.27\,\Omega$, $C_b^+ = 1944$ pF, $L_e^+ = 4.74$ μH, $C_c^+ = 1338$ pF

Embedding used:

$$C_b^+ = 1940 \text{ pF}, \quad L_e^+ = 4.9 \text{ μH}, \quad C_c^+ = 1325 \text{ pF}$$

Measured values:

$$1/G_b^+ = 35\,\Omega \qquad f = 2.03 \text{ MHz.}$$

This set of experimental results shows that the measured values agree very reasonably with those calculated from the design expressions.

5.8 The Design of a High "Q" Oscillator

In this section we shall consider the design of a three terminal oscillator, using a series resonant circuit as an embedding admittance. The resonant arm consists of a silver mica capacitor of 50 pF and a Marconi calibrated inductor of 100 μH. The measured frequency characteristics of its conductance and susceptance are shown in Fig.5.17. On examining Fig. 5.17, it is noticed that the frequency characteristic of the resonant arm can be separated into four distinct regions. These are:

(1) Region A: G is positive; B is positive; $(\partial G/\partial \omega)$ is positive; $(\partial B/\partial \omega)$ is positive.

(2) Region B: G is positive; B is positive; $(\partial G/\partial \omega)$ is positive; $(\partial B/\partial \omega)$ is negative.

(3) Region C: G is positive; B is negative; $(\partial G/\partial \omega)$ is negative; $(\partial B/\partial \omega)$ is negative.

(4) Region D: G is positive; B is negative; $(\partial G/\partial \omega)$ is negative; $(\partial B/\partial \omega)$ is positive.

Since the stability of the steady state oscillation involves the frequency characteristic of the circuit parameters, stable oscillation can only occur in a region where the stability criterion given by condition (4.21) is satisfied. This is the reason for the observed frequency pulling effect in oscillator circuits using resonant circuits. With such circuits the frequency of oscillation is always found to be slightly different from the actual resonant frequency.

Stability investigation of each of the four regions would mean

prescribing an arbitrary embedding network to operate in each of the regions, and then evaluating the inequality of (4.21). This is very time consuming. An alternative way is to make preliminary experiments to ascertain which region of operation is best for a given transistor. For the OC 44 transistor, it was found that using the resonant arm as Y_e^+ made it easy to obtain stable oscillation. From previous investigations, oscillation at $|v_c| = 100$ mV, $f_o = 2.00$ MHz and with large G_e^+ requires B_e^+ to be negative. Thus we require the resonant arm to operate in region B or D.

An unwelcome feature of the series resonant circuit is that the dissipation increases as we approach the resonant frequency. This is clearly indicated by the sharp rise of G in Fig. 5.17. (It should be pointed out that the dotted lines in Fig. 5.17 are extrapolations. To obtain satisfactory measurements very close to the resonant frequency, a frequency synthesizer giving small frequency increments is required). The gain of a single transistor is normally not sufficient to cover the large dissipation in region C. Thus we are left to operate the oscillator in region D.

Design

Data

Transistor OC 44, $V_{cb} = 5V$, $I_e = 5$ mA.

Design parameters given in Fig. 5.5b.

Object

To design an oscillator employing OC 44 and the resonant arm. Require low sensitivity.

Method

In previous discussions, it has been pointed out that for a low frequency - sensitive oscillator, we require a frequency controlling element having a large frequency gradient. This means that we are required to operate as far up the G curve in Fig. 5.17 as possible. Therefore the maximum* load configuration is most suitable. The operation point on the G curve will be determined by the "maximum"* load calculated for the given design parameters. Using expressions (4.18), the values for the maximum load and its associated lossless embedding susceptances are:

$G_e^+ = 13.96$ m℧

$B_b^+(G_e^+) = 16.32$ m℧ (1297 pF)

$B_e^+(G_e^+) = -12.48$ m℧

$B_c^+(G_e^+) = 16.46$ m℧ (1308 pF)

G = 14 m℧ on the G curve corresponds to a frequency of 2.06 MHz, and the associated resonant arm susceptance is -36 m℧ . If the resonant arm is to act as Y_e^+ of the maximum load configuration, an auxilliary susceptance $B_{aux}^+ = 23.52$ m℧ must be added in parallel to the resonant arm. The constructed oscillator circuit is shown in Fig. 5.18.

---

* The "maximum" load here is calculated from large signal "Y" parameters.

It is instructive to see what difference a frequency controlling element (one with large frequency gradient) makes to the evaluation of the sensitivity expressions. From Fig. 5.16 we find $(\partial G/\partial\omega) = -484 \times 10^{-6}$ [m℧] [rad./s]$^{-1}$ and $(\partial B/\partial\omega) = 484 \times 10^{-6}$ [m℧] [rad./s]$^{-1}$. With $C_b^+ = 1297$ pF and $C_c^+ = 1308$ pF, we find $(\partial B_b^+/\partial\omega) = 1.3 \times 10^{-6}$ [m℧] [rad./s]$^{-1}$ and $(\partial B_c^+/\partial\omega) = 1.3 \times 10^{-6}$ [m℧] [rad./s]$^{-1}$. Thus for small changes of frequency (within 1% of f_o), all circuit parameters remain substantially constant except for G and B. Therefore in the expressions for $(\partial M/\partial\omega)$ and $(\partial N/\partial\omega)$ it is only necessary to consider the terms containing $\partial B/\partial\omega$) and $\partial G/\partial\omega$. We obtain

$$\partial M/\partial\omega = (G_C + G_B)(\partial G/\partial\omega) - (B_C + B_B)(\partial B/\partial\omega)$$
$$= -10778 \times 10^{-6} \text{ [m℧]}^2 \text{ [rad./s]}^{-1}$$
$$\partial N/\partial\omega) = (G_C + G_B)(\partial B/\partial\omega) + (B_C + B_B)(\partial G/\partial\omega)$$
$$= 6084 \times 10^{-6} \text{ [m℧]}^2 \text{ [rad./s.]}^{-1}$$

The design parameters for the two adjacent states $S(a_o, \omega_o)$ and $S(a_o + \Delta a, \omega_o)$ are:

$S(a_o, \omega_o)$

$Y_B = 5.00 + j\ 1.25$

$Y_E = 9.78 + j\ 2.85$

$Y_C = 12.42 + j\ 3.60$

$Y_O = 4.46 - j15.27$

$S(a_0 + \Delta a, \omega_0)$

$$Y_B = 4.90 + j\,1.12$$

$$Y_E = 9.90 + j\,2.92$$

$$Y_C = 12.34 + j\,3.46$$

$$Y_0 = 4.38 - j15.40$$

(all admittances are in m℧ units).

From these design parameters, $\partial M/\partial a$ and $\partial N/\partial a$ can be obtained. They are:

$$\partial M/\partial a = 0.79\,[m℧]^2\,[mV]^{-1} \qquad (5.25a)$$

$$\partial N/\partial a = 1.69\,[m℧]^2\,[mV]^{-1} \qquad (5.25b)$$

From data (5.24) and (5.25) we find

$$(\partial M/\partial a)(\partial M/\partial \omega) - (\partial M/\partial \omega)(\partial N/\partial a) = 23021.18 \times 10^{-6}\,[mV]\,[rad./s.]^{-1} \qquad (5.26)$$

The sensitivity measures S_B^a and S_B^ω for this circuit can be calculated in a manner similar to that in Section 5.5a. The comparison between the calculated and measured values are given in Table 5.2.

TABLE 5.2

Quantities	Calculated	Measured
$S_B^a(\Delta a, \Delta B_b^+)$	- 0.86	- 1.97
$S_B^a(\Delta a, \Delta B_c^+)$	- 0.63	- 1.31
$S_B^\omega(\Delta \omega, \Delta B_b^+)$	3.3×10^{-4}	4.7×10^{-4}
$S_B^\omega(\Delta \omega, \Delta B_c^+)$	2.5×10^{-4}	2.3×10^{-4}

The calculated and measured values in Table 5.2 agree in order of magnitude. The difficulty of obtaining close agreement is due to the same reasons as those pointed out in connection with Table 5.1b. It is noticed that the frequency sensitivity has improved by a factor of 10^{-3} over that in Table 5.1b.

The introduction of a frequency controlling element into the circuit, simplifies the frequency sensitivity expressions. Consider for example S_B^{ω}. We have

$$S_B^{\omega}(\Delta\omega, \Delta B_b^+) = \Delta\omega/(\Delta B_b^+/B_b^+)$$

$$= \left[\frac{(B_E+B_C)(\partial N/\partial a)-(G_E+G_C)(\partial M/\partial a)}{(\partial M/\partial a)(\partial N/\partial\omega) - (\partial M/\partial\omega)(\partial N/\partial a)}\right] \quad B_b^+ \qquad (5.27)$$

$$\partial M/\partial\omega = \partial(\sum G_B G_E - \sum B_B B_E + G_0^2 - B_0^2)/\partial\omega \qquad (5.28)$$

$$\partial N/\partial\omega = \partial\left[(G_E+G_C)B_B+(G_C+G_B)B_E+(G_B+G_E)B_C+2G_0B_0\right]/\partial\omega \qquad (5.29)$$

assuming that the frequency controlling element is $G_e^+ + jB_e^+$. In Section 4.11, it has been pointed out that near, the resonant frequency, $\partial G_e^+/\partial\omega$ and $\partial B_e^+/\partial\omega$ can be expressed as linear functions of the quality factor Q of the resonant arm. Let $\partial G_e^+/\partial\omega = k_1 Q$ and $\partial B_e^+/\partial\omega = k_2 Q$ where $k_1 \ll Q$ and $k_2 \ll Q$. Since all other circuit parameters remain constant for small frequency changes, we get

$$\partial M/\partial\omega = (G_C+G_B)(\partial G_e^+/\partial\omega)-(B_C+B_B)(\partial B_e^+/\partial\omega) \qquad (5.30)$$

$$\partial N/\partial\omega = (G_C+G_B)(\partial B_e^+/\partial\omega)+(B_C+B_B)(\partial G_e^+/\partial\omega) \qquad (5.31)$$

From expressions (5.27), (5.30) and (5.31) we obtain

$$S_B^{\omega}(\Delta\omega, \Delta B_b^+) = \frac{1}{Q}\left\{\frac{(B_E+B_C)(\partial N/\partial a) - (G_E+G_C)(\partial M/\partial a)}{[(G_C+G_B)k_2+(B_C+B_B)k_1][\partial M/\partial a] - [(G_C+G_B)k_1-(B_C+B_B)k_2][\partial N/\partial a]}\right\} \quad (5.32)$$

From expression (5.32) it is noticed that the frequency sensitivity of the high "Q" oscillator is governed in the first instance by the quality factor of its frequency controlling element. However its actual value will depend on the oscillator configuration and the nonlinearity present in the system.

5.9 Conclusion for Chapter 5

In this Chapter, the geometrical model of the oscillation mechanism is verified experimentally. Starting with the design parameters (these are constructed from the indefinite admittance matrix of the transistor) of three adjacent states $S(a_0,\omega_0)$, $S(a_0+\Delta a,\omega_0)$ and $S(a_0, \omega_0 + \Delta\omega)$, it is possible to investigate the steady state oscillation of the system. Oscillators corresponding to points on the locus of steady state oscillation have been constructed and their performance found to agree with calculations. The effect of loading the oscillator is to shrink the locus of steady state oscillation, thereby narrowing the number of possible configurations realizable for any given

state $S(a_0, \omega_0)$. Calculations have been made on the sensitivity measures S_B^a, S_B^ω, S_G^a, S_B^ω etc. These agree in order of magnitude with measured values. If the oscillator is deliberately designed to be selective for a particular frequency f_0, the stability of the initial state can be investigated in a manner similar to that carried out in Section 5.5a. The mechanism of frequency stability has been investigated with a high "Q" oscillator. The greatest obstacle to achieving high frequency stability (i.e. low frequency sensitivity) is due to dissipation in the frequency controlling element. The generalized "maximum" load configuration (calculated using large signal "Y" parameters) is suggested as the best configuration for achieving high frequency stability in conjunction with a frequency controlling element. Reasonable agreement between calculations and measurements has been found.

Chapter 6

CONCLUSIONS

6.1 General Conclusions

In this thesis the transistor harmonic oscillator is analyzed so that a better understanding of the mechanism behind the steady state oscillation may be gained. In the course of this work, it has been found that a purely linear theory based on the deliberate design of potential instability is inadequate. On the other hand classical nonlinear theory requires a knowledge of the nonlinear element present in the system. Two factors combine to make a design theory for transistor harmonic oscillator elusive: the nonlinear action of the oscillator and the nonrational dependence of the transistor parameters upon frequency. In order to find a guide line to a new approach, the idealized transistor oscillator based on the Ebers Moll model has been examined. The controlling variable responsible for the nonlinear action in the transistor oscillator is identified as the port voltage v_{eb}. The describing function method is used to characterize the transistor for subsequent design. It is found that Aizerman's filter hypothesis justifies the describing function method and that the existence of a strong filter action in the oscillator can be designed deliberately. Measurements and experiments have shown that the describing function method can be used even at higher frequencies. The transistor can be characterized by large signal "Y" parameters. These

are measured directly on a transformer ratio-arm bridge.

In order to relate circuit parameters to the nonlinear action, a geometrical model of the steady state oscillation is constructed using the large signal "Y" parameters. Points on the locus of steady state oscillation in this model, can be interpreted as algebraic limit cycles. Each of these points correspond to a single nonlinear dynamic system whose stability has to be investigated individually. Therefore the construction of the geometrical model is in fact a method of finding steady state solutions of dynamic systems comprising the transistor and possible embedding networks. The adjacent states in the neighbourhood of a well stabilized steady state are also stable, this means that a small change in circuit environment will induce the oscillator to operate in one of its adjacent states. Sensitivity expressions have been derived. These agree reasonably with experimental measurements. The mechanism of stabilizing the frequency of oscillation with a single frequency controlling element has been investigated. It is found that the obstacle to achieving high frequency stability in a Clapp oscillator, is the large dissipation in the resonant arm at frequencies close to resonance. The actual operation of such a high "Q" oscillator depends on the activity of the transistor. A transistor with a large gain will be able to tolerate large losses and thus operate at a more advantageous point on the frequency characteristic of the resonant arm. In connection with providing active power the generalized "maximum" load configuration turns out to be useful.

The work carried out for this thesis, has led to a better

understanding of the transistor oscillator. A new design theory based on synthesizing points on the locus of steady state oscillation is proposed.

6.2 Future Research

(1) Design for large output power

The experiments carried out in this thesis involve circuits generating very low output power. To increase the output power of the circuit, its "conductance state" has to be optimized. For example, it might be more efficient to operate the oscillator on a "hyperbolic" locus of steady state oscillation rather than on an " "elliptical" locus. However it is the author's opinion that not much can be gained by such optimisation. If this is the case, then the designer will have to contend with designing a well stabilized circuit and amplifying the generated signal subsequently.

(2) Design for a variable frequency oscillator with a large frequency band

This is the reverse of designing for good frequency stability. The requirements here are (1) high frequency sensitivity together with (2) a large cluster of stable states in the geometrical model. The investigation will involve examining different points on the locus of steady state oscillation and comparing their stability and their

frequency sensitivity.

(3) Design of CR oscillators

It is expected that the dissipation in a CR embedding network will be large. Investigation should be made into the design of oscillators involving more than one transistor. The object should be to have one transistor contributing to the nonlinear action and the others providing additional generative power.

(4) Sensitivity of performance to transistor parameter variations

The spread in performance in using different transistor with the same embedding network should be examined. This might lead to finding the best transistor characteristics of the transistor for oscillator construction.

Appendix 1

Design Expressions for the Maximum Load

The maximum load configuration corresponds to the point at which the associated plane touches the hyperboloid.

Equation of the hyperboloid is:

$$xy + yz + zx = P \qquad (A.1)$$

Equation of the associated plane is:

$$ax + by + cz = p \qquad (A.2)$$

(see relationships 4.15, for expressions of P, p, a, b and c).

Consider a straight line passing through the point $P(\alpha, \beta, \gamma)$ and intersecting the hyperboloid at points O and Q. Let the directional cosines of the straight line be l, m and n. Let the distance between P and O be r. Then the co-ordinates of O will be given by $O((\alpha + lr), (\beta + mr), (\gamma + nr))$. This point lies on the hyperboloid (A.1), therefore we obtain,

$$(\alpha + lr)(\beta + mr)+(\beta + mr)(\gamma + nr)+(\gamma + nr)(\alpha + lr) = P \qquad (A.3)$$

Rewriting this we get,

$$\alpha\beta + \beta\gamma + \gamma\alpha + r(l\beta + m\alpha + m\gamma + n\beta + n\alpha + l\gamma) + r^2(lm + mn + nl) = P \qquad (A.4)$$

If $\alpha\beta + \beta\gamma + \gamma\alpha = P$, then the point $P(\alpha, \beta, \gamma)$ lies on the hyperboloid. This is because one of the roots of r will be zero. If in addition

we have

$$\alpha(m + n) + \beta(n + l) + \gamma(l + m) = 0 \qquad (A.5)$$

then the other root must also be zero; i.e. $P(\alpha, \beta, \gamma)$, O and Q must all be the same point or $P(\alpha, \beta, \gamma)$ must be the point of tangency. The equation of the tangent plane at $P(\alpha, \beta, \gamma)$ can be obtained by eliminating the quantities l, m, n in equation (A.5). This can be done by using the relationship for the directional cosines:

$$(x - \alpha)/l = (y - \beta)/m = (z - \gamma)/n \qquad (A.6)$$

Equation of the tangent plane is

$$x(\alpha + \beta) + y(\beta + \gamma) + z(\gamma + \alpha) = 2(\alpha\beta + \beta\gamma + \gamma\alpha) \qquad (A.7)$$

If the condition for oscillation is to be satisfied, equation (A.7) must also represent the associated plane given by equation (A.2). If the two planes are to be identical, they must be parallel and their perpendicular distances from the origin must be the same. Equating the squared perpendicular distances, we obtain

$$\frac{(\alpha\beta + \beta\gamma + \gamma\alpha)^2}{(\alpha + \beta)^2 + (\beta + \gamma)^2 + (\gamma + \alpha)^2} = \frac{G_0^2 + B_0^2}{(G_E + G_C)^2 + (G_C + G_B)^2 + (G_B + G_E)^2} \qquad (A.8)$$

On equating the directional cosines of the planes represented by equation (A.7) and (A.2) we get

$$\begin{aligned} (\alpha + \beta)/K_1 &= (G_E + G_C)/K_2 \\ (\beta + \gamma)/K_1 &= (G_C + G_B)/K_2 \\ (\gamma + \alpha)/K_1 &= (G_B + G_E)/K_2 \end{aligned} \qquad (A.9)$$

where,

$$K_1 = \sqrt{\left[(\alpha + \beta)^2 + (\beta + \gamma)^2 + (\gamma + \alpha)^2\right]}$$

$$K_2 = \sqrt{\left[(G_E + G_C)^2 + (G_C + G_B)^2 + (G_B + G_E)^2\right]}$$

In order to satisfy equations (A.8) and (A.9) we must have

$$\begin{aligned} \alpha &= -(G_0/B_0)G_B \\ \beta &= -(G_0/B_0)G_E \\ \gamma &= -(G_0/B_0)G_C \end{aligned} \qquad \text{(A.10)}$$

Substituting values (A.10) into (A.8) and rearranging, we get

$$\sum G_B G_E + G_E G_C + G_C G_B = B_0^2 \qquad \text{(A.11)}$$

Assuming that equation (A.11) is achieved by a single additional external load G_b^+, then equation (A.11) becomes

$$\sum G_b G_e + G_b^+(G_e + G_c) = B_0^2 \qquad \text{(A.12)}$$

where

$$\sum G_b G_e = G_b G_e + G_e G_c + G_c G_b$$

This gives

$$G_b^+ = (B_0^2 - \sum G_b G_e)/(G_e + G_c)$$

Similarly we find

$$\begin{aligned} G_e^+ &= (B_0^2 - \sum G_b G_e)/(G_c + G_b) \\ G_c^+ &= (B_0^2 - \sum G_b G_e)/(G_b + G_e) \end{aligned} \qquad \text{(A.13)}$$

Expressions (A.13) and (A.10) are the expressions for the maximum loads and their "associated" susceptances.

Appendix 2

The Bounds on the Lossless Embedding Elements

The locus of steady state oscillation will be fixed by the frequency of operation and the external load. If the locus is a closed one, then there must be bounds on co-ordinates of points on the locus. By considering the points at which the locus touches the three reference planes xoy, yoz and zox, we can calculate the upper and lower bounds placed on the values of the elements of the lossless embedding (see Fig. 4.13).

Consider the equation for the hyperboloid (A.1) and the associated plane (A.2). On eliminating y from these equations we get

$$-ax^2 + x\left[p - z(c + a - b)\right] + pz - cz^2 - pb = 0 \qquad (A.14)$$

At the upper and lower bound of z, there will be correspondingly only one value of x. Using this constraint and the property of a quadratic we obtain

$$-z^2(\sum G_B G_E) - z(2G_0 B_0 G_C) + G_0^2 B_0^2 - (\sum G_B G_E + G_C^2)(\sum G_B G_E - B_0^2 + G_0^2) = 0 \qquad (A.15)$$

The roots of z are given by

$$\overset{\wedge\vee}{z} = \overset{\wedge\vee}{B_C} = \frac{G_0 B_0 G_C \pm \sqrt{(\sum G_B G_E + G_C^2)(B_0^2 - \sum G_B G_E)(\sum G_B G_E + G_0^2)}}{\sum G_B G_E} \qquad (A.16)$$

The associated value of x is found from equation (A.14) to be:

$$\overset{\wedge\vee}{x} = \overset{\wedge\vee}{B_B} = (-G_0 B_0 + \overset{\wedge\vee}{B_C} G_E)/(G_E + G_C) \qquad (A.17)$$

Similarly we find

$$\overset{\wedge\vee}{y} = \overset{\wedge\vee}{B_E} = (-G_O B_O + \overset{\wedge\vee}{B_C} G_B)/(G_C + G_B) \qquad (A.18)$$

Expression (A.16) gives the boundary values of B_C along the z axis.

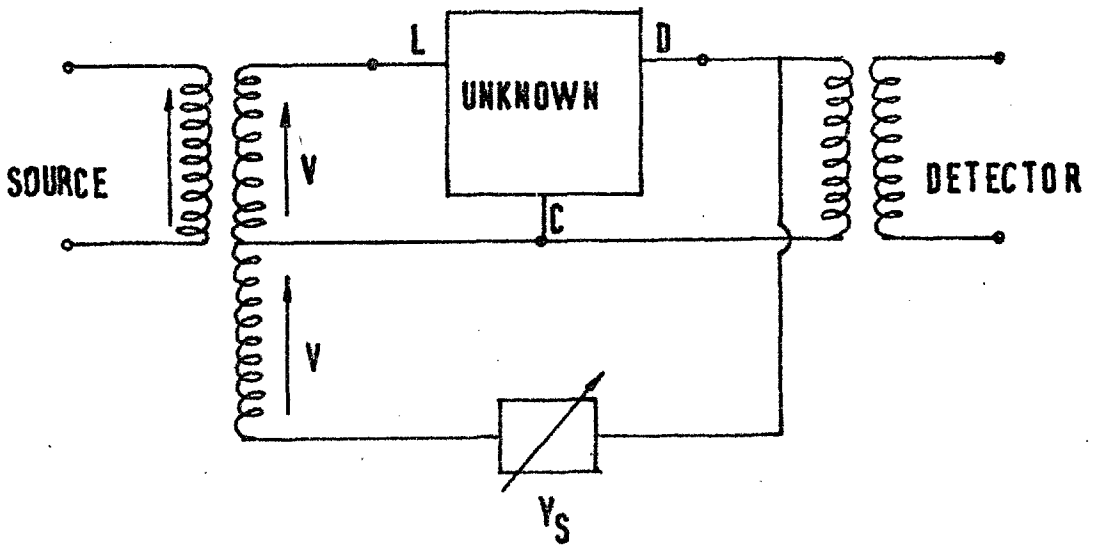

Fig. 5.1 The transformer ratio-arm bridge

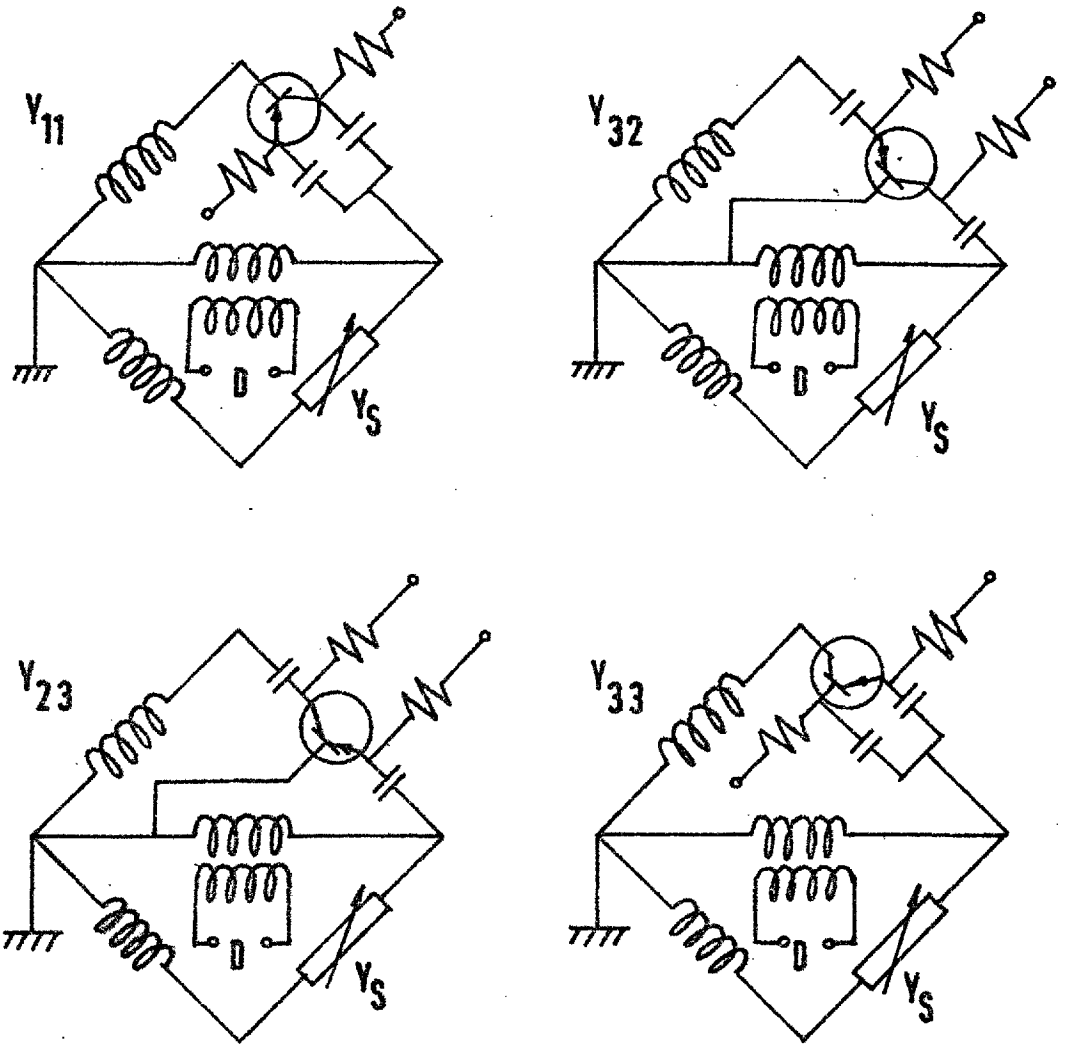

Fig. 5.2 Schematic diagrams of arrangements for measuring "Y" parameters

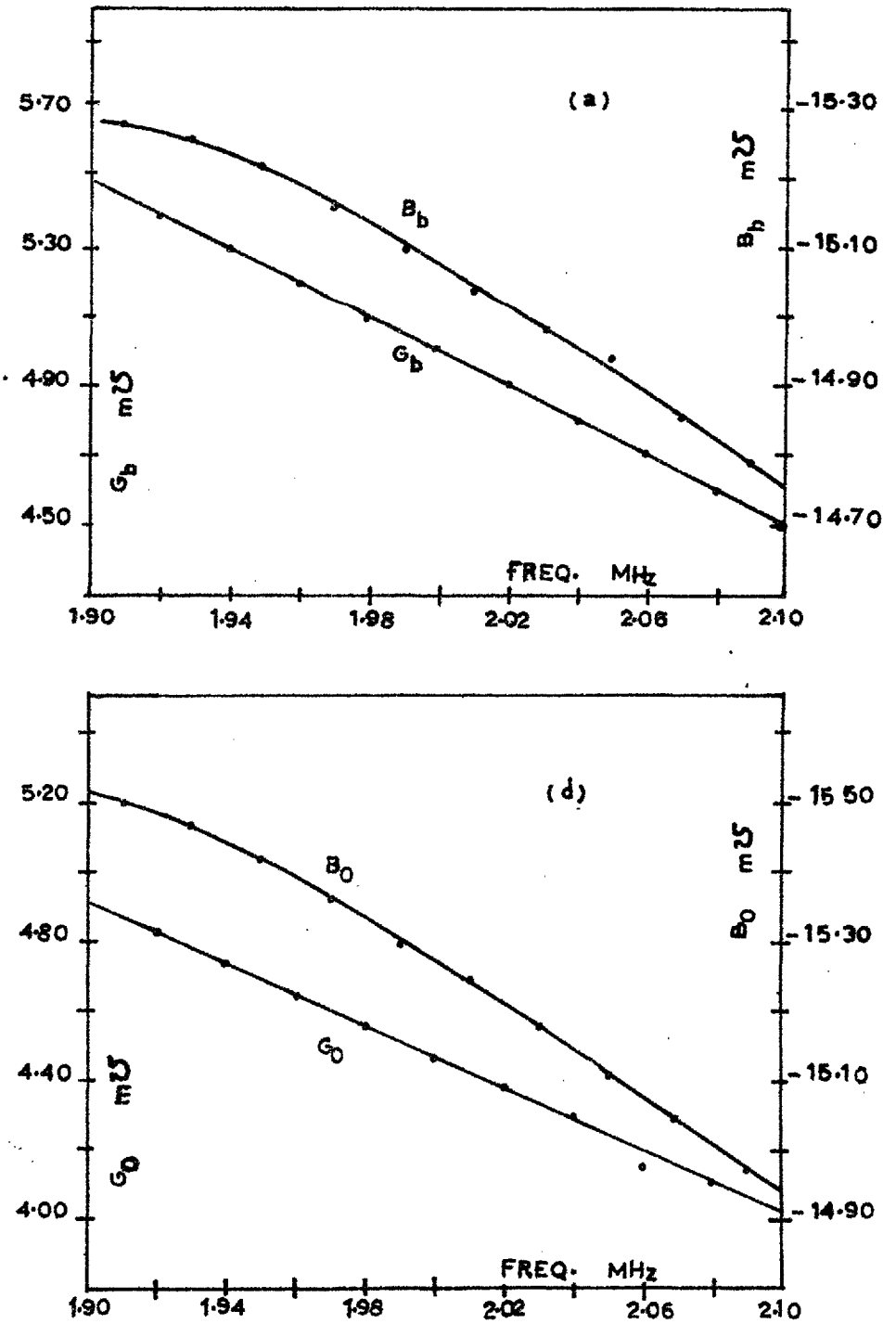

Fig. 5.3 (a) and (d) Values of G_b, B_b, G_o and B_o as functions of frequency

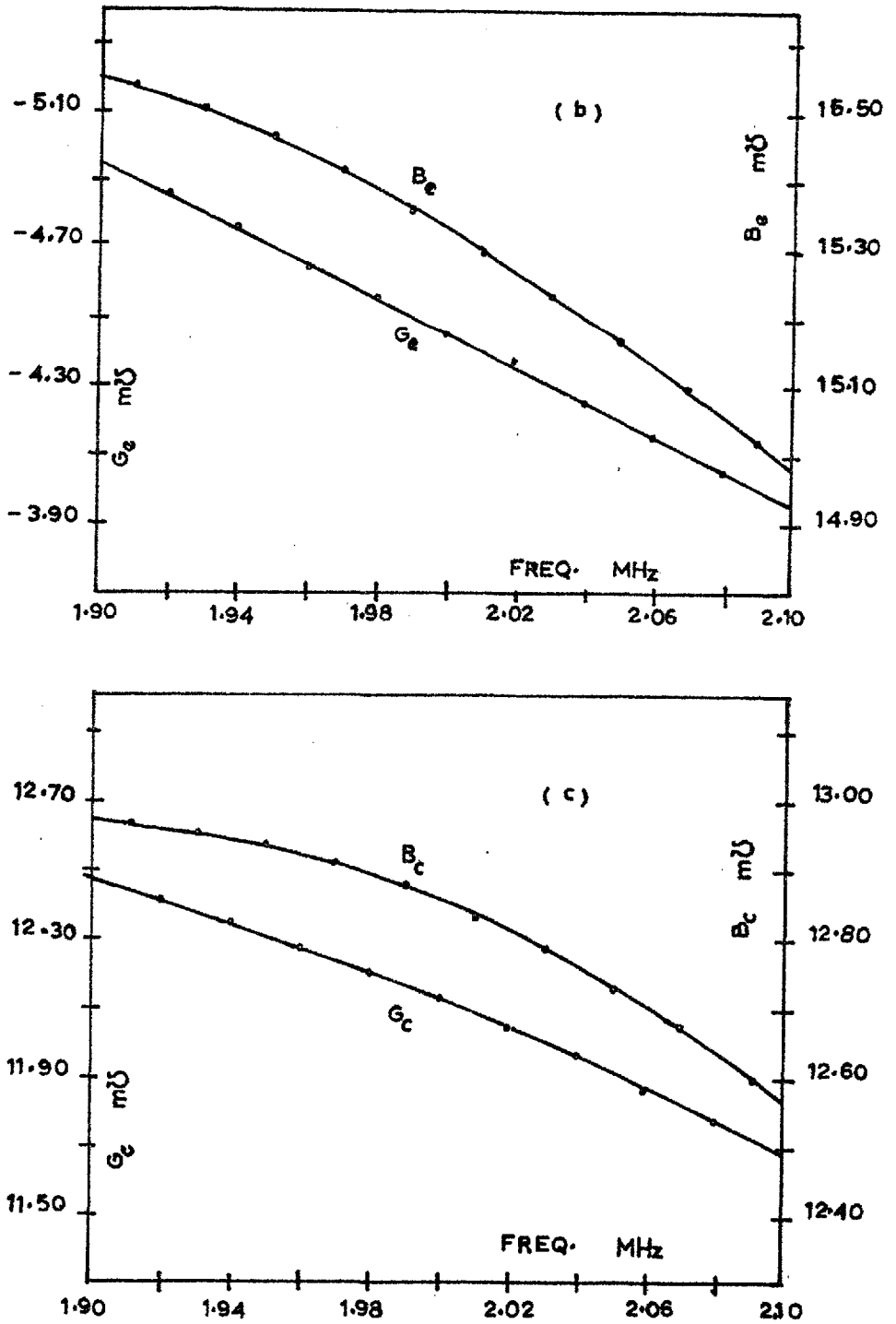

Fig. 5.3 (b) and (c) Values of G_e, B_e, G_c and B_c as functions of frequency

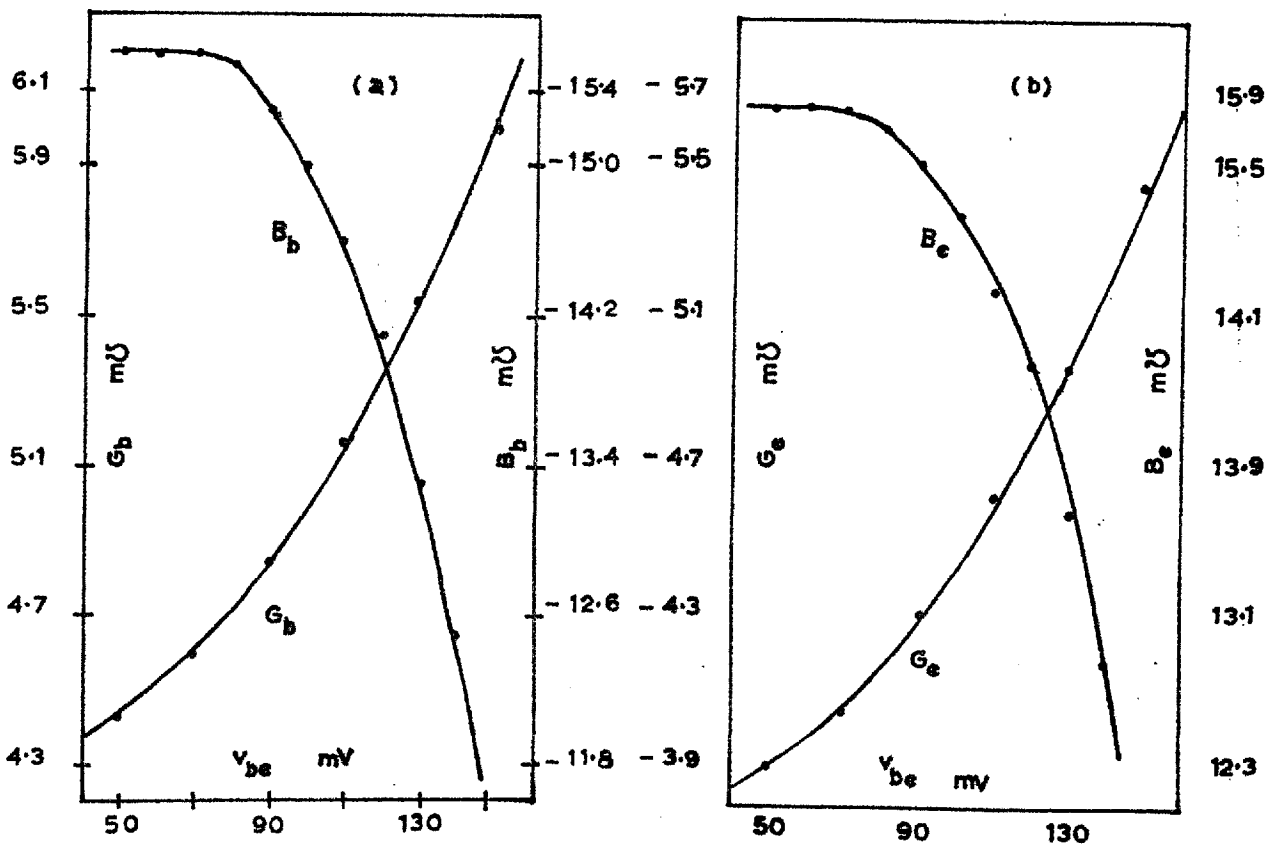

Fig. 5.4 (a) and (b) Values of G_b, B_b, G_e and B_e as functions of $|V_c|$

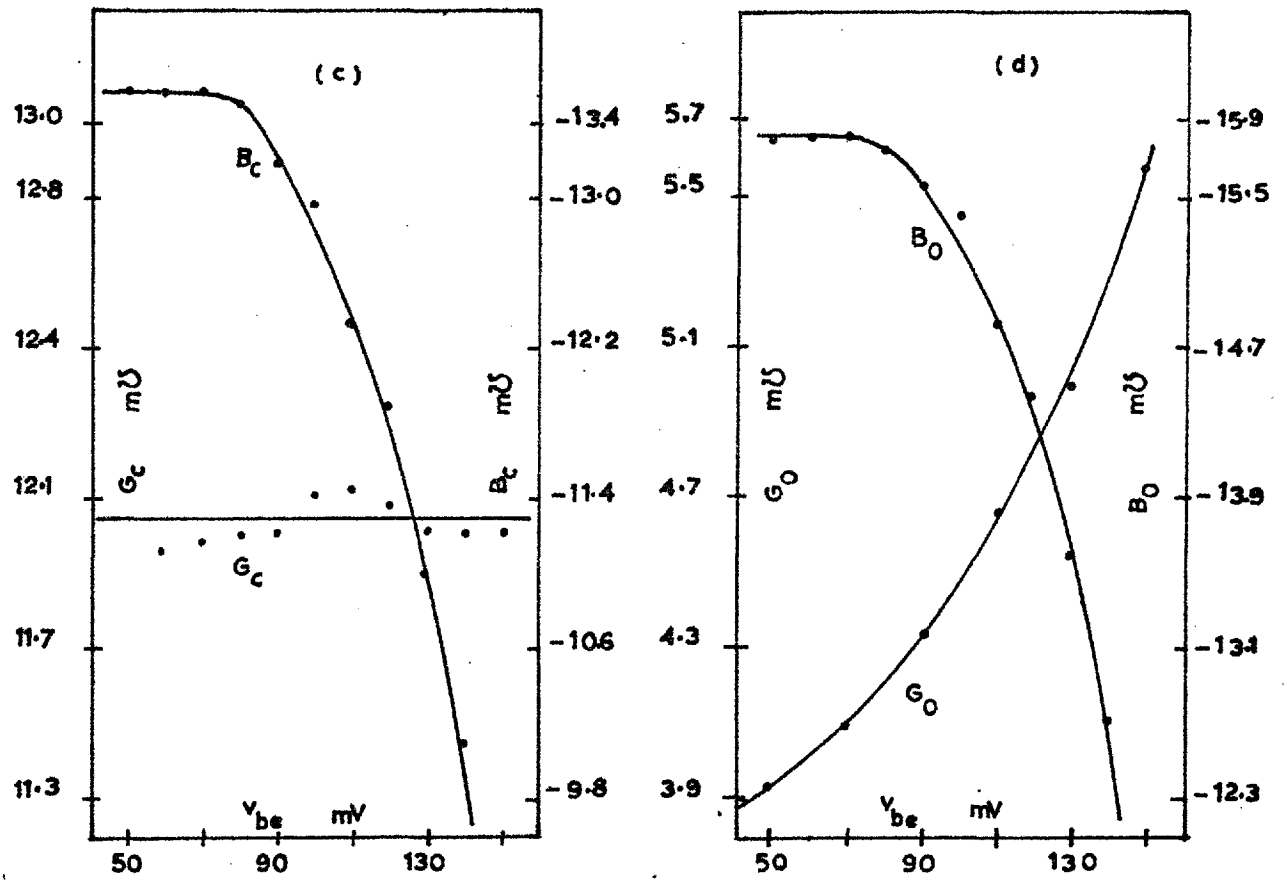

Fig. 5.4 (c) and (d) Values of G_c, B_c, G_o and B_o as functions of $|v_c|$

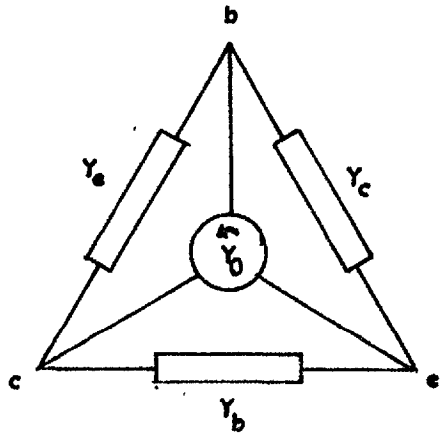

$a_o = v_e = 100$ mV (r.m.s.)

$f_o = \omega_o/2\pi = 2.0$ MHz.

$Y_b = 5.00 - j\ 15.07$ m℧

$Y_e = -4.44 + j\ 15.33$ "

$Y_c = 12.12 - j\ 12.86$ "

$Y_o = 4.46 - j\ 15.27$ "

Fig. 5.5.a. Gyrator representation of the transistor for the operational state $S(a_o, \omega_o)$

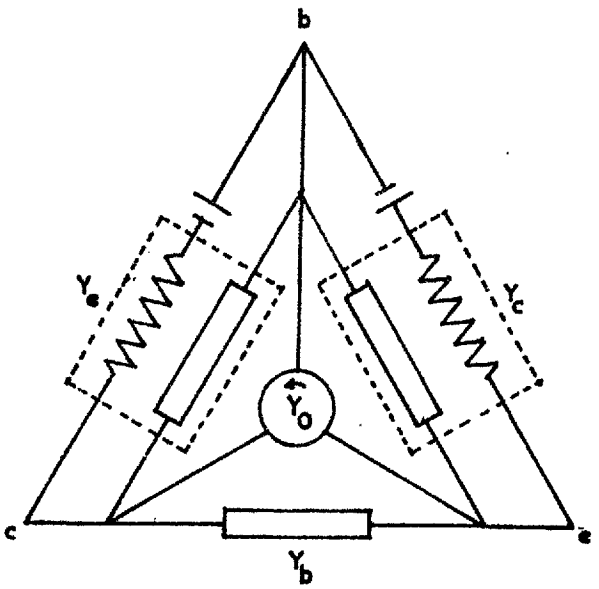

$a_o = v_c = 100$ mV (r.m.s.)

$f_o = \omega_o/2\pi = 2.0$ MHz.

$Y_b = 5.00 - j\ 15.07$ m℧

$Y_e = -4.14 + j\ 15.33$ "

$Y_c = 12.42 - j\ 12.86$ "

$Y_o = 4.46 - j\ 15.27$ "

Fig. 5.5.b. Gyrator representation of the transistor whose biasing resistors are lumped into the arm conductance

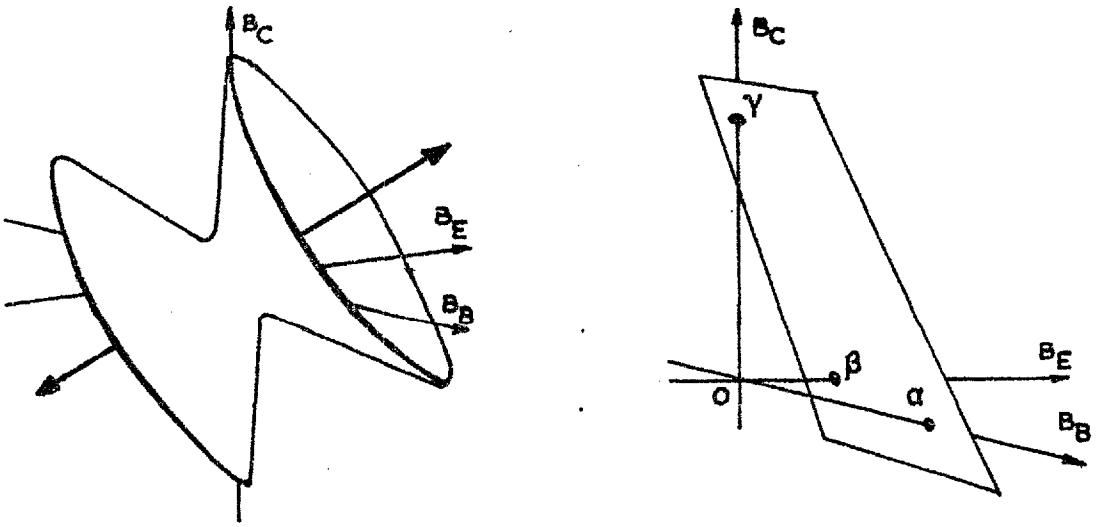

Fig. 5.6.a. The hyperboloid and its "associated" plane for the gyrator representation given in Fig. 5.5.a.

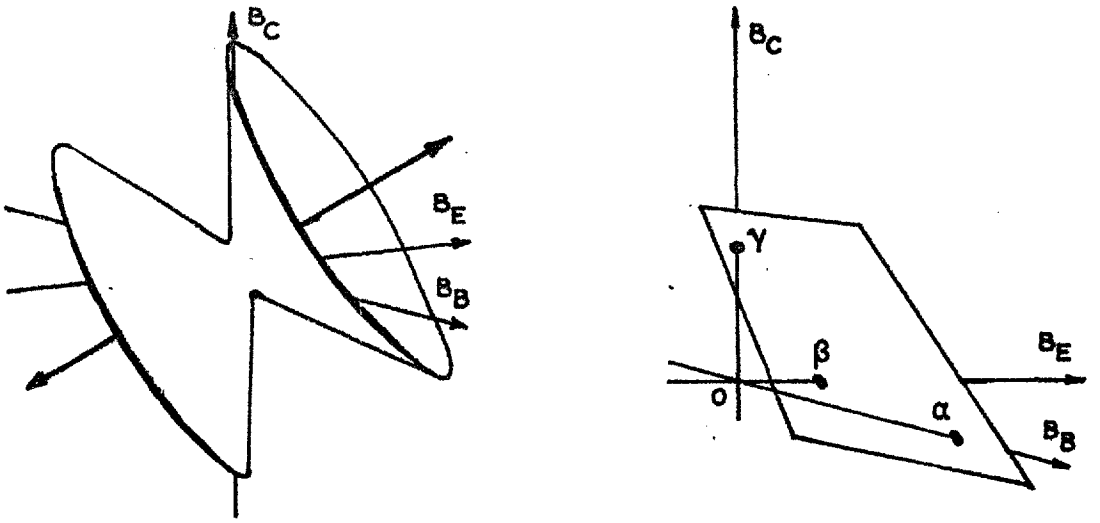

Fig. 5.6.b. The hyperboloid and its associated plane for the gyrator representation given in Fig. 5.5.b.

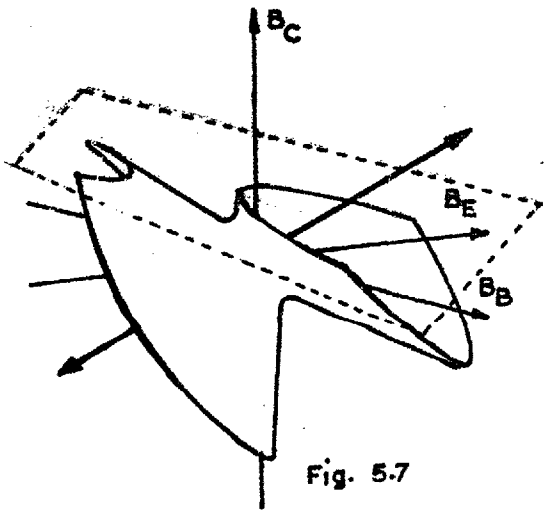

Fig 5.7 The locus of steady state oscillation assuming the form of a "quasi hyperbola"

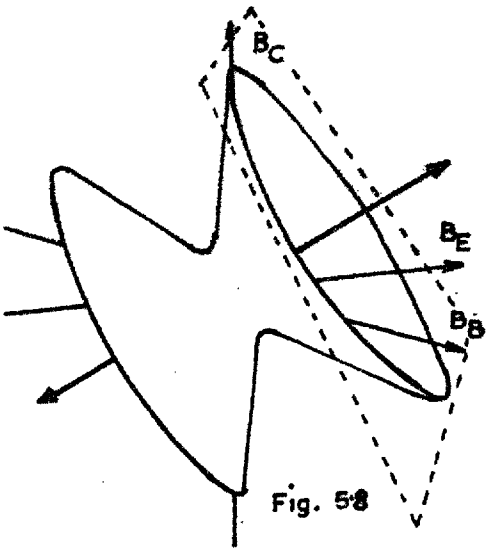

Fig. 5.8 The locus of steady state oscillation assuming the form of a "quasi ellipse"

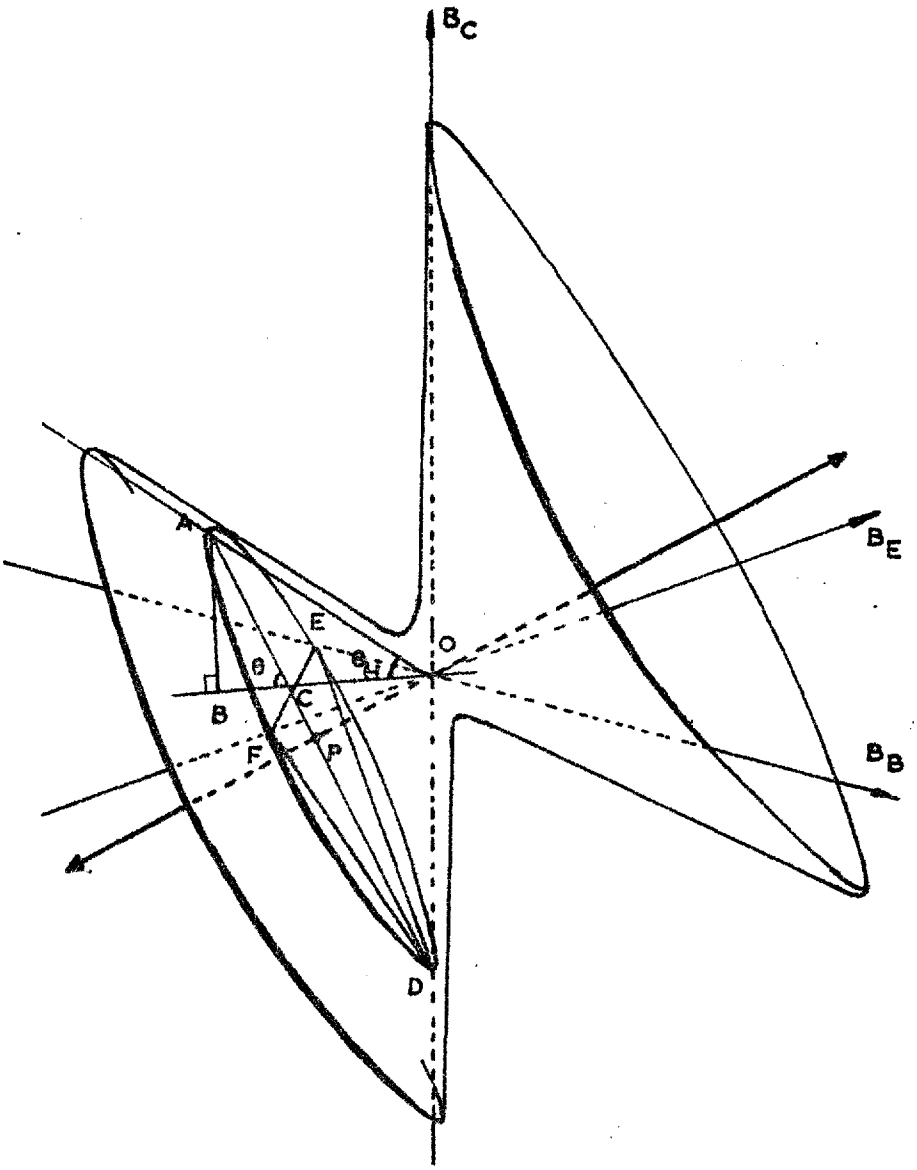

Fig. 5.9 The "associated" right angle cone of the hyperboloid surface

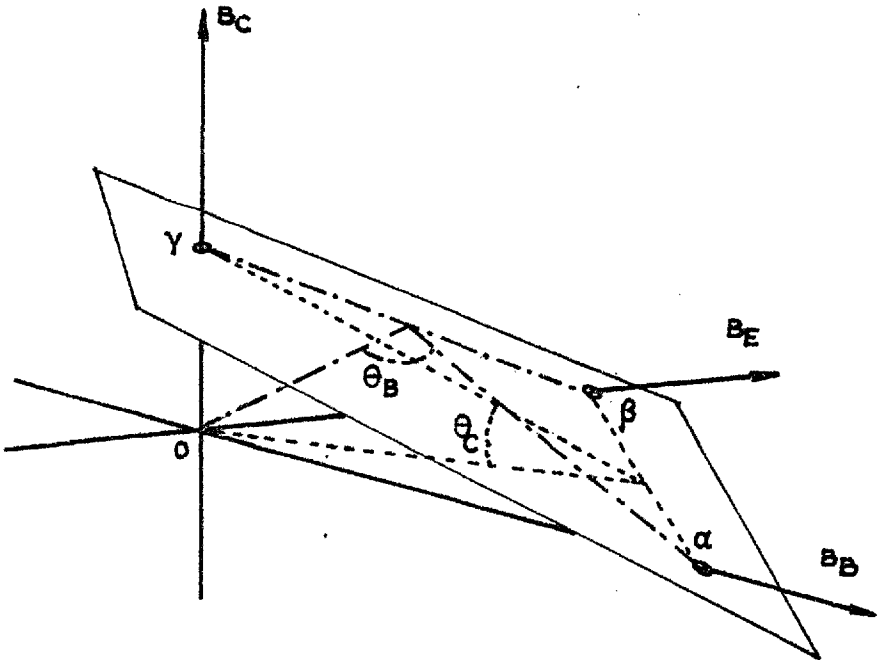

Fig. 5.10 The angles of inclination of the associated plane, θ_B and θ_C are shown. θ_E is defined similarly.

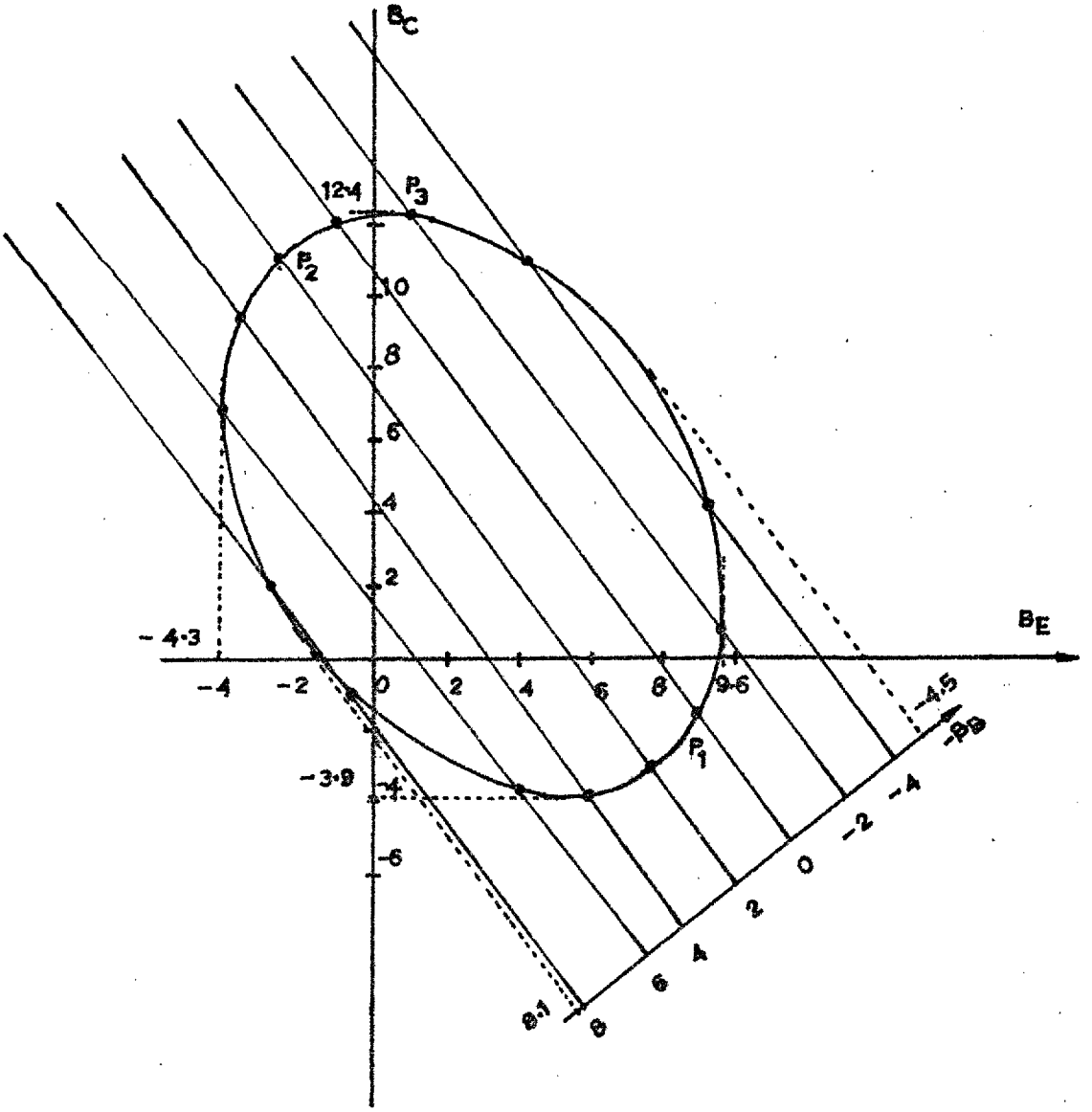

Fig. 5.11 The locus of steady state oscillation for a particular conductance state

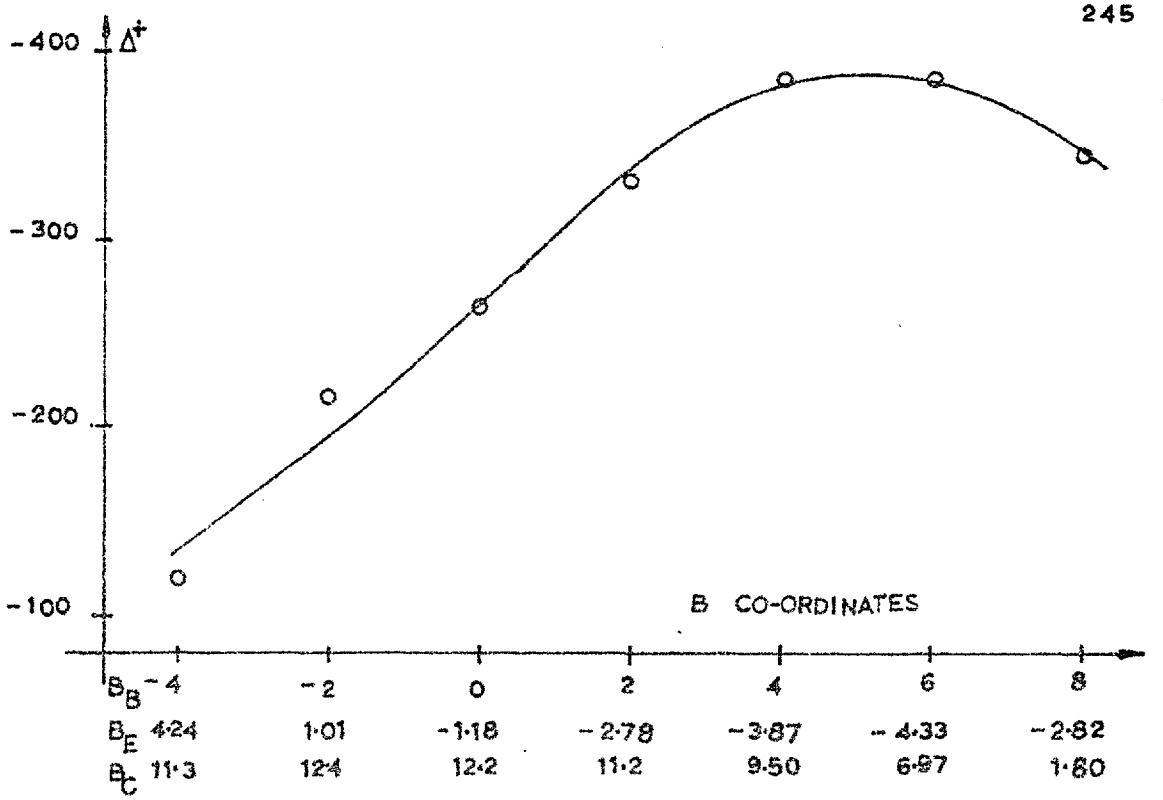

B_B	-4	-2	0	2	4	6	8
B_E	4·24	1·01	-1·18	-2·78	-3·87	-4·33	-2·82
B_C	11·3	12·4	12·2	11·2	9·50	6·97	1·60

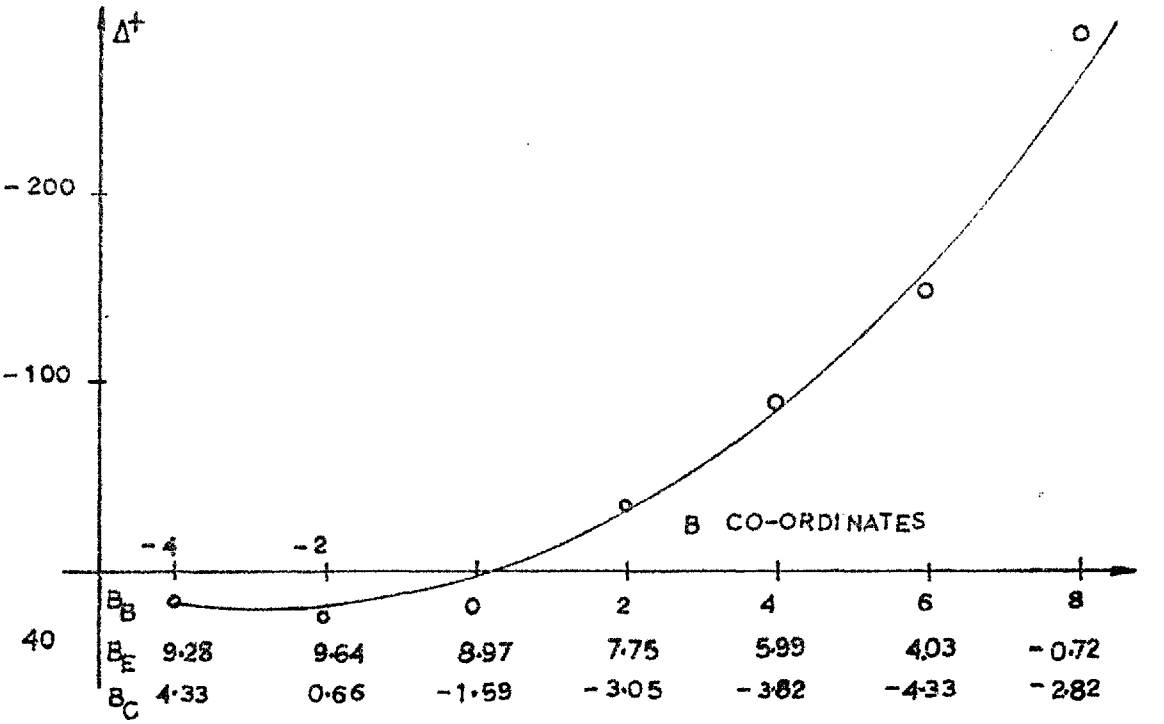

B_B	0	2	4	6	8
B_E	9·28	9·64	8·97	7·75	5·99	4·03	-0·72
B_C	4·33	0·66	-1·59	-3·05	-3·82	-4·33	-2·82

40

Fig. 5.12 Δ^+ as a function of co-ordinates on the locus of oscillation

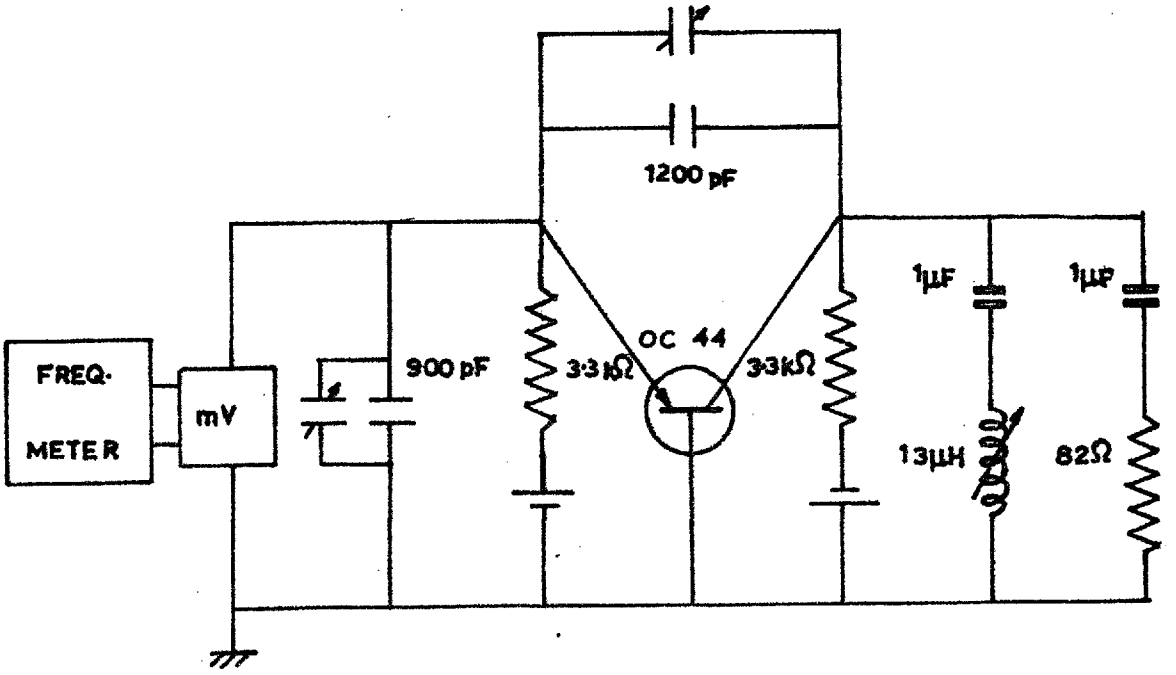

Fig. 5.13 Schematic diagram of the synthesized oscillator

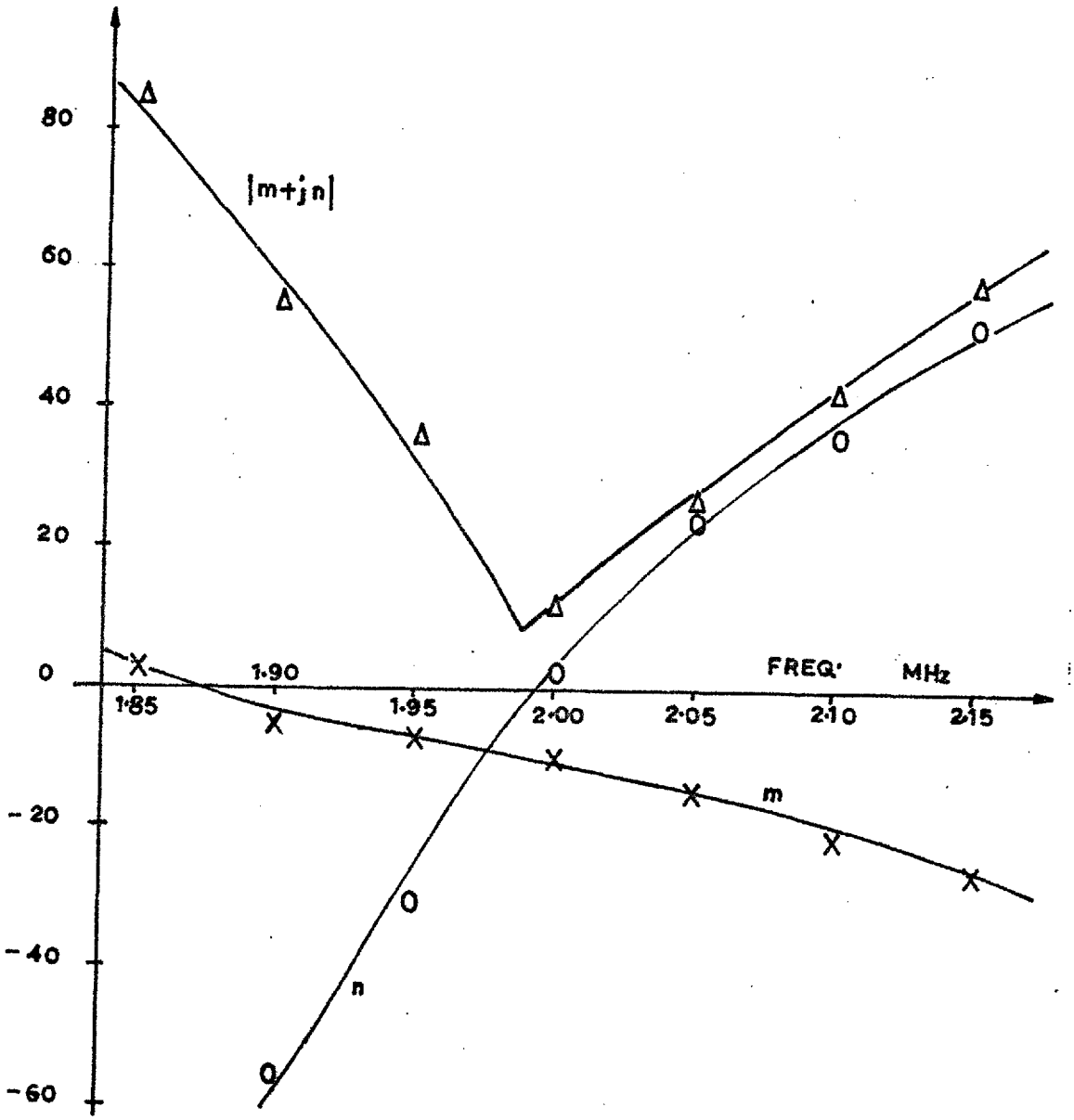

Fig. 5.14 Frequency plots of m, n, and $\sqrt{m^2 + n^2}$

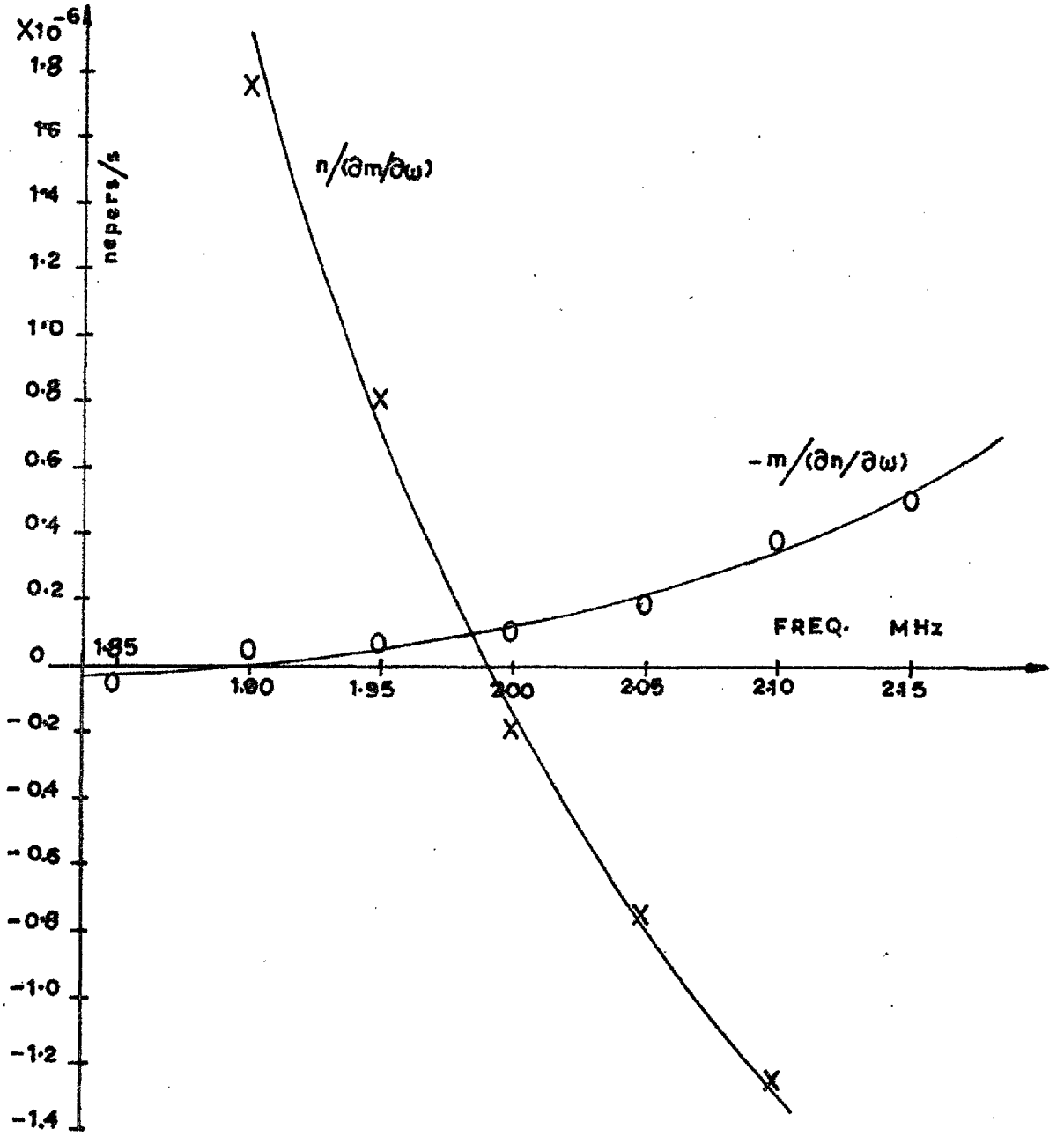

Fig. 5.15 Frequency plots of $-m/(\partial n/\partial\omega)$ and $n/(\partial m/\partial\omega)$

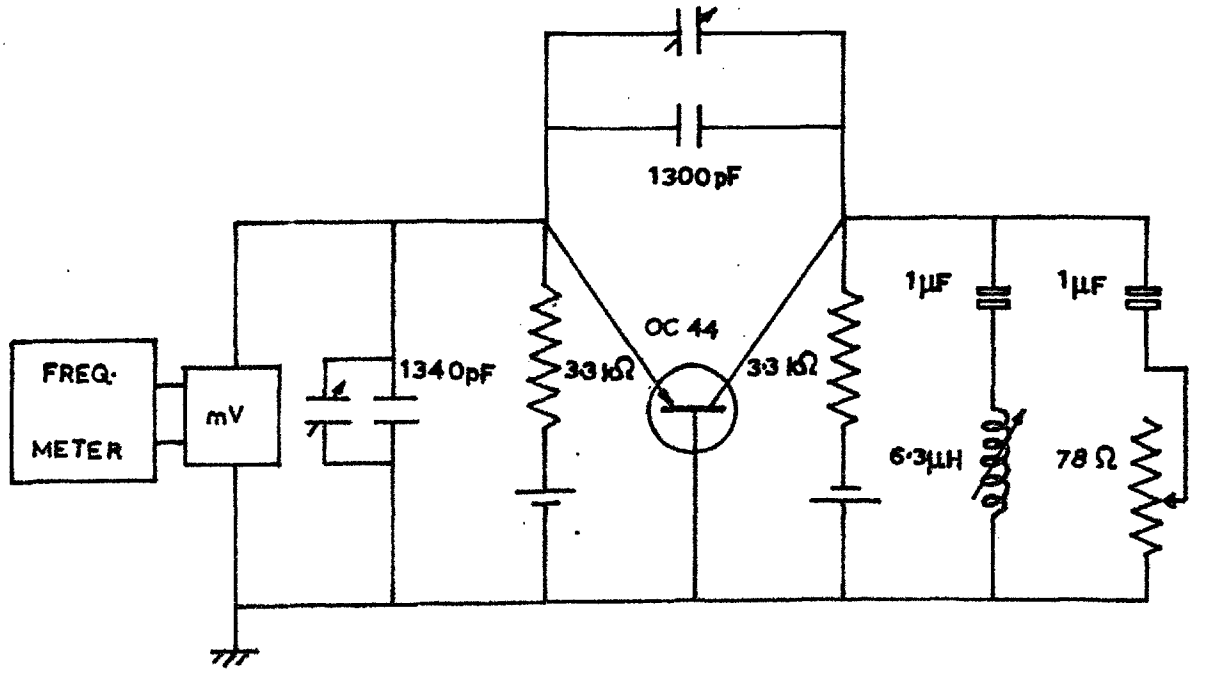

Fig. 5.16 Experimental verification of the maximum load $\hat{G}_b^+$

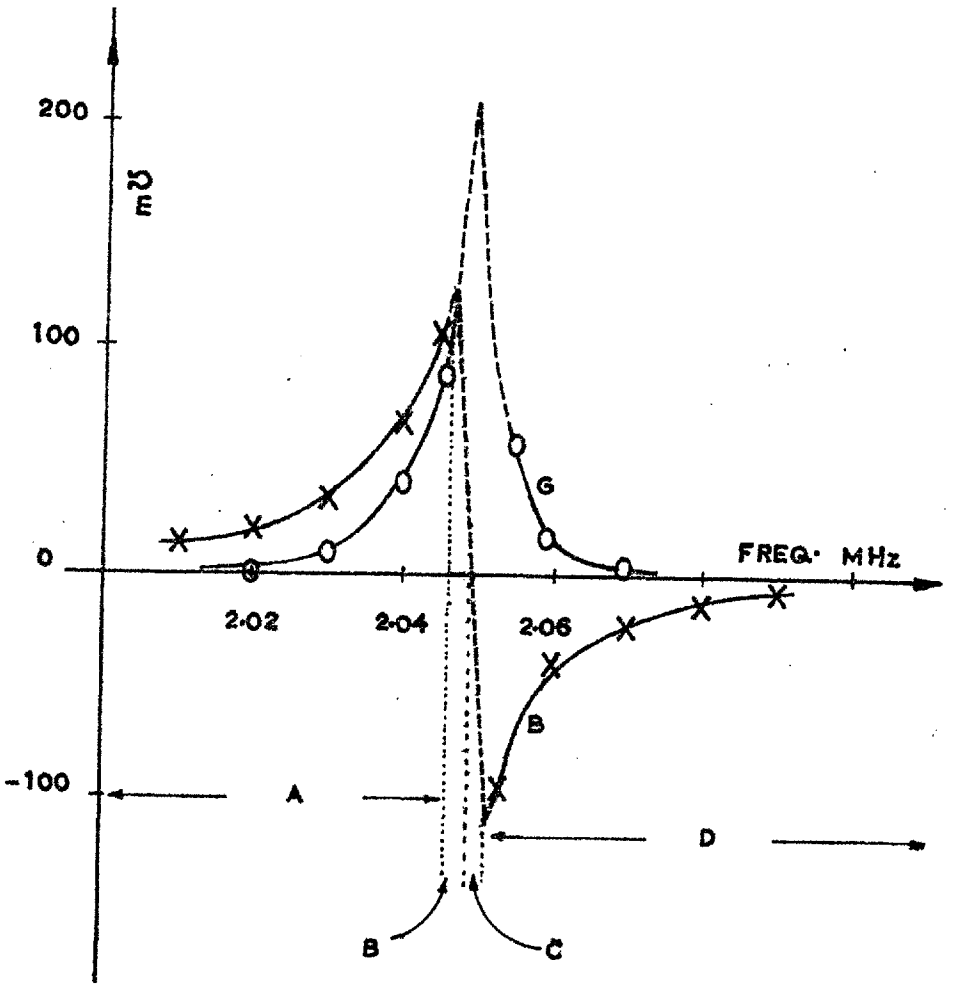

Fig. 5.17 Frequency characteristics of G^+ and B^+

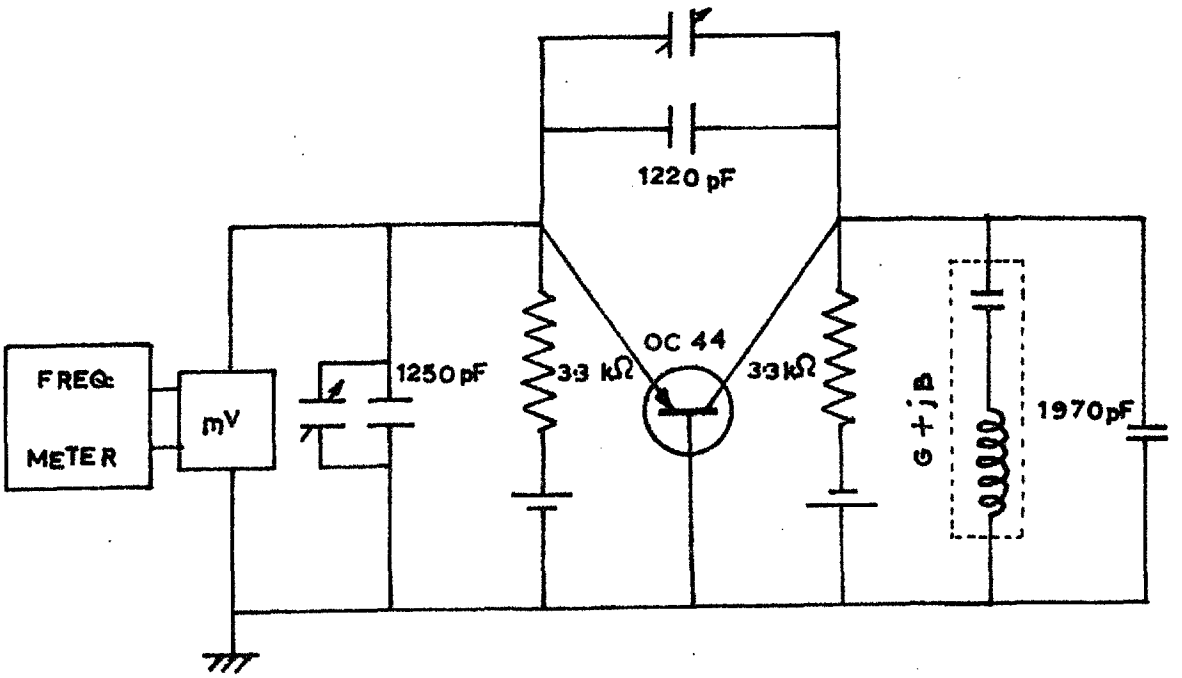

Fig. 5.18 Experimental verification of the design for a Clapp oscillator